GEOSCIENCE AUSTRALIA

Australian Government
Geoscience Australia

Geology of the Fairway and New Caledonia Basins in the Tasman Sea:

sediment, pore water, diapirs and bottom simulating reflectors (*Franklin* Cruise FR9/01 and Geoscience Australia Survey 232)

Neville Exon, Peter Hill, Yves Lafoy, Melissa Fellows, Kirsten Perry, Patrick Mitts, Richard Howe, George Chaproniere, Gerald Dickens, Bill Ussler and Charlie Paull

Record
2004/26

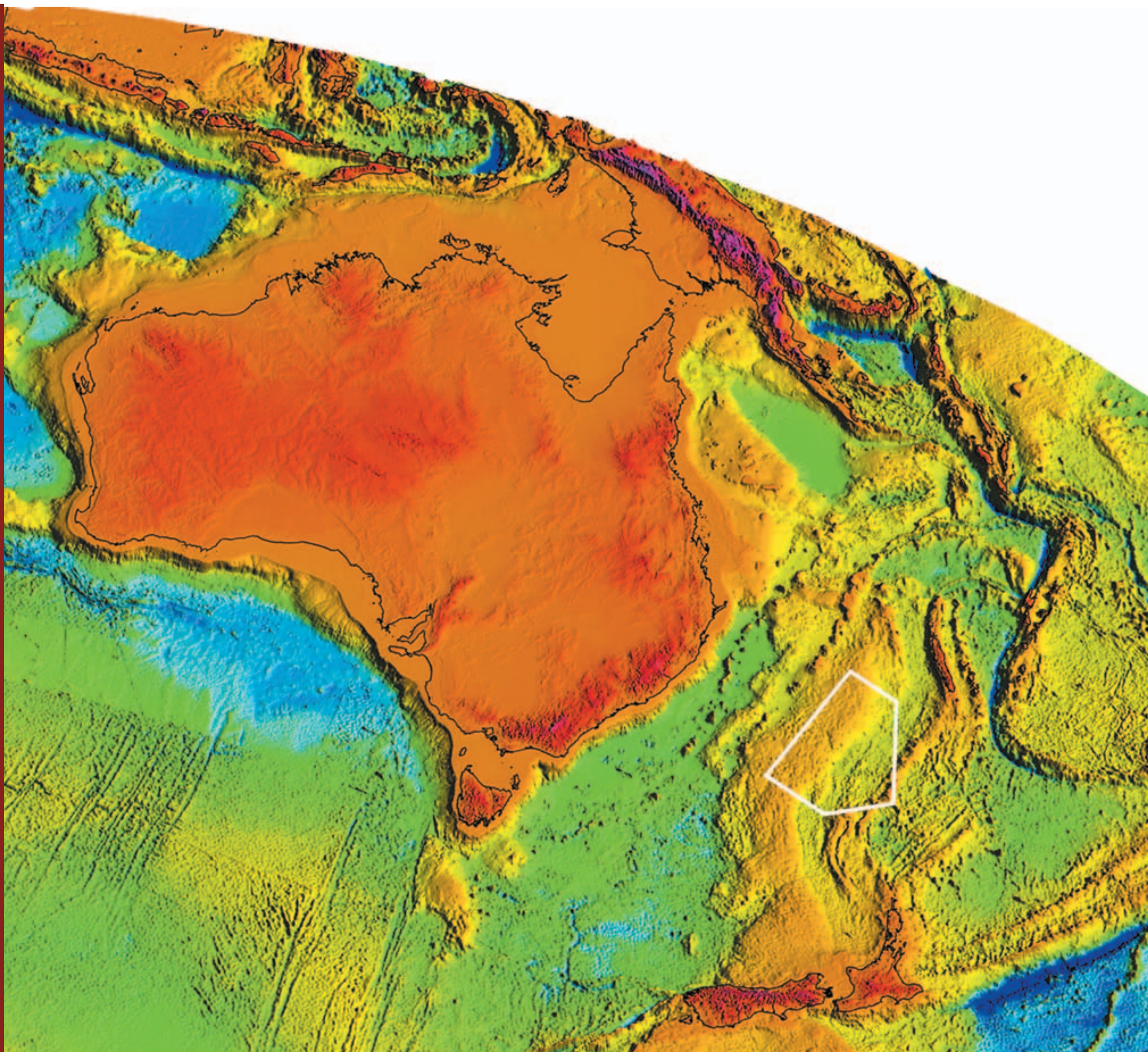

SPATIAL INFORMATION FOR THE NATION

Australian Government

Geoscience Australia

Petroleum and Marine Division

Geoscience Australia Record 2004/26

Geology of the Fairway and New Caledonia Basins in the Tasman Sea: sediment, pore water, diapirs and bottom simulating reflectors (*Franklin* Cruise FR9/01 and Geoscience Australia Survey 232)

Neville Exon[1], Peter Hill[1], Yves Lafoy[2], Melissa Fellows[1], Kirsten Perry[3], Patrick Mitts[4], Richard Howe[1], George Chaproniere[5], Gerald Dickens[6], Bill Ussler[4] and Charlie Paull[4]

Canberra 2004

[1]Geoscience Australia, GPO Box 378, Canberra, Australia 2601
[2]Direction de l'Industrie des Mines et de l'Energie, BP 465, 98 845 Nouméa, Nouvelle-Calédonie
[3]James Cook University, School of Science and Engineering, Townsville, Queensland, Australia 4811
[4]Monterey Bay Aquarium Research Institute, 7700 Sandholt Road, Moss Landing, California, USA 95039
[5]Department of Geology, Australian National University, Canberra, Australia 0200
[6]Rice University Department of Earth Science, MS 126, PO Box 1892, Houston, Texas, USA 77251-1892

Geoscience Australia
Chief Executive Officer: Dr Neil Williams

Department of Industry, Tourism & Resources
Minister for Industry, Tourism & Resources: Senator The Hon. Ian Macfarlane, MP
Parliamentary Secretary: The Hon. Warren Entsch, MP
Secretary: Mark Patterson

ISSN 1448-2177
ISBN 1 920871 27 7

GeoCat No. 61124

Bibliographic reference: Neville Exon, Peter Hill, Yves Lafoy, Melissa Fellows, Kirsten Perry, Patrick Mitts, Richard Howe, George Chaproniere, Gerald Dickens, Bill Ussler and Charlie Paull. Geology of the Fairway and New Caledonia Basins in the Tasman Sea: sediment, pore water, diapirs and bottom simulating reflectors (*Franklin* Cruise FR9/01 and Geoscience Australia Survey 232)

TABLE OF CONTENTS

Figures

Tables

Appendices

ABSTRACT

The Lord Howe Rise and Norfolk Ridge are major north-south structural highs in the Tasman Sea that are separated by the Fairway and New Caledonia Basins. The Fairway Basin is the shallower of the two basins and is in water generally shallower than 3000 m. The New Caledonia Basin lies further east in water generally deeper than 3000 m. In terms of petroleum potential, pre-existing seismic and sampling data showed that the Fairway Basin and western New Caledonia Basin contain:

- Sedimentary sequences more than 3 km thick, probably thick enough to generate petroleum if source rocks are present, and consisting largely of siliciclastic Cretaceous sediments and Cainozoic oozes and chalk
- Sedimentary diapirs, probably in Cretaceous mudstone, and possibly capable of being petroleum source rocks and forming petroleum traps
- A bottom simulating reflector (BSR) 500-600 m below the sea bed in Cainozoic chalk in water depths of 1500-3600 m, which might represent gas hydrates. Given the lack of organic matter in the chalks, any hydrates would probably be of thermogenic origin.
- Small quantities of possibly thermogenic gas identified in gravity cores

In the area studied on *Franklin* research cruise FR9/01, the Fairway and New Caledonia Basins together are about 300 km wide and 900 km long. About 2800 km of 24 channel seismic profiles were recorded in this very poorly known region. They have helped us to clarify the structural framework and nomenclature of the area, showing that the Fairway Basin and New Caledonia Basin are separated by an intermittent ridge, and that both terminate at roughly 31º30'S. In the Central Fairway Basin in the north, known to have petroleum potential, two new east-west seismic sections found more diapirs, evidence of a BSR suggesting the presence of gas hydrates, and young faults.

In the south, there are now six east-west seismic profiles in an area of Australian jurisdiction where there were previously none. These seismic profiles show that the deep water depression south of 26º20'S is an extension of the Fairway Basin. Water depths are 1200-3600 m. The South Fairway Basin is limited by the Lord Howe Rise to the west and the northern extension of the West Norfolk Ridge to the east, and is roughly 600 km long and 150 km wide: an area of 90,000 km^2. The basin contains sediments more than 2000 m thick in places, shallow and deep diapirs (especially north of 29°S), and a BSR in some places. Clearly, the South Fairway Basin has some petroleum potential, despite the apparent maximum thickness of sediment (<3 km) found so far.

In the southern New Caledonia Basin (near Norfolk Island) maximum water depths are 3000-3600 m. The true sediment thickness is unclear, because basement commonly was not reached on our two seismic profiles, but it reaches 1500 m in places. The sedimentary section is flat-lying in general, with some areas of folding and diapirism. The generally seismically diffuse lower sequence, of probable Paleocene-Eocene age, contains rare strong reflectors. The upper sequence is transparent on both sides of the basin, but contains well-bedded sequences, probably turbidites, in the basin centre.

In terms of petroleum potential, the new seismic data prove that diapirs and the BSR extend further south. Recent waveform inversion modelling on a pre-existing seismic profile suggests that the BSR may be generated by a thin gas hydrate layer with no gas below it. Twenty-two Quaternary gravity cores were recovered along the seismic profiles across the basins, partly to further investigate the nature of the BSR (gas hydrate or not?). Their average length is 350 cm. The cores contain negligible quantities of gas, despite many being located in apparently favourable positions above diapirs. Furthermore, the pore waters do not show the sharp chemical gradients of sulphate, chloride and methane which would indicate significant accumulations of methane in gas hydrates. However, these negative results may well be caused by the highly oxidised nature of the sediment throughout the cores, so our results shed no new light on the nature of the BSR. Overall, the regional evidence does not support the presence of a diagenetic BSR, but the evidence for a gas hydrate BSR is not conclusive. Only sampling across the BSR, at depth or from outcrops on the continental slope, will conclusively prove whether it is associated with gas hydrates.

The cores recovered a variety of foram-bearing nannofossil oozes and nannofossil oozes, in water depths of 1297-3517 m and latitudes of 24-32ºS. Uniformly pale core colours in the north suggest purely oxidising conditions, but multicoloured cores in the south indicate fluctuations in redox conditions, and are probably related to inflow of varied bottom water through time. Twenty-one samples from core bases, and three from dredges, have been examined for planktic foraminifera and calcareous nannofossils: in the cores both groups are abundant and well preserved. All core-base samples are Pleistocene and the foraminiferal assemblages are typically subtropical to warm temperate, dominated largely either by the *Globorotalia (Truncorotalia)* or the *Gr. inflata* groups. The more precise nannofossil ages show a clear relationship between location and the age of the core bases. As most cores are of similar lengths, there is probably a systematic variation in sedimentation rates. The four oldest cores, all from the north, have the lowest average sedimentation rates (~4 mm/1000 years), but they are on slopes and may be winnowed. The other northern cores have lower sedimentation rates (~10 mm/1000 years) than the southern cores (25 mm/1000 years), perhaps because productivity has been higher south of 26º45'S than further north.

The northern dredge 1, from the Fairway Basin, contains chalk and radiolarite with Early Eocene foraminifera and late Early to early Middle Eocene nannofossils. The southern dredge 5, from the eastern Lord Howe Rise, contains a volcanic breccia with poorly preserved Early Pliocene foraminifera and Late Miocene to Late Pliocene nannofossils in micrite infillings. The associated ferromanganese crust contains Late Middle Miocene foraminifera.

Key words: Lord Howe Rise, Fairway Basin, New Caledonia Basin, seismic profiles, Cretaceous diapirs, BSR, Cainozoic chalks, Pleistocene gravity cores, pore water gradients, R.V. *Franklin*

1. INTRODUCTION

The regional setting of the study area is shown in Figures 1 and 2. In the 1000 km between Australia and New Caledonia are the following major structural features, generally trending north-south:

- The Australian continental slope, with average slopes of less than 5º
- The relatively flat sea floor of the oceanic northern Tasman Basin, more than 4000 m deep, cut by volcanic seamounts of the north-south Tasmantid chain
- The relatively narrow Dampier Ridge
- The Middleton Basin
- The broad continental Lord Howe Rise, with its crest at less than 1000 m depth
- The Fairway Basin forming the eastern flank of the Lord Howe Rise
- The relatively flat New Caledonia Basin, more than 4000 m deep
- The slope of New Caledonia and its southern extension, the Norfolk Ridge

A more detailed view of the study area is displayed as an image of satellite gravity data draped on bathymetry (Figure 3). This shows the area between the Lord Howe chain of seamounts on the western side of Lord Howe Rise in the west, and the New Caledonian and Norfolk Ridges to the east. A noteworthy feature of this map is that both the Fairway Basin and the New Caledonia Basin are characterised by axial gravity highs. Like Lafoy *et al*. (in prep.) we consider that the Fairway Basin overlies thinned continental crust. The situation in the New Caledonia Basin is not clear, but Lafoy *et al*. (in prep.) argue that the northern New Caledonia Basin probably overlies highly extended continental crust, and the southern north-south trending part of the New Caledonia Basin probably overlies oceanic crust.

The aim of the present report is to present the general results from *Franklin* Cruise FR9/01 in the Fairway and New Caledonia Basins, with emphasis on seismic profiles and Quaternary cores. There are major sections on nannofossil and foraminiferal biostratigraphy, and pore water geochemistry. Figure 4 is a map of bathymetry, national boundaries, seismic profiles and sampling sites.

1.1. Previous studies

Lord Howe Rise (Figures 1 and 4) is a bathymetric high and thinned fragment of continental crust that detached from Australia during Cretaceous rifting, and then subsided to its present depths in the early Cainozoic (e.g., Hayes & Ringis, 1973; Weissel & Hayes, 1977; Launay *et al*., 1977; Shaw, 1978; Willcox *et al*., 1980, 1981, 2001; Kroenke, 1984; Hinz *et al*. 1985; Roeser *et al*., 1985; Schreckenberger *et al*., 1992; Walley, 1992; Gaina *et al*., 1998; van de Beuque *et al*., 1998a, 2003; Stagg *et al*., 2002). The Lord Howe Rise is a ribbon continent and is probably composed of Paleozoic basement with Tasman Fold Belt orogenic affinities, overlain by a number of rift basins with up to 4 km of sedimentary fill of Mesozoic and Cainozoic ages. This ribbon continent in the Tasman Sea, between Australia, New Caledonia and New Zealand, averages 400 km in width, and extends about 1600 km northward from the Challenger Plateau off New Zealand to the Chesterfield Plateau west of New Caledonia. Crestal water depths are 750 to 1200 metres below sea level. It rifted from Australia to the west in the latest Cretaceous and Paleocene (82-52 Ma). The resultant Tasman Basin to the west is floored with oceanic crust. The Lord Howe Rise has Cainozoic seamount chains, probably related to mantle plumes, on its crest (McDougall and Duncan, 1988; Exon *et al*., 2004).

The Lord Howe Rise also rifted from the Norfolk Ridge and New Caledonia to the east, but the timing of the formation of the resultant New Caledonia Basin is unclear, and it is also not clear whether oceanic crust is involved (van de Beuque *et al*., 1998b, 2003; Auzende *et al*. 2000a; Stagg

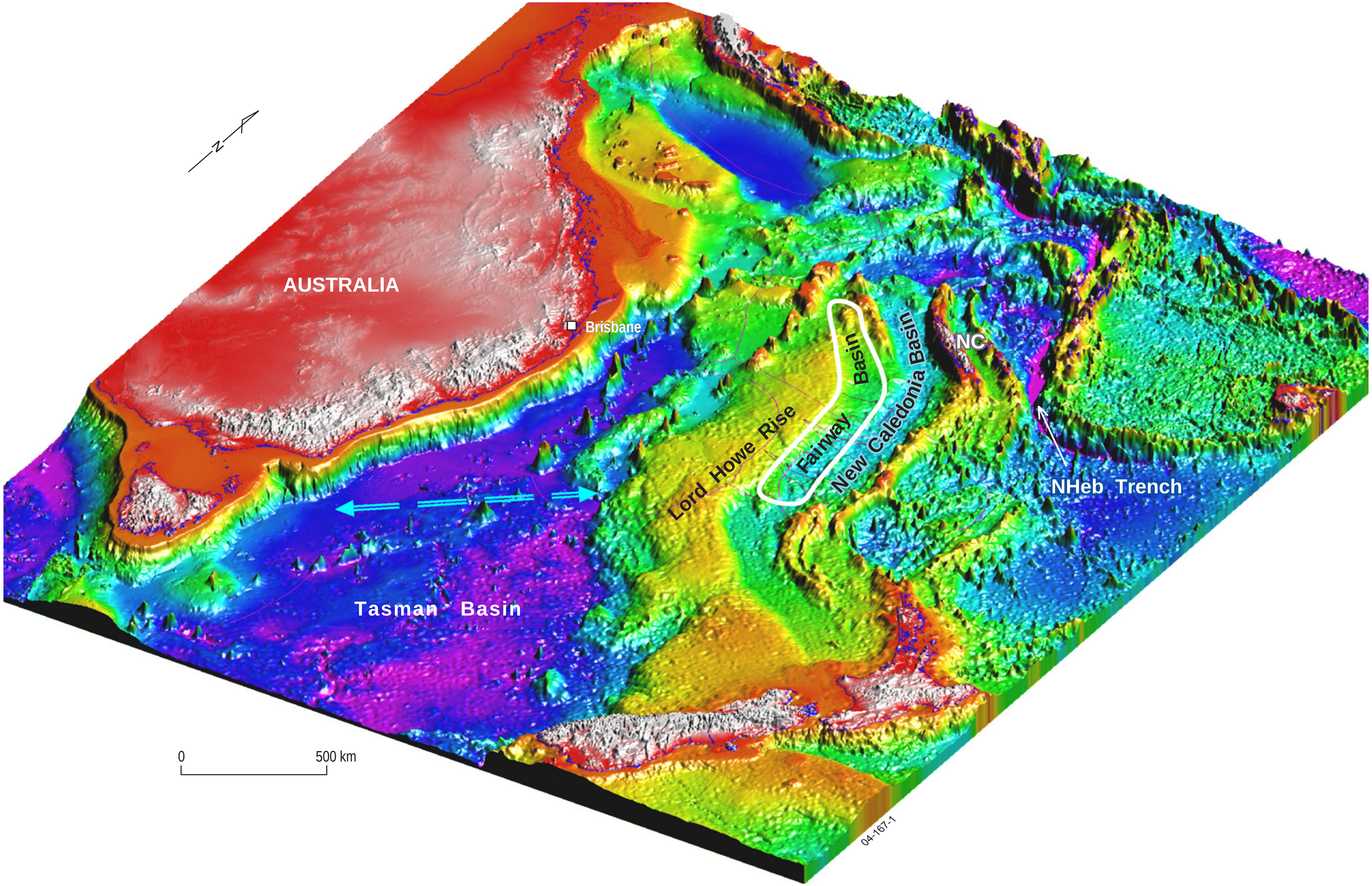

Figure 1. Bathymetric relief of Southwest Pacific Ocean showing Fairway Basin

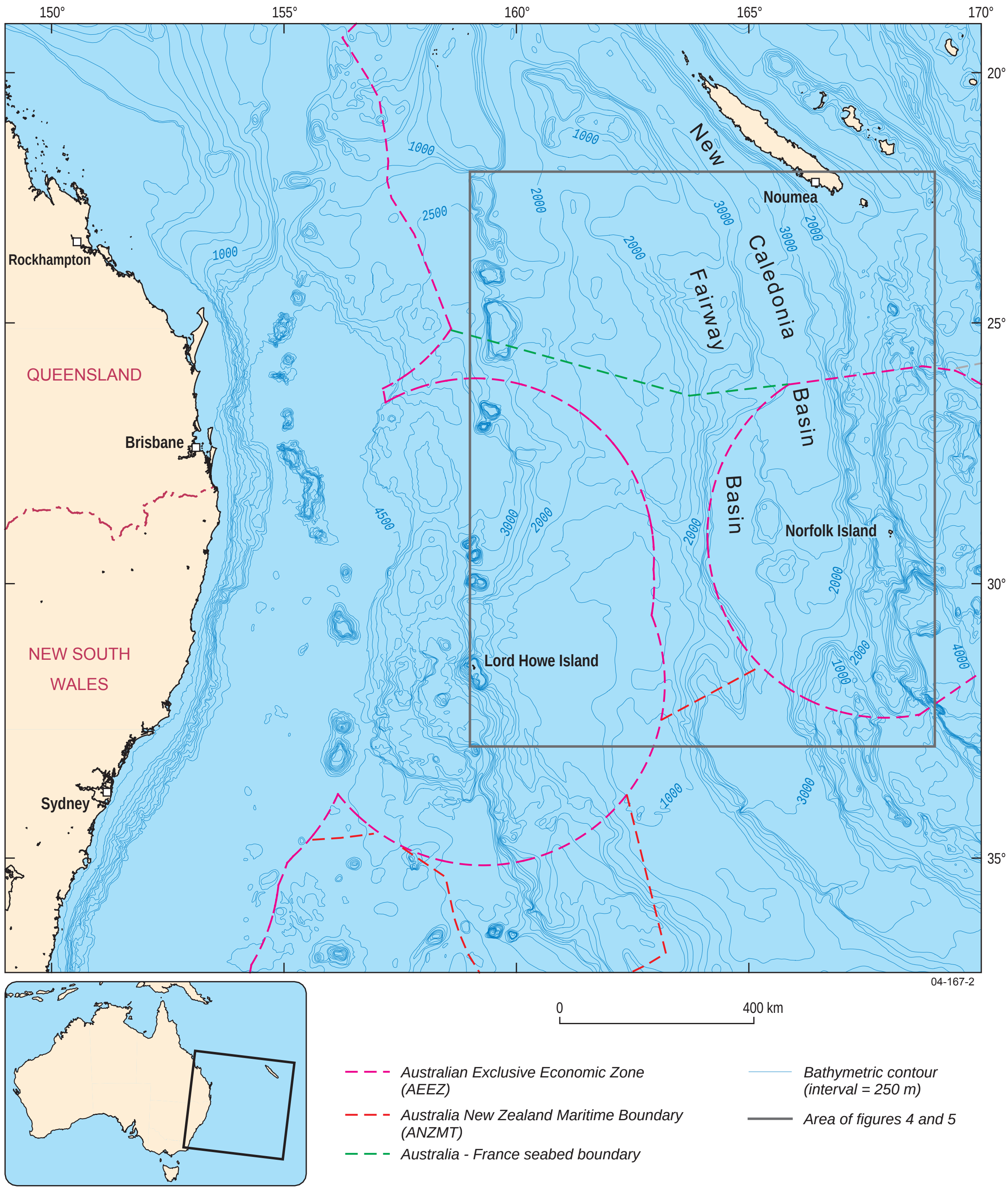

Figure 2. Regional setting of Fairway Basin region

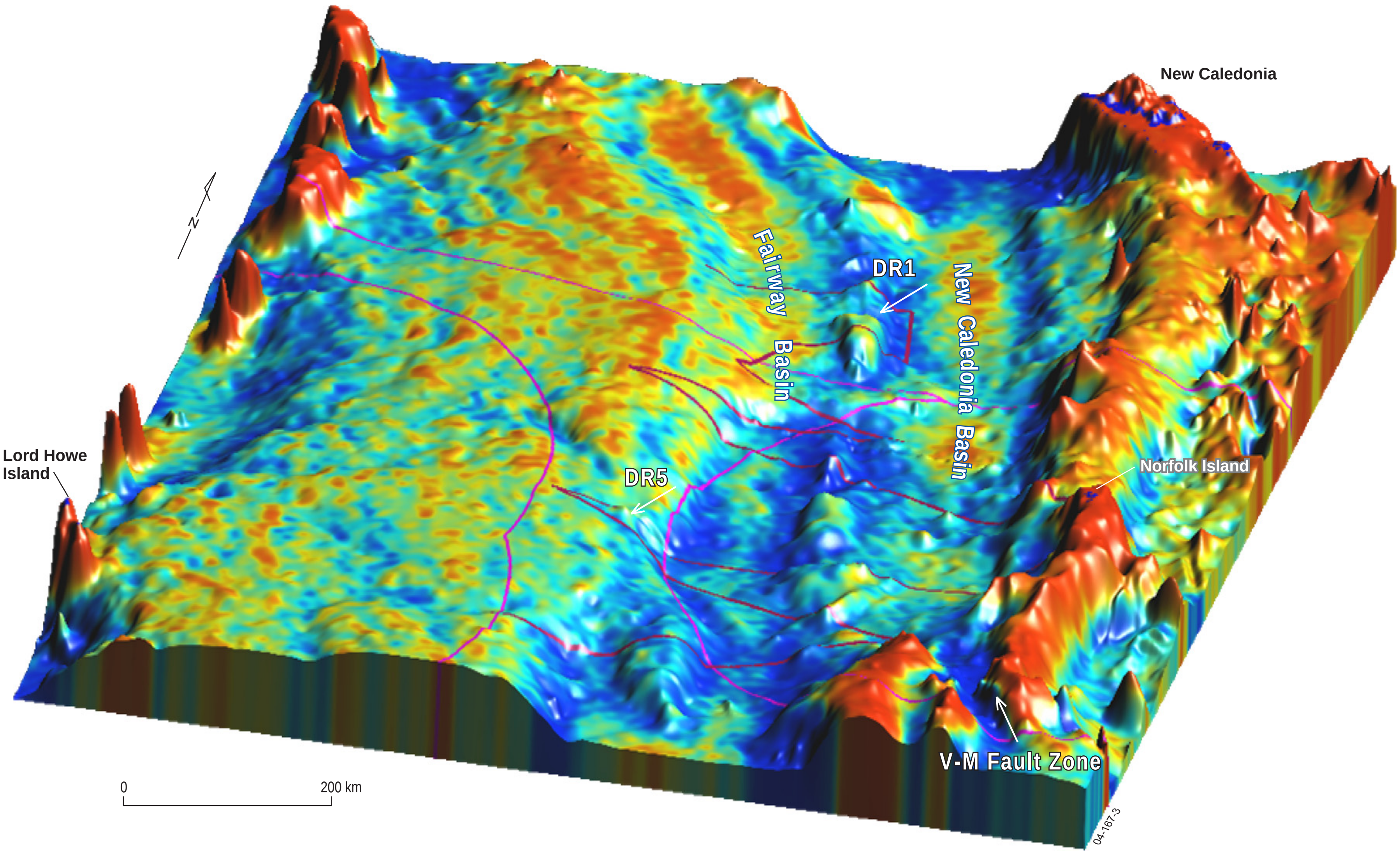

Figure 3. Satellite gravity draped on topography: Lord Howe chain to Norfolk Ridge

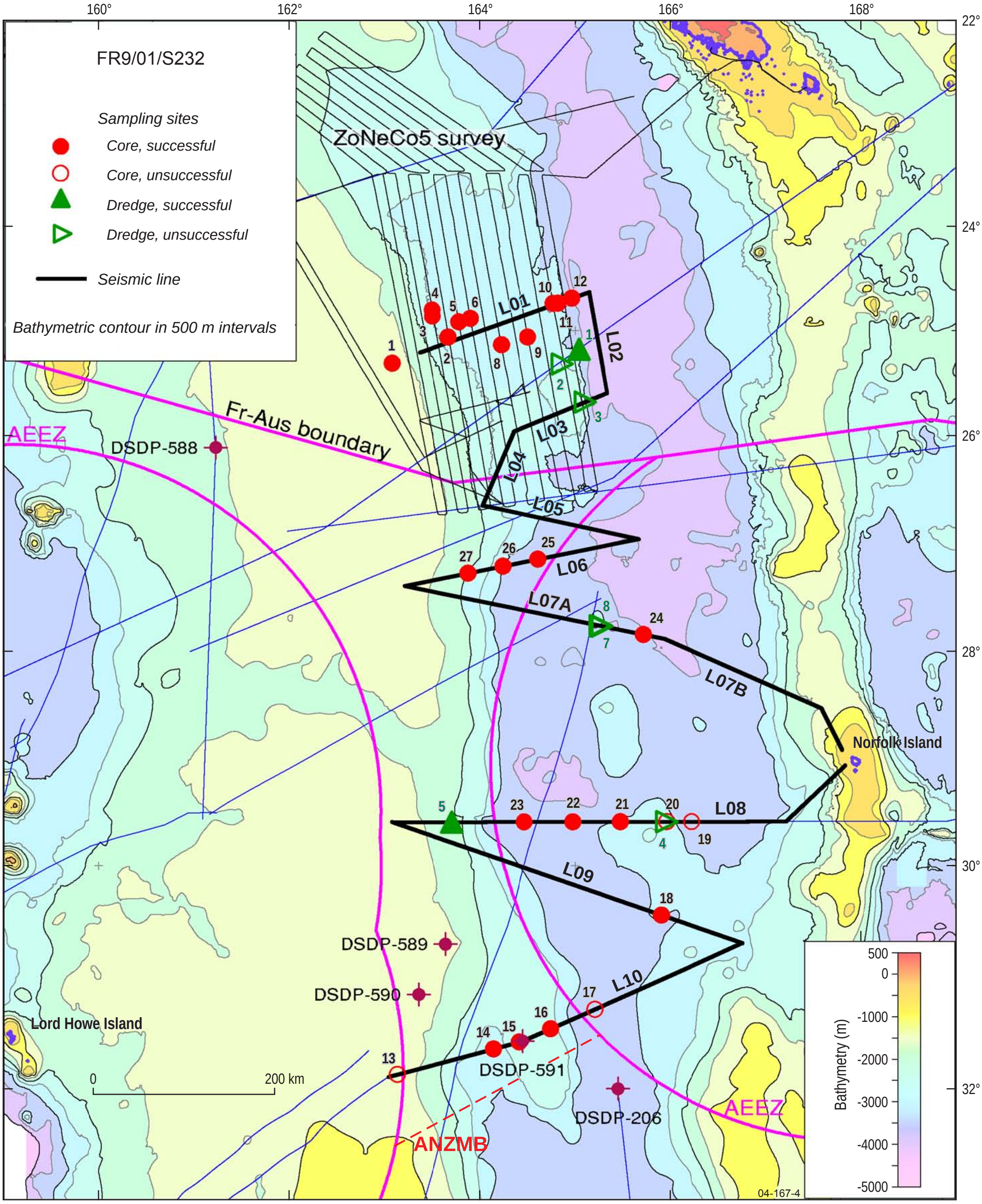

Figure 4. Bathymetric map showing *Franklin* cruise FR9/01 seismic tracks (solid lines) and geological sampling program in the region. Solid circles = successful cores; open circles = unsuccessful cores; solid triangles = successful dredges; open triangles = unsuccessful dredges.
Map also shows Deep Sea Drilling Project (DSDP) sites, Australian Exclusive Economic Zone (AEEZ) boundary and Australia New Zealand Maritime Boundary (ANZMB)

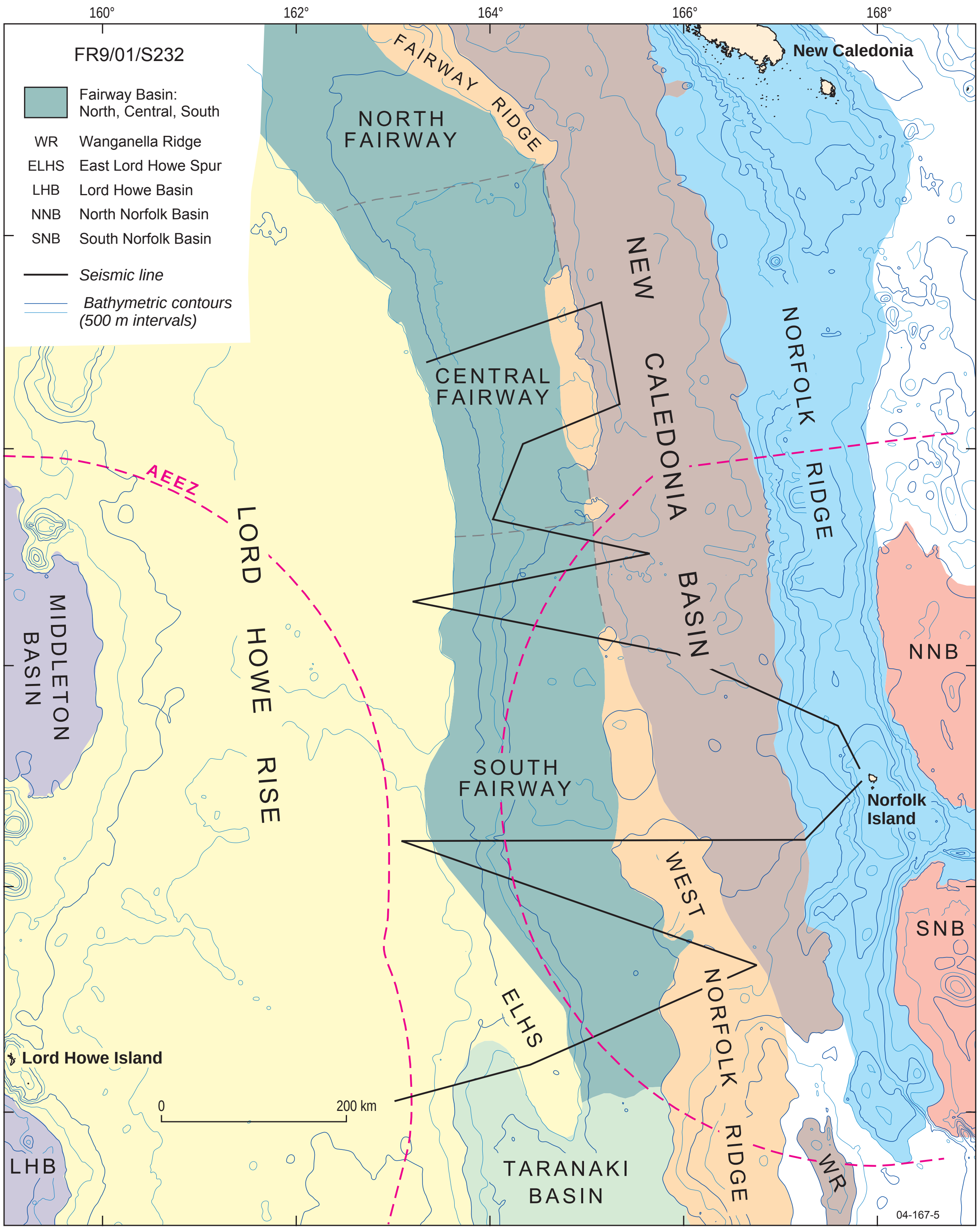

Figure 5. Structural elements with *Franklin* cruise FR9/01 seismic tracks

et al., 2002). However, during the rifting process the Fairway Basin formed as a transitional basin in the slope between the structurally high Lord Howe Rise and the structurally low New Caledonia Basin (Figure 3).

Other significant papers summarising the regional geology relevant to the eastern Lord Howe Rise, Fairway Basin and New Caledonia Basin include those on the results of the Deep Sea Drilling Project (DSDP) legs in the region (Burns, Andrews *et al*., 1973; Bradshaw *et al*., 1973; Kennett, Houtz et al., 1974; Kennett, Houtz, Andrews *et al*., 1974; McDougall and van der Linden, 1974; and Kennett and von der Borch, 1986), and on regional tectonics from seismic data (Dubois *et al*., 1974; Ravenne *et al*., 1977; Lafoy *et al*., 1994, 1998a, b; Bernardel *et al*., 1999; Lafoy *et al*., in prep.).

Recent geophysical investigations (Exon *et al*., 1998; Auzende *et al*., 2000a, b, c) have shown that much of the Fairway Basin (eastern Lord Howe Rise) and part of the New Caledonia Basin contain sediment diapirs, possible gas hydrate as represented by a bottom simulating reflector (BSR), and probably free gas (Dickens *et al*., 2001). All these features suggest that the two basins may have some petroleum prospects. The BSR occurs in Cainozoic chalks 500-600 m beneath the sea bed in water depths of 1500-3600 m (e.g. Exon *et al*., 1998), and is frequently associated with fields of diapirs that appear to be generated in Cretaceous sediments (e.g. Auzende *et al*., 2000c). Relevant general papers dealing with gas hydrates are by Dillon and Paull (1983), Kvenvolden and Cooper (1987), Kvenvolden (1993, 1995), Dickens and Quinby-Hunt (1997) and Dickens *et al*. (1997a, b). Recently, petroleum modelling of the northern part of the Fairway Basin has shown that both depth and thermal conditions are adequate for gas hydrates to be stable within the upper part (more than 500 m) of the sedimentary cover (Vially *et al*., 2003). Furthermore, the same study shows that within the deeper part of the northern, NW-SE trending New Caledonia Basin, the thickness of the Cretaceous sediments is sufficient to generate liquid and gaseous hydrocarbons.

Various papers have been written on the southern part of the Norfolk Ridge (e.g., Eade, 1988; Herzer *et al*., 1997, 1999). Uruski and Wood (1991) reviewed the New Zealand part of the New Caledonia Basin. As regards the Quaternary sediments in this region there are many papers: three important ones are those of Nees (1997), Hiramatsu and DeDeckker (1997), and Dickens *et al*. (2001).

DSDP drilled five sites in our area of interest (Figure 4), providing vital core information throughout the Cainozoic (Table 1). DSDP Leg 21 drilled Site 206 in deep water in the Taranaki Basin (Burns, Andrews *et al*., 1973): ~420 m of Miocene to Recent foram-bearing nannofossil ooze, and ~310 m of Paleocene to Upper Eocene nannofossil chalk. Foraminifera and siliceous microfossils occur throughout, with the siliceous content high in the Paleocene and Eocene. There is a major Late Eocene through Early Oligocene unconformity. One could expect a strong seismic reflector at the ooze-chalk boundary (~420 m), which corresponds roughly to the Oligocene-Miocene boundary, and at the Eocene-Oligocene unconformity (~610 m).

DSDP Leg 90 drilled four sites in our area of interest in shallower water on the Lord Howe Rise (Kennett, von der Borch *et al*., 1986). Site 589 drilled 97 m of Quaternary sediment and is not considered further here. Sites 588, 590 and 591 contain 250-450 m of foram-bearing Middle Miocene to Recent nannofossil ooze, and up to 220 m of Middle Eocene to Middle Miocene nannofossil chalk. There is a major Late Eocene through Early Oligocene unconformity at Site 588. One could expect a strong seismic reflector at the ooze-chalk boundary in the Middle Miocene.

Table 1. Representative DSDP drill sites nearby

Character	Site 588 * Lord Howe Rise	Site 590 * Lord Howe Rise	Site 591 * Lord Howe Rise	Site 206 ** Taranaki Basin
Location	26º06.7'S 161º13.6'E	31º10.02'S 163º21.51'E	31º35.06'S 164º26.92'E	32º00.75'S 165º27.15'E
Water depth	1533 m	1299 m	2131 m	3196 m
Pleistocene	20 m foram-bearing nannofossil ooze	35 m foram nannofossil ooze	50 m foram-bearing nannofossil ooze	105 m foram-bearing nannofossil ooze, with some radiolarians
Pliocene	95 m foram-bearing nannofossil ooze	160 m total: 65 m late Pliocene foram-bearing nannofossil ooze; 95 m early Pliocene nannofossil ooze	165 m total: 55 m late Pliocene foram-bearing nannofossil ooze; 110 m early Pliocene foram-bearing nannofossil ooze	82 m foram-bearing nannofossil ooze, with some radiolarians
Miocene	300 m total: 110 m late Miocene foram-bearing nannofossil ooze; 80 m middle Miocene calcareous ooze grading to nannofossil chalk; 110 m nannofossil chalk.	310 m total: 90 m late Miocene nannofossil ooze; 175 m middle to late Miocene foram-bearing nannofossil ooze; >45 m early Miocene recrystallised nannofossil chalk	290 m total proximal slope limestone: 75 m late Miocene foram-bearing nannofossil ooze; 155 m middle and late Miocene nannofossil chalk; 60 m early and middle Miocene recrystallised chalk	230 m foram-bearing nannofossil ooze with some clay, diatoms and radiolarians: 40 m late Miocene; 90 m middle Miocene; 100 m early Miocene
Oligocene	70 m late Oligocene nannofossil chalk			190 m middle to late Oligocene clayey foram-bearing nannofossil chalk, with diatoms and radiolarians
Paleocene to Eocene	>20 m middle Eocene foram-bearing nannofossil chalk, with chert, sponge spicules and diatoms			> 120 m total: 63 m middle to earliest late Eocene radiolarian-rich nannofossil chalk; 57 m early Paleocene to middle Eocene nannofossil chalk with radiolarians and chert
Total thickness	488 m	499 m	500 m	734 m

* Nelson (1986) **Burns, Andrews *et al*. (1973)

There are few direct seismic ties to boreholes in or near the Fairway Basin region. Various authors have used extrapolated borehole information and seismic stratigraphy to build up an interpretation of the strata revealed by seismic lines that cross the region. Typical such attempts are those of van de Beuque *et al*. (1998), Auzende *et al*. (2000c) and van de Beuque *et al*. (2003). In general, using high to moderate quality seismic lines, they separate out:

- Lower Cretaceous siliciclastic sediments resting on basement
- Upper Cretaceous and Paleocene siliciclastic sediments
- Eocene and Oligocene chalks
- Oligocene to Middle Miocene chalk
- Middle Miocene to Recent chalk and ooze

1.2. Scientific objectives

Recent geophysical investigations had shown that much of the Fairway Basin (eastern Lord Howe Rise) and some of the New Caledonia Basin in the Tasman Sea contain sediment diapirs, possible gas hydrate as represented by a bottom simulating reflector (BSR) 500-600 m beneath the sea bed, and probably free gas (Exon *et al*., 1998; Auzende *et al*., 2000a, b, c; Dickens *et al*., 2001). Water depths are largely 1500-3200 m. The RV *Franklin* was used to:

- continue seismic mapping of basin sequences, sediment diapirs and bottom simulating reflectors (BSR, suggesting gas hydrate layers) within the Australian and New Caledonian/French seabed jurisdictions;
- core to help determine the origin and composition of gas on the Lord Howe Rise, especially in any identified seafloor structures above sediment diapirs;
- ground-truth seismic data by sampling older outcropping sequences;
- and core to establish the composition, character and climate history of shallow sediment of Holocene and Pleistocene age.

2. SHIPBOARD ACTIVITIES

The area of activity, the geophysical profiles and the sampling stations are shown in Figure 4. The cruise was an overall success, although the coring did not recover any of the gas that is assumed to be related to the BSR. The methods employed were seismic profiling, gravity coring and dredging. We were blessed by good weather. The logistical results of the cruise are summarised in Table 2, and the seismic results are documented in Table 3. Almost all down time was due to problems with the hired diesel seismic compressor, and most of it was concentrated in the first six seismic lines (~945 km). Ship's speed was generally 8 knots, but was reduced at times to ensure good data quality in rough seas. In New Caledonian waters we acquired 480 km of seismic data in 3.5 days of profiling. In Australian waters we acquired 2315 km of seismic data in 8.5 days. The seismic profiles were processed to migration stage aboard ship. All samples were labelled with the prefix 232 for *Geoscience Australia Cruise 232*, rather than FR9/01, as they are to be stored in Canberra under the Geoscience Australia system.

Table 2. Data gathered on Cruise FR9/01

Data type	Results
Seismic profiles	2795 km of 24 channel (3 fold) data
Magnetic profiles	~2400 km of data (163 hours)
Bathymetric profiles	~7400 km of data (acquired throughout voyage)
Gravity cores	26 total: 22 successful, total 80 m, average 360 cm
Dredges	7 total: 2 successful

All but four of the 26 Quaternary gravity cores attempted were successful. The successful cores recovered foram-bearing nannofossil ooze and nannofossil ooze, in water depths of 1297-3517 m. Average recovery was 360 cm, and total recovery 80 m. Two of the four unsuccessful cores (two of which were also repeated) apparently failed to penetrate current-swept foram sand in shallower water (1200 m), or foram sand turbidites in deep water (3320 m). Such sands require the use of a piston corer. Another Quaternary core failed when the core catcher failed, and the final core failure was an attempt to recover basement rock.

The cores in their liners were cut to 1 m lengths, and split and described aboard ship. The working half was sampled for sediment and pore water analyses, while the archive half was logged and described. Colours were determined on wet sediment using a Munsell Soil Colour Chart. The cores were stored in a cool facility below deck.

Generally one shallow and one deep sample were taken from each core to investigate the molecular and isotopic composition of gas, using a procedure developed by Keith Kvenvolden (USGS, pers. comm.). A piece of half-core with diameter of 9.5 cm and length 10 cm (about 300 cm^3) was placed in a 500 cm^3 paint can with a septa, and covered with clean sea water until the can was full. Precisely 100 cc of water were removed with a syringe to get a known volume of headspace. One cm^3 of $HgCl_2$ was added to kill bacteria. Two needles were then placed into the septa and the headspace was purged with helium for several minutes at low pressure. The can was hammered shut, shaken to mix in the bactericide, and frozen upside down for transport back to Geoscience Australia. Sediment samples were canned within 30 minutes of splitting the core to reduce degassing at atmospheric pressure and room temperature, but the average delay in sampling after core recovery was an hour for shallow samples and two hours for deep samples.

One shallow and one deep sample also were taken from most cores to analyse for potential hydrocarbon biomarkers. About 150 cc of sediment were added to a 500 cc plastic bottle. The samples were then sealed and frozen, with no bactericide, for subsequent analysis by solvent extraction and gas chromatography-mass spectrometry.

Pore water samples (see also Appendix 1) were taken using a squeezing apparatus consisting of a nitrogen tank, a brass gas manifold, and a series of pressure chambers made of heavy plastic, each with a hole in the bottom covered with a wire mesh and filter. For each pore water sample, a furrow was cut into the centre of a split core with a clean knife. About 100 cm^3 of sediment were collected and packed into one of the pressure chambers. The chamber was sealed with a clamp. Nitrogen at pressure was passed through the manifold and into the sediment-filled chamber, squeezing pore water through the hole into a second filter and empty syringe. A nitrogen pressure of 1.9 bars typically produced about 7 to 10 ml of pore water, although some samples produced less than 5 ml. Pore waters were injected from the syringes into plastic vials, sealed, and stored in a refrigerator. Between three and seven pore water samples were taken from each core. For three pore waters, two sets of samples were taken. In addition, four aliquots of a seawater sample were collected, stored and shipped with the pore water samples. This seawater had an average $S = 34.6$, as determined by passing water through an environmental data logger that continuously measured conductivity and hence salinity.

The seven dredges attempted were far fewer than planned, because of time constraints and the fact that most possible hard rock targets were only marginally suitable. In fact, only two attempts succeeded, one in recovering volcaniclastic basement and the other Eocene chalk. Some samples were slabbed aboard ship. The samples were examined with a hand lens and described in some detail aboard ship, sampled and packed up. Sub-samples were set aside for palaeontology and thin sectioning.

2.1. Acknowledgements

We are very grateful to the Master, Ian Taylor, and his maritime crew for their wholehearted support and professional seamanship throughout the cruise, and especially to the engineers, Gordon Gore and Greg Pearce, for their wonderful support to Craig Wintle in overcoming numerous problems with the diesel compressor. The deck crew, led by bosun Malcolm McDougall, were helpful at all times. The excellent food kept spirits high. We thank the CSIRO Marine Division staff of Lindsay Pender and Steve Thomas for ensuring that all the necessary scientific support was provided. The Geoscience Australia technical group did an excellent job, and was led well by Jon Stratton; especial mention must be made of Craig Wintle in his ultimately successful struggles with the recalcitrant compressor. We thank Tony Stephenson and Barry Willcox of Geoscience Australia for reviewing this publication. We also thank Angie Jaensch for finalising the figures and Jim Mason for final Record production.

3. STRUCTURAL NOMENCLATURE

Modified nomenclature for this region is used here (Figure 5), in line with that of Lafoy *et al.* (in prep.). Most features run north-south.

- *Lord Howe Rise* for the broad basement ridge in water generally shallower than 1500 m, in the west of the area.
- *Norfolk Ridge* for the relatively narrow basement ridge that includes New Caledonia and Norfolk Island, in the east of the area.
- *New Caledonia Basin* for the sedimentary and morphological basin in water generally deeper than 3000 m, west of the Norfolk Ridge.
- *Fairway Ridge* for the northwest-trending basement ridge west of the northern part of the New Caledonia Basin and north of ~23°30'S.
- *Northern West Norfolk Ridge* for the intermittent basement ridge west of the central part of the New Caledonia Basin from 23°30'S to 26°30'S.
- *West Norfolk Ridge* for the basement ridge west of the southern part of the New Caledonia Basin from 26°30'S to 31°S.
- *Fairway Basin* for the sedimentary basin on the eastern flank of the Lord Howe Rise, generally in water depths of 1500-3000 m, and bounded to the east by the Fairway Ridge, the intermittent northern West Norfolk Ridge, and the West Norfolk Ridge proper.
- *North Fairway Basin* for the northwest-trending part of the basin, north of 23°30'S and lying between the Fairway Ridge and the Lord Howe Rise.
- *Central Fairway Basin* for the shallower part of the north-south trending Fairway Basin between the Lord Howe Rise and the intermittent northern West Norfolk Ridge, which lies north of 26°40'S and is generally in water less than 3000 m deep.
- *South Fairway Basin* for the deeper part of the sedimentary basin between the Lord Howe Rise and the intermittent northern West Norfolk Ridge and the West Norfolk Ridge proper. To the south it is separated from the Taranaki Basin by the generally high area between the East Lord Howe Rise Spur and the West Norfolk Ridge at ~31°30'S.
- *East Lord Howe Spur* for the bathymetric ridge extending ESE from the Lord Howe Rise through DSDP Site 591.

4. SEISMIC PROFILES

4.1. Seismic profiles in New Caledonian jurisdiction

The seismic survey started in the north (~25°10'S) and ended in the south (~26°40'S). The results are summarised in Table 3. The seismic survey in New Caledonian waters was plagued by problems with the hired Charge-Air DC330/2000 diesel compressor. Acquiring the 480 km of data (Figure 4) took nearly three days, as compared to the planned one day, mainly because of compressor breakdowns, but also partly because the optimal towing speed proved to be 8 rather than 9 knots.

Table 3. Seismic line statistics

Line	Start WP (lat/long)		End WP (lat/long)		Intermediate WP(s)	Length (km)
FB-01	25 12.5S	163 22.1E	24 35.8S	165 09.0E		205
FB-02	24 35.7S	165 08.3E	25 35.6S	165 20.1E		110
FB-03	25 35.6S	165 20.1E	25 57.6S	164 21.0E		107
FB-04	25 57.5S	164 21.2E	26 39.6S	164 01.5E		95
FB-05	26 39.5S	164 01.6E	26 58.4S	165 39.9E		187
FB-06	26 58.4S	165 39.9E	27 24.9S	163 12.4E		242
FB-07A	27 24.8S	163 12.7E	27 54.4S	165 56.2E		269
FB-07B	27 54.4S	165 56.2E	28 56.1S	167 48.1E		291
FB-08A	29 04.7S	167 49.9E	29 35.6S	167 12.8E		80
FB-08B	29 35.6S	167 12.8E	29 36.0S	163 05.0E		460
FB-09	29 36.0S	163 05.0E	30 42.0S	166 45.0E		370
FB-10	30 42.0S	166 45.0E	31 35.1S	164 26.9E	DSDP 591B	241
FB-11	31 35.1S	164 26.9E	31 54.3S	163 02.7E		138

Total kilometres = 2795
New Caledonian kilometres = 480
Australian kilometres = 2315
DSDP 591B = 31°35.06S, 164°26.92E

Line 1, from west to east and 205 km long (Figure 6), generally shows 2 seconds of penetration. It starts in 1800 m water depth on the Lord Howe Rise (LHR), passes through the Fairway Basin (FB), and finishes in 3500 m water depth in the New Caledonia Basin (NCB). It is characterised by very strong reflectors in the mid-Cainozoic that are often unconformably overlain by the younger sequence, diapiric structures and large scale folding, volcanics at depth, and some evidence of BSRs and possible flat spots. The eastern margin of the FB is marked by a high basement block with as little as 50 metres of overlying younger sediments. The older sedimentary section onlaps basement and shows some broad gentle folding. The section thickens off the basement high into the New Caledonia Basin. Cores 1-12 were taken on or near this line (Figure 4), and they proved to be either Early-Middle Pleistocene or Late Pleistocene at their base (Table 4).

Line 2, 110 km long and from north to south in the New Caledonia Basin (Figure 7), shows a very flat sea floor at 3500 m. A basement high in the north is 0.8 seconds below seabed. Basement drops southward about 1 second along an assumed fault zone, and there an older sequence onlaps the high. Further south, basement gradually shallows to 0.5 seconds below sea bed, toward the culmination of a large basement high to the west.

Line 3, 107 km long, rose from east to west out of the New Caledonian Basin up into the Central Fairway Basin (Figure 8), the sea bed shallowing from 3500 m to 2600 m deep. In the short section across the NCB there is initially about 1 second of section above basement. The older section thins westward to the foot of the northern West Norfolk Ridge but the transparent younger section maintains its 0.4 second thickness. The scarp of the northern West Norfolk Ridge is lightly sedimented and ~600 m high, and is underlain by a local basement high. Beyond the first high, folded sediments are unconformably overlain by a transparent younger section that is ~0.4 second thick across the northern West Norfolk Ridge and FB. A second basement high is possibly planated, and is immediately overlain by a thin bedded section, which thickens westward into the FB where the total section above basement (?volcanic) is 1.5 seconds thick. At the western end of the line the total section is at least 2 seconds thick. Some folding and diapirs occur.

Line 4, 95 km long, runs from north to south in the southernmost Central Fairway Basin (Figure 9), shallowing from 2600 m to 2100 m. Total sediment thickness reaches 2.5 seconds in places, with a transparent sequence 0.4 seconds thick overlying a bedded sequence that contains numerous folded and diapiric structures. The largest of these structures rises ~1 second at the southern end of the line, where even the sea bed is irregular. The southernmost third of this line is in Australian jurisdiction.

The main results of the survey carried out within New Caledonia's EEZ have been summarized by Lafoy et al. (2001, in prep.). The northern part of the Fairway Basin trends NW-SE and the central part trends NNW-SSE, separated at 23°30S. The basin is characterized by an average sedimentary fill of 3 km, plus a BSR and associated diapir-like features (sedimentary and volcanic intrusions) within the Cretaceous deposits.

4.2. Seismic profiles in Australian jurisdiction

This seismic survey also started in the north (~26°40'S) and ended in the south (~31°50'S). The results are summarised in Table 3. The seismic survey in Australian waters was also plagued by problems with the hired diesel compressor.

Line 5, 187 km long, runs ESE from the southernmost Central Fairway Basin to the easternmost part of the South Fairway Basin, and across the northern West Norfolk Ridge (Figure 10). The water depth increases from 2100 m to 3600 m. The maximum sediment thickness is ~2 seconds, with an upper transparent section 0.4 seconds thick and a lower bedded section containing folds and diapirs. The northern West Norfolk Ridge has a surface expression of 150 m, and basement below it comes to within ~0.5 seconds of the sea bed. Sea bed drops 150 m into the New Caledonia Basin to a flat 3600 m, but the section remains similar there except that flows or sills disguise basement at the eastern end of the line.

Line 6, 242 km long, runs WSW from the westernmost New Caledonia Basin across the South Fairway Basin to the edge of the Lord Howe Rise (Figure 11). The water depth decreases from 3600 m to 1300 m. In the east the sedimentary section is 1-1.5 seconds thick. The upper transparent section is 0.4 seconds thick. The entire section is disturbed along the northern West Norfolk Ridge, with folding and diapirism apparent throughout, and with surface relief in the transparent material of as much as 200 m. In the deepest part of the South Fairway Basin the section is almost 2 seconds thick and contains two large diapirs, one of which has surface expression. On the slope up to the Lord Howe Rise (see also Figure 12) the surface and deeper sections undulate and small (and occasionally large) diapirs are present. The thickness of the section decreases up the slope from 2 seconds to 1 second. On the easternmost Lord Howe Rise the basement comes to within 0.3 seconds of the sea bed and is unconformably overlain by transparent sediments. The unconformity appears to be of subaerial origin and is unconformbly underlain by a wedge of sediments up to 0.8 seconds thick in a local half graben. Cores GC25-27 in the South Fairway Basin (Figures 4 and 11) were either Early to Middle Pleistocene or Late Pleistocene at their base (Table 5).

Line 7 runs 560 km ESE from the Lord Howe Rise to the Norfolk Ridge (Figures 13 and 15). On the LHR it is very near Line 6 and shows similar features (Figures 13 and 14), indicating north-south structural trends. The section thickens down-slope from 1200 m water depth, into the axis of the South Fairway Basin 3300 m deep. There the section is two seconds thick, folded and cut by diapirs, some of which affect the sea bed surface. Here the northern West Norfolk Ridge consists of two basement highs, the larger of which dams the Fairway Basin, rising 600 m above the Fairway Basin and 1000 m above the New Caledonia Basin. Basement is exposed on the eastern flank of the larger, western high, and the transparent sequence is up to 0.4 seconds thick.

In the New Caledonia Basin (Figure 15), the Line 7 section is ~1.5 seconds thick, with its base characterised by either flat reflective basement or by highs of diffuse material. The sedimentary section is largely flat-lying, with some areas of folding and diapirism. The upper sequence, up to 0.5 second thick, is transparent on both sides of the basin, but well-bedded in the basin centre. The sea floor is flat-lying at 3600 m in the centre of the basin, above the well-bedded sequence. As the sea floor rises toward the Norfolk Ridge, basement is not apparent, probably because of volcanic strata in the mid-Cainozoic. The young sediments are cut, probably by canyons, with perhaps some slumping of the upper sequence. Near the Norfolk Ridge is a large free-standing volcano or guyot rising to within 900 m of the surface (Figure 16). Younger sediments fill its caldera, which is at least 17 km across. This volcano is part of a north-south chain apparent in satellite gravity data. Small satellite cones east of the main volcano give way to a sedimentary section ~1.2 seconds thick. This section in turn gives way, in 500 m water depth, to the hard volcanic outcrop of the pedestal of Norfolk Island. The pedestal is planated at about 75 m below sea level. Core GC 24 in the New Caledonia Basin (Figures 4 and 15) was Late Pleistocene at its base (Table 5).

Line 8 is 550 km long, and extends westward from the Norfolk Ridge to the eastern flank of Lord Howe Rise (Figures 17 and 18). West of the planated pedestal, at about 700 m water depth, a sedimentary section at least 0.5 second thick thickens westward into the New Caledonia Basin. The upper, flat-lying sedimentary sequence is up to 1.6 seconds thick and overlies large bulges of weakly reflective material. Basement is not readily apparent. The flat-lying sequence consists of a lower, largely transparent part, and an upper part unconformably overlying the lower. As on Line 7, the upper sequence is more transparent on the margins, and is well-bedded in the flat central basin where the water depth is 3200 m. On the eastern side of the basin, the generally transparent sequence contains some volcanics, perhaps reworked as contourites, and is canyoned and slumped. On the western side of the basin the transparent sequence is more disturbed than the synchronous well-bedded material further east.

On Line 8 (Figures 17 and 18), the New Caledonia Basin is terminated westward by a basement ridge, the northern West Norfolk Ridge, which outcrops and rises to within 2400 m of sea level. This ridge towers above a broad rise extending westward for 90 km and falling slowly to 3000 m below sea level. The rise consists of two sequences, cut by another high of acoustic basement in its midst. The lower sequence is strongly reflective, folded and faulted, with a maximum revealed thickness of 0.5 seconds. The upper, also deformed, sequence is generally transparent and ~0.6 seconds thick. Seafloor above it is irregular. The lower folded sequence drops away westward beneath the South Fairway Basin to at least 1.7 seconds below the sea bed, which is flat-lying and 3400 m below sea level. In the basin, flat-lying sediments are only weakly reflective at depth, but the top 0.4 seconds of section is strongly reflective. Cores GC 21-23 (Figures 4 and 18) were Late Pleistocene at their base (Table 5). A volcaniclastic edifice in the westernmost South Fairway Basin (Figure 19), which is onlapped by the transparent sequence, contains calcareous microfossils in

Dredge 5 that are as old as Late Middle Miocene (Appendix 8). This suggests that the transparent pelagic carbonates are Middle Miocene and younger in age.

Line 9 runs 370 km ESE from the eastern flank of the Lord Howe Rise in water 1300 m deep to the southern end of the New Caledonia Basin in water 3000 m deep (Figures 20 and 22). On the rise at the western end of the line, Cretaceous sediments are planated and lie 0.5 seconds below sea bed (bsb), with basement at least 1.5 seconds bsb (Figure 21). Basement deepens rapidly to 2 seconds bsb for over 50 km and forms a basin, before rising to 1.1 seconds bsb in a large marginal block on the easternmost rise. In the basin 1 second of transparent section lies between the basement blocks. About 0.5 seconds of younger well-bedded section overlaps onto the blocks and is overlain by 0.5 seconds of transparent sequence. Two diapirs are apparent. The three sequences thicken down the slope into the Fairway Basin, where they reach 1.7 seconds thick. In the central flat part of the basin in water ~3400 m deep, the two lower sequences give way to one transparent sequence, and the upper sequence becomes well-bedded, presumably by the addition of turbidites. Several large diapirs are present, including one that appears to have eroded away the underside of the upper well-bedded sequence. A basement high to the east, in the northern extension of the West Norfolk Ridge, rises 400 m above the Fairway Basin and the New Caledonia Basin. It is planated and capped by 200 m of eroded transparent sequence. The New Caledonia Basin is about 3000 m deep. The sedimentary sequence is up to 1.6 seconds thick and fairly transparent. It is cut by large diapirs, some of which bow the sea bed upward. Core GC 18 on the West Norfolk Ridge (Figures 4 and 22) is Late Pleistocene at its base.

Line 10 runs 241 km WSW from the southernmost New Caledonia Basin to DSDP Site 591, where latest Early Miocene chalk is at total depth of 500 m below sea floor (Figure 23). The small part of the New Caledonia Basin that was surveyed is flat, in water ~2900 m deep, and underlain by at least 1.4 seconds of largely transparent section above faulted basement. The broad northern extension of the West Norfolk Ridge is 100 km across and in water ~2700 m deep. An irregular volcanic surface lies 0.6-1.3 seconds below the sea bed. Most of the overlying sequence is transparent, but the upper 0.3 seconds contains some bedding in a broad depression, and another bedded sequence 0.2 seconds thick lies about 0.7 seconds deep. The western side of the ridge drops 600 m down into the Fairway Basin, which is about ~3300 m deep and 75 km wide (Figure 23). The sedimentary section is up to 1.6 seconds thick and largely transparent. An upper well-bedded section thickens into the basin from 0.1 to 0.3 second, and the failure of GC17 suggests that it probably contains Quaternary sand turbidites. The broad East Lord Howe Spur (new name) extends SSE from the Fairway Basin, and here it is 75 km wide and ~2100 m deep. Basement lies 1-1.6 seconds below sea bed (Figure 24). The upper section is transparent and 0.5 second thick; it is underlain by a well-bedded section 0.2-0.3 second thick that may be volcanogenic. A BSR occurs 0.6 seconds below the sea bed and there are several small diapiric structures. DSDP Site 591 lies at the western end of the line and the western side of the ridge, where the BSR is no longer apparent.

Line 11 runs 138 km WSW, from ODP Site 591 on the western side of the SSE-trending East Lord Howe Spur up onto the Lord Howe Rise (Figure 25). Core GC15, Late Pleistocene at its base, was taken above a deep diapir a couple of kilometres from DSDP Site 591. In Site 591, calcareous ooze gives way to foraminifera-bearing nannofossil chalk at 290 m below sea floor, and it terminates in the late Early Miocene 500 m below sea floor. The base of Site 591 is shortly above the base of the transparent sediment, suggesting that the calcareous ooze and chalk are all Early Miocene or younger in age.

A fault-bounded graben, 30 km wide and ~2700 m deep, trends NNW and separates the East Lord Howe Spur from the Fairway Basin (Figure 25). It contains up to 1.8 seconds of moderately bedded and generally flat-lying sedimentary section, and we regard it to be the northernmost part of the Taranaki Basin. A deep diapir is overlain by a surface mound and a shallow flat spot, and that location was cored by GC14, which contains Late Pleistocene microfossils at its base. West of the graben, the Fairway Basin extends about 45 km upslope toward the Lord Howe Rise. Basement is visible only in places, and is up to 2.2 seconds deep. The sedimentary section is largely transparent, with a bedded section 0-6-0.8 second deep. At least one diapir is visible at depth. Basement is upthrown 0.5 second at ~1650 m water depth to 1.2 seconds below sea bed, where the Lord Howe Rise begins 50 km from the end of the line. It rises steadily westward to 0.5 seconds below sea bed in water ~1350 m deep at the end of the line, the shallower part being planated, presumably by wave action during gradual subsidence. The older sequences onlap the rising basement westward, with only the upper sequence (probably Miocene and younger) overlying planated basement. The lower part of this sequence is well-bedded and the upper part transparent. Near the end of the line, core GC13 (Figure 4) contained only a little foraminiferal sand.

5. SEDIMENTARY BASINS

Adding DSDP and our own information to the regional seismic interpretations of van de Beuque *et al*. (1998), Auzende *et al*. (2000c) and van de Beuque *et al*. (2003), we suggest that the following sequences are probably present:

- Lower Cretaceous siliciclastic sediments resting on basement in places
- Upper Cretaceous siliciclastic sediments commonly resting on basement
- Paleocene and Eocene chalks and radiolarites with chert
- Oligocene to Middle Miocene chalk
- Middle Miocene to Recent ooze and volcaniclastic turbidites

5.1. Central Fairway Basin

The north-south trending Central Fairway Basin (Figures 1, 4, 5, 6, 8 and 9) lies between the Lord Howe Rise and the northern extension of the West Norfolk Ridge, from 23°30’S to 26°40’S. It is about 400 km long and 150 km wide, and is generally in water shallower than 3000 m. The Fairway Ridge and West Norfolk Ridge probably formed by compressional uplift in the Late Eocene, and the contiguous North and Central Fairway Basins were separated at that time from the New Caledonia Basin (e.g. Lafoy et al., 1994). These two parts of the basin, with their different trends, had been subject to different regional tectonic forces.

The sedimentary section is up to 2000 m thick and is probably entirely Cainozoic. Diapiric structures, possibly in mud (Lines 1 and 4: Figures 6 and 9), and large scale folding are common, and there is evidence of BSRs and possible flat spots. The older sedimentary section (Figure 6) onlaps basement on both sides of the basin, shows some broad gentle compressional folding, and is intruded in places. It is ~500 m thick and probably consists of Upper Cretaceous mudstone and sandstone. An overlying, less folded interbedded sequence ~750 m thick, on the evidence of nearby Dredge 1 (location in Figure 4) includes pelagic Eocene radiolarites, chalk and chert. We assume the sequence to span the Palaeogene. Very strong reflectors within this sequence are probably turbidites, and some of these turbidites were probably derived from erosion of the Lord Howe Rise and Fairway Ridge during and after Eocene compression and uplift. The Palaeogene sequence is unconformably overlain (Oligocene unconformity) by a younger largely transparent sequence ~600 m thick, that is assumed to consist of Miocene and younger oozes and chalks that were deposited as pelagic rain.

5.2. South Fairway Basin

The north-south trending South Fairway Basin (Figures 1, 4, 5, 10-14, 18-24) is the deeper water part of the Fairway Basin. It lies between the Lord Howe Rise and the northern West Norfolk Ridge

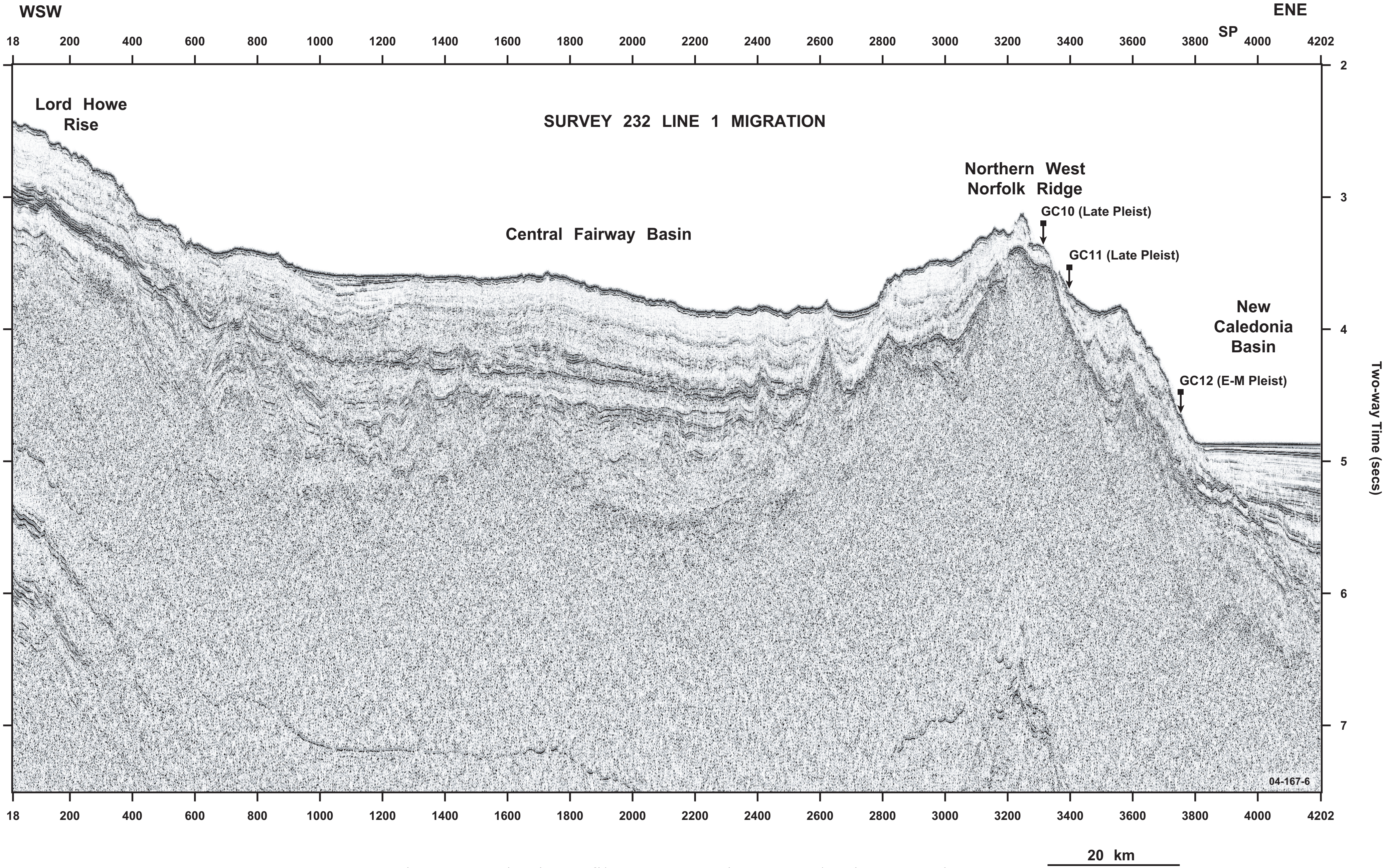

Figure 6. Seismic profile 232-1 crossing Central Fairway Basin

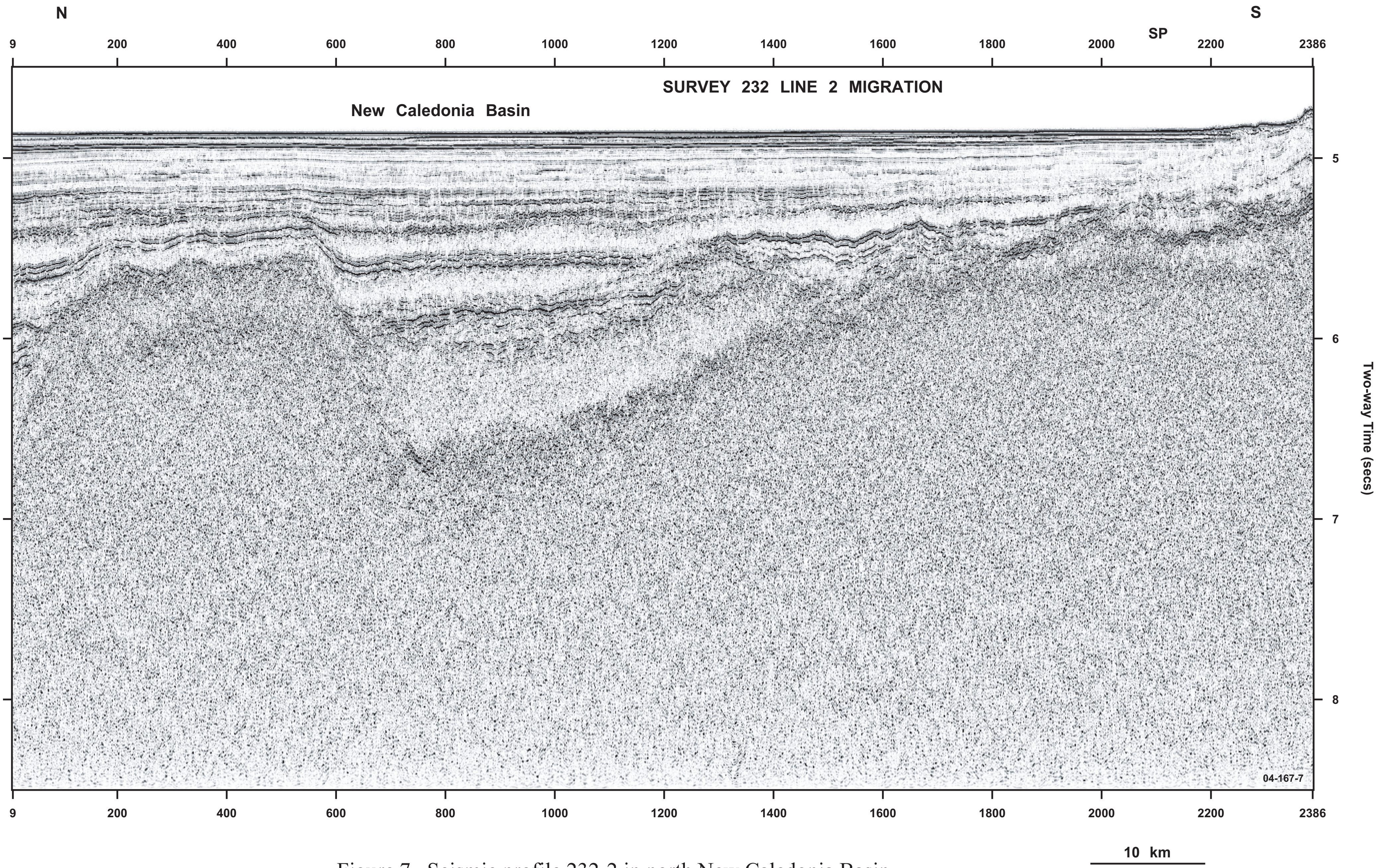

Figure 7. Seismic profile 232-2 in north New Caledonia Basin

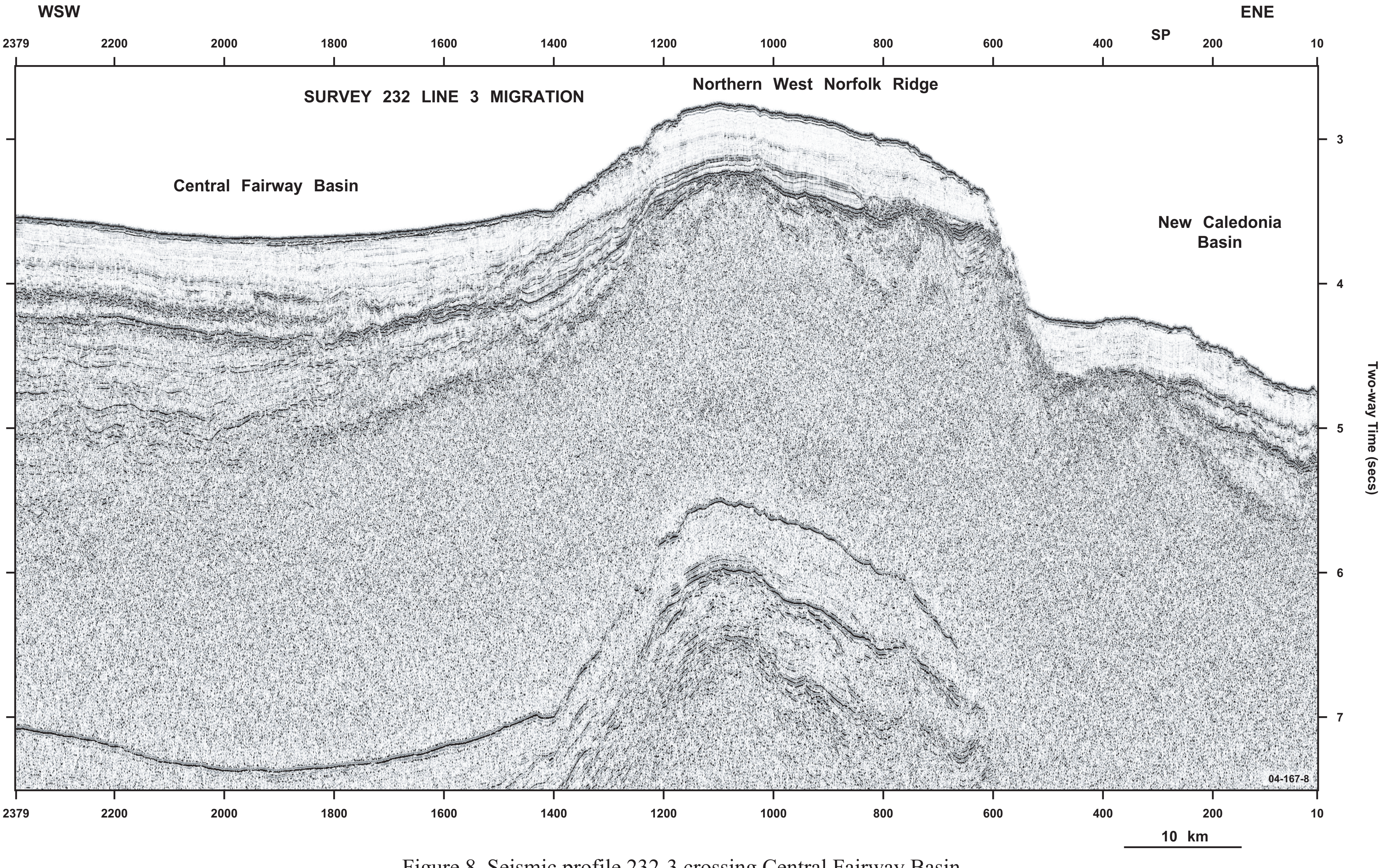

Figure 8. Seismic profile 232-3 crossing Central Fairway Basin

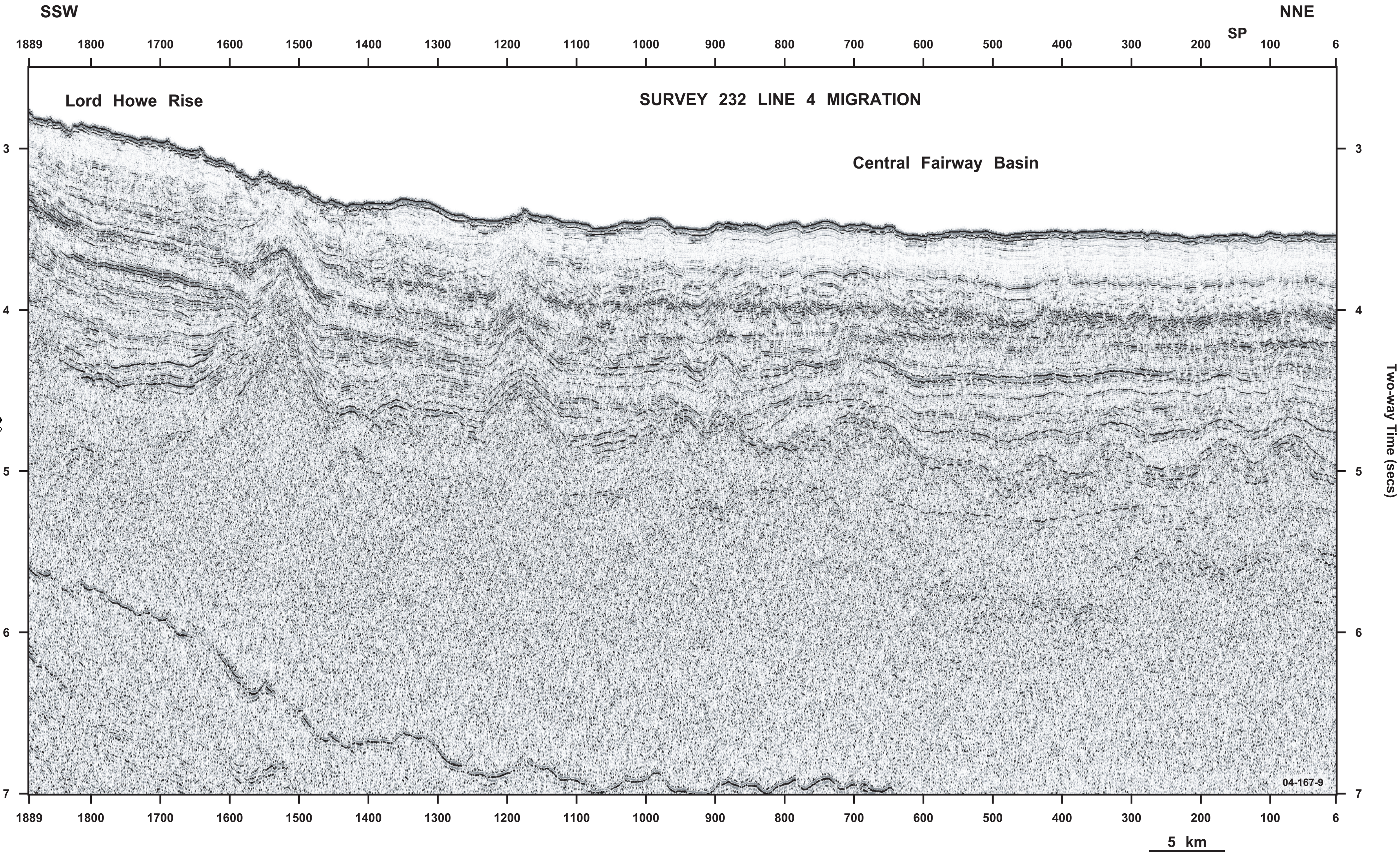

Figure 9. Seismic profile 232-4 in Central Fairway Basin

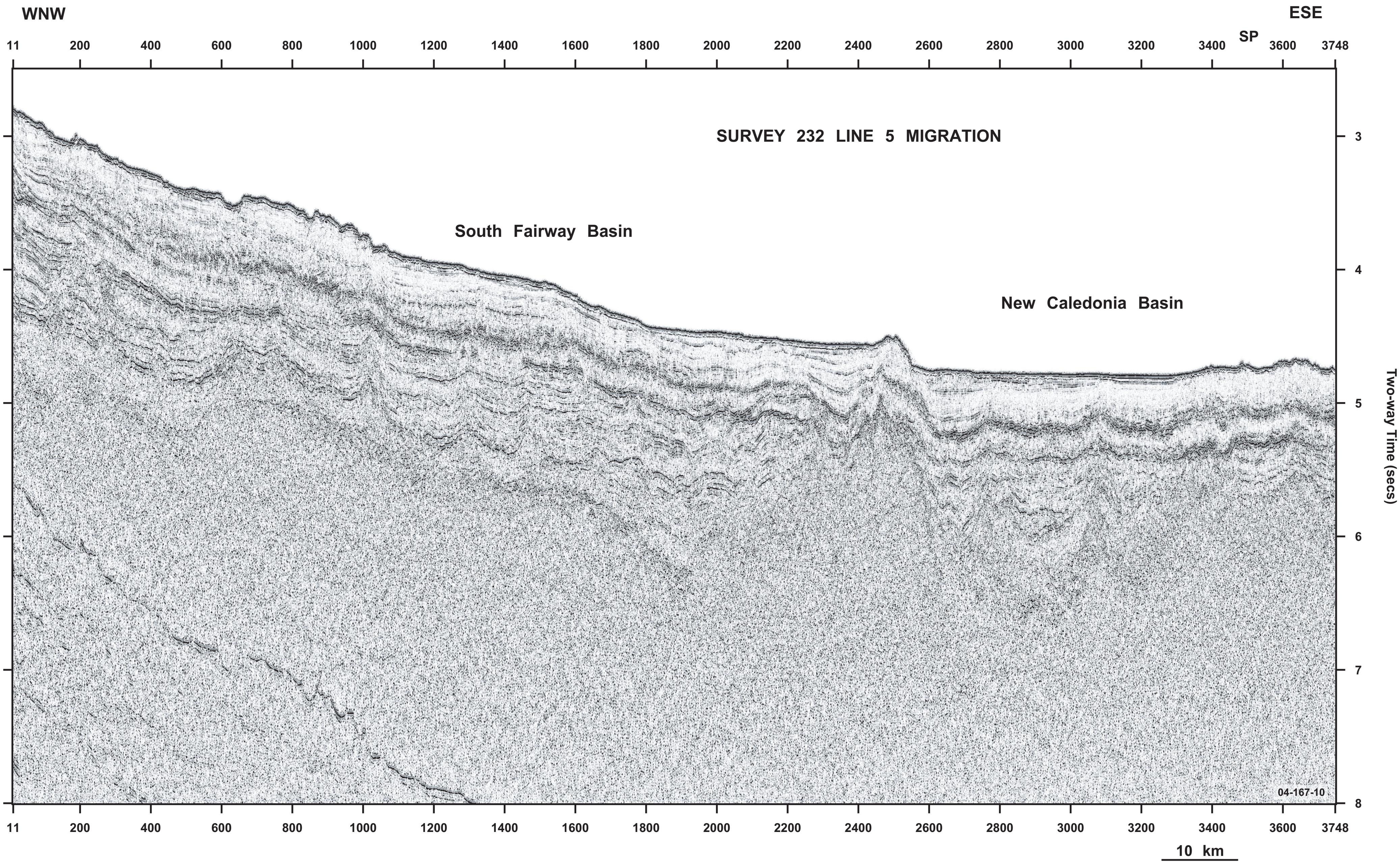

Figure 10. Seismic profile 232-5 crossing South Fairway Basin

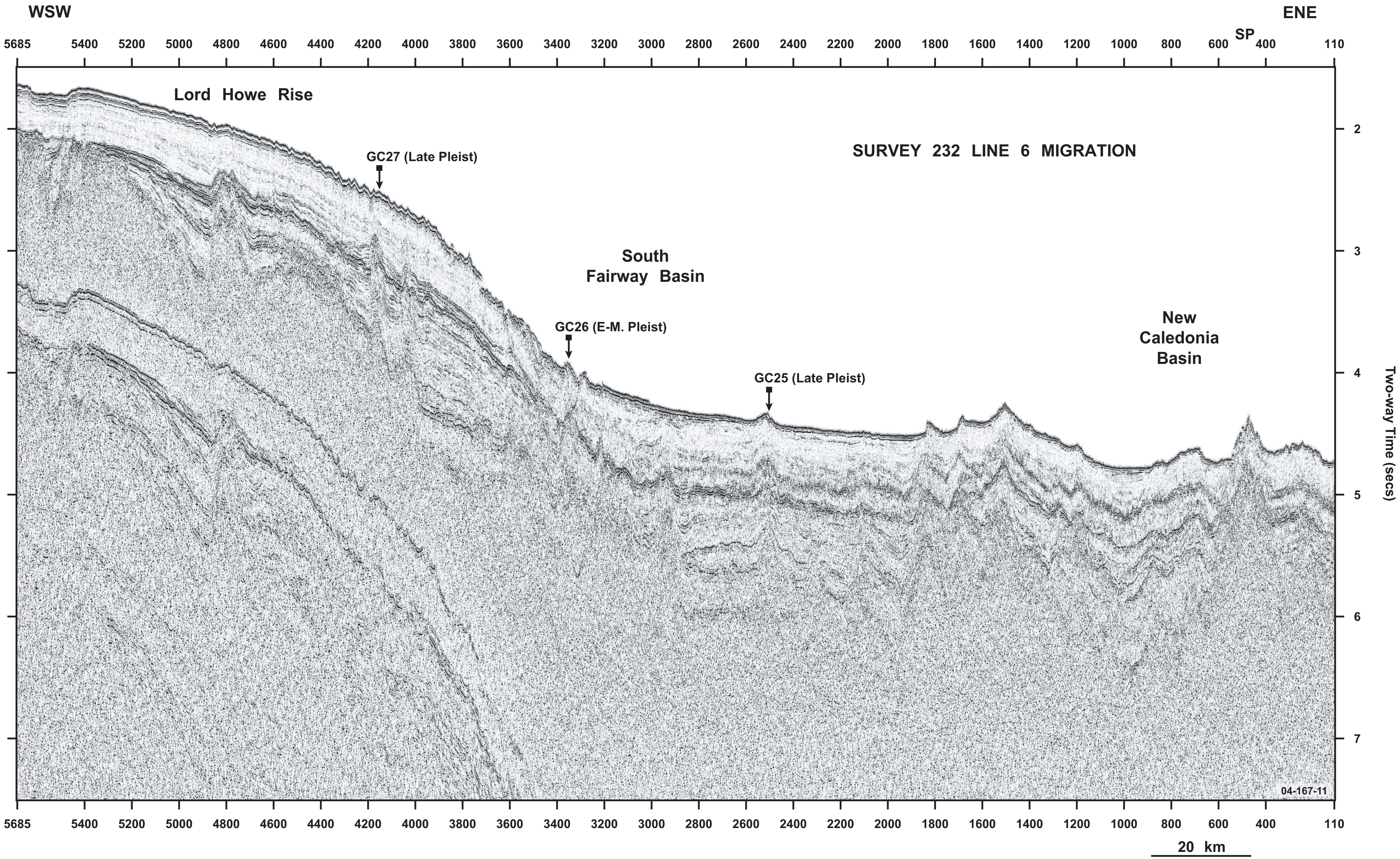

Figure 11. Seismic profile 232-6 crossing South Fairway Basin

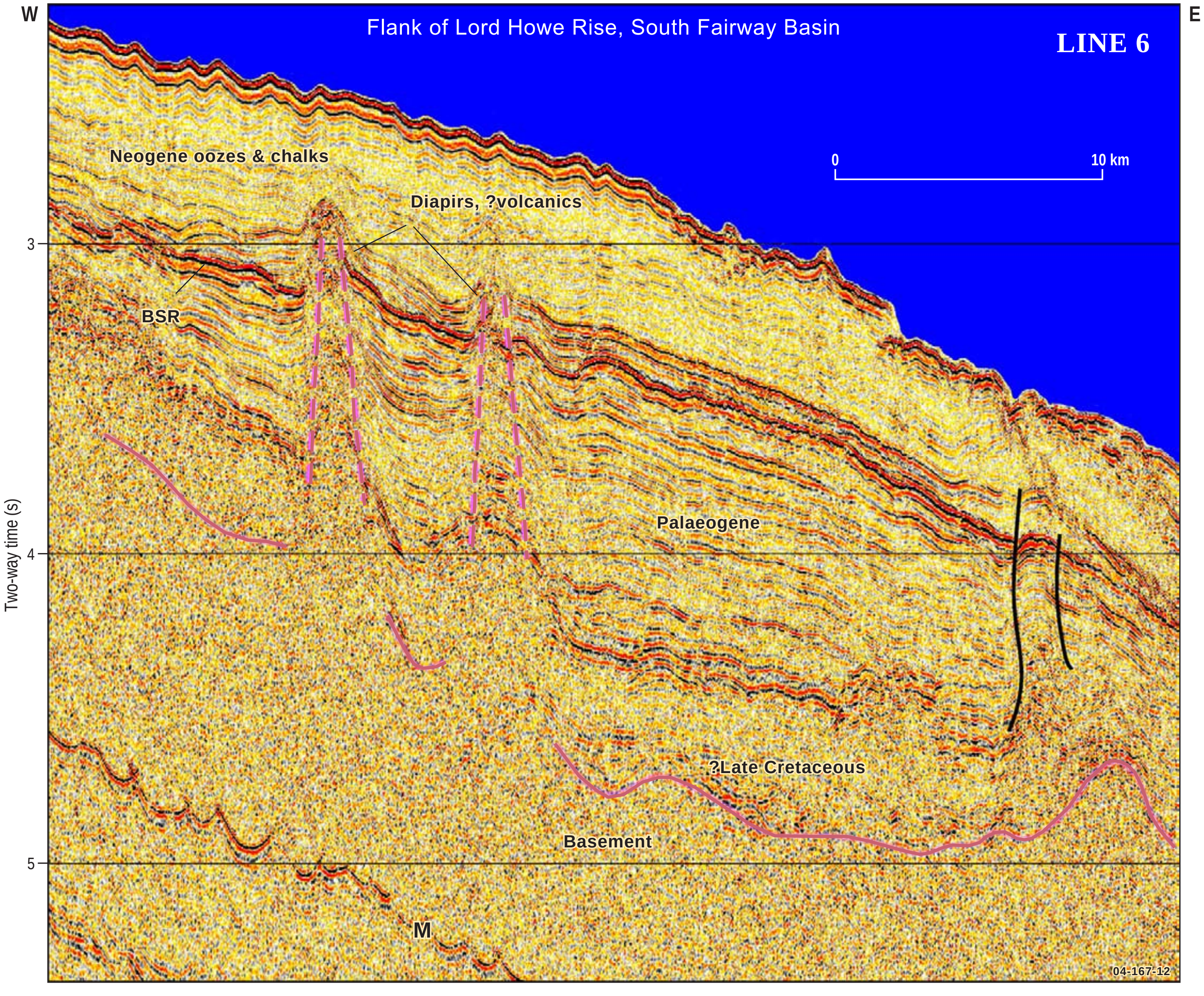

Figure 12. Detail of profile 232-6 on flank of Lord Howe Rise

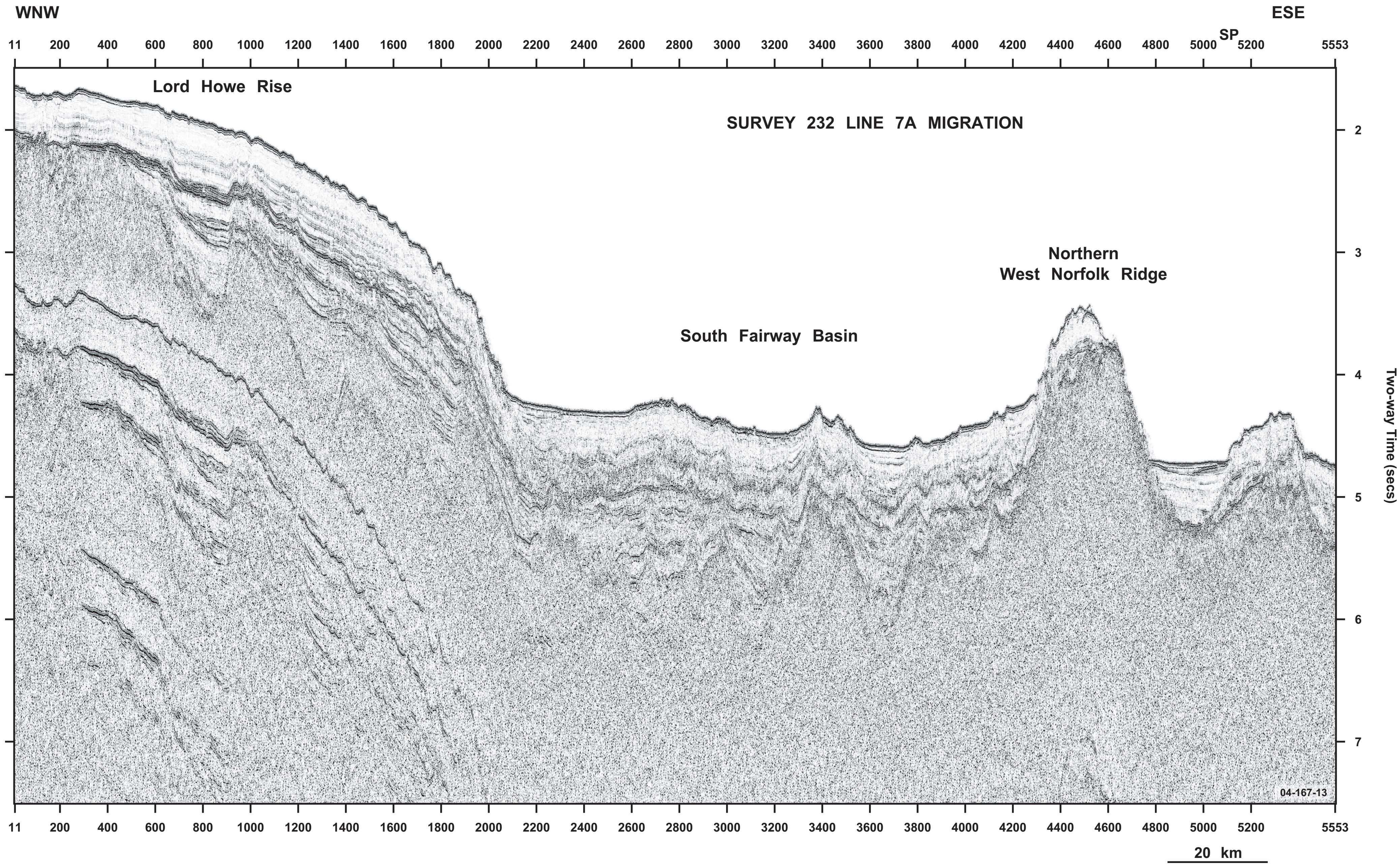

Figure 13. Seismic profile 232-7A crossing South Fairway Basin

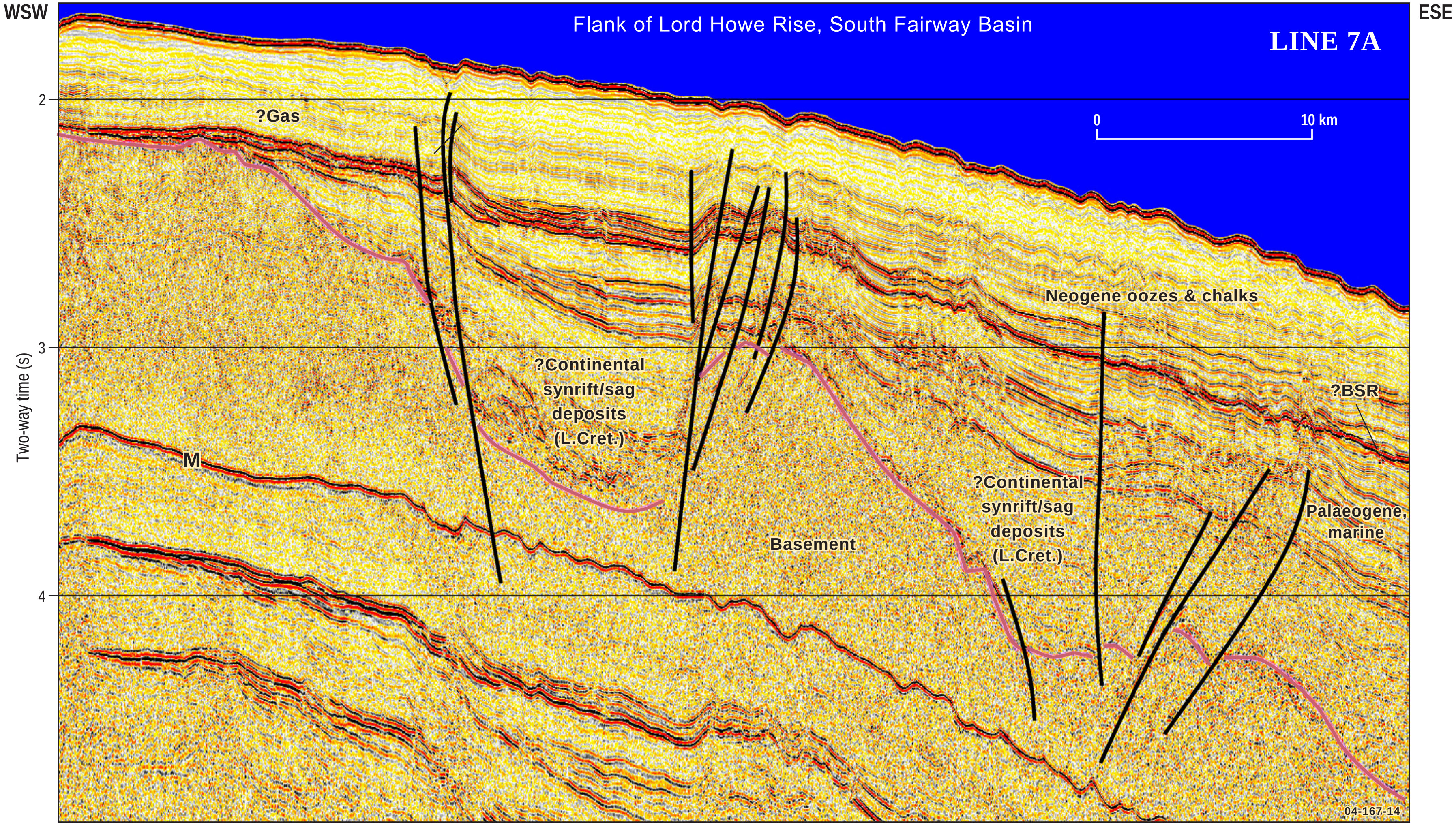

Figure 14. Detail of profile 232-7A in South Fairway Basin

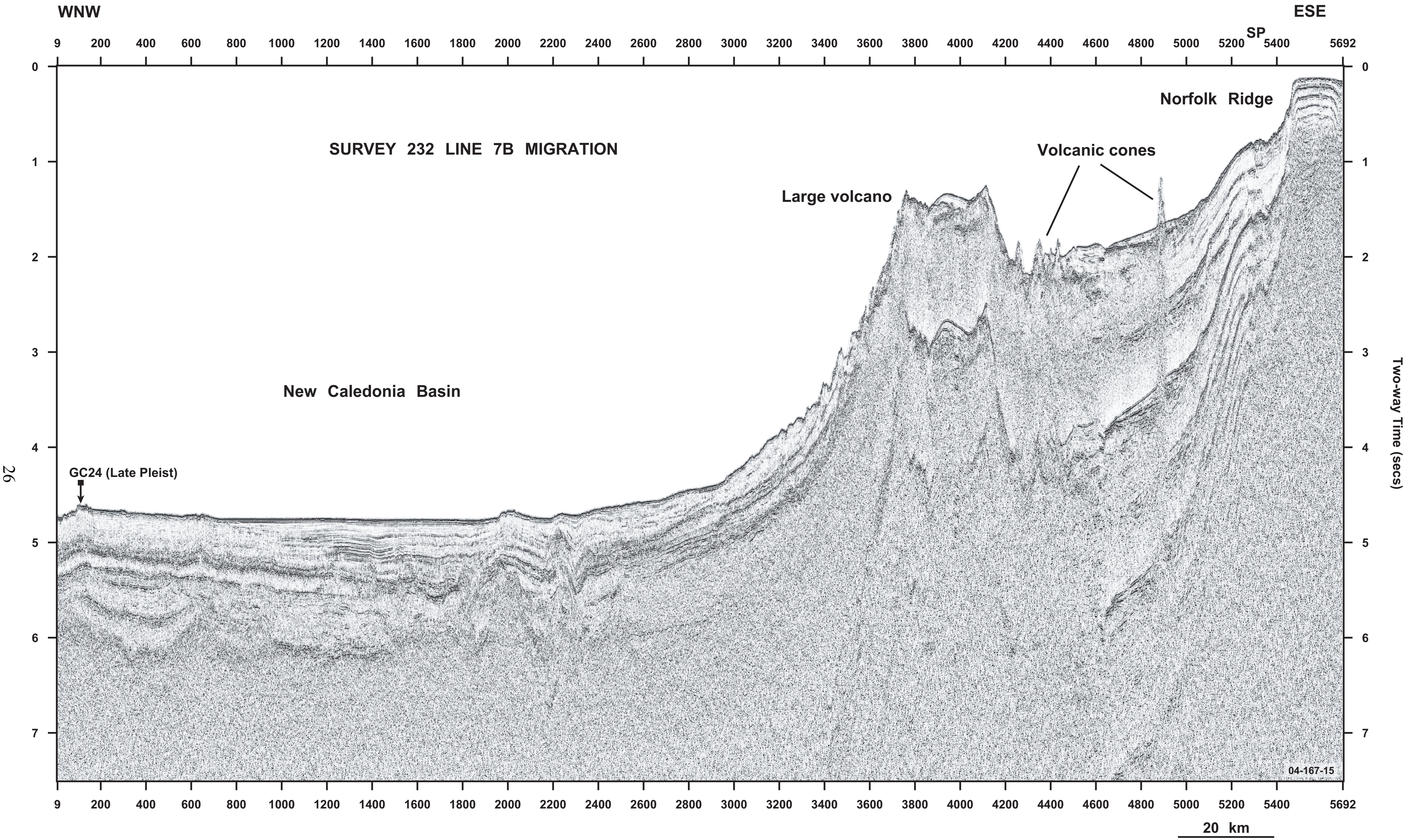

Figure 15. Seismic profile 232-7B crossing New Caledonia Basin

Volcanics, west flank of Norfolk Ridge

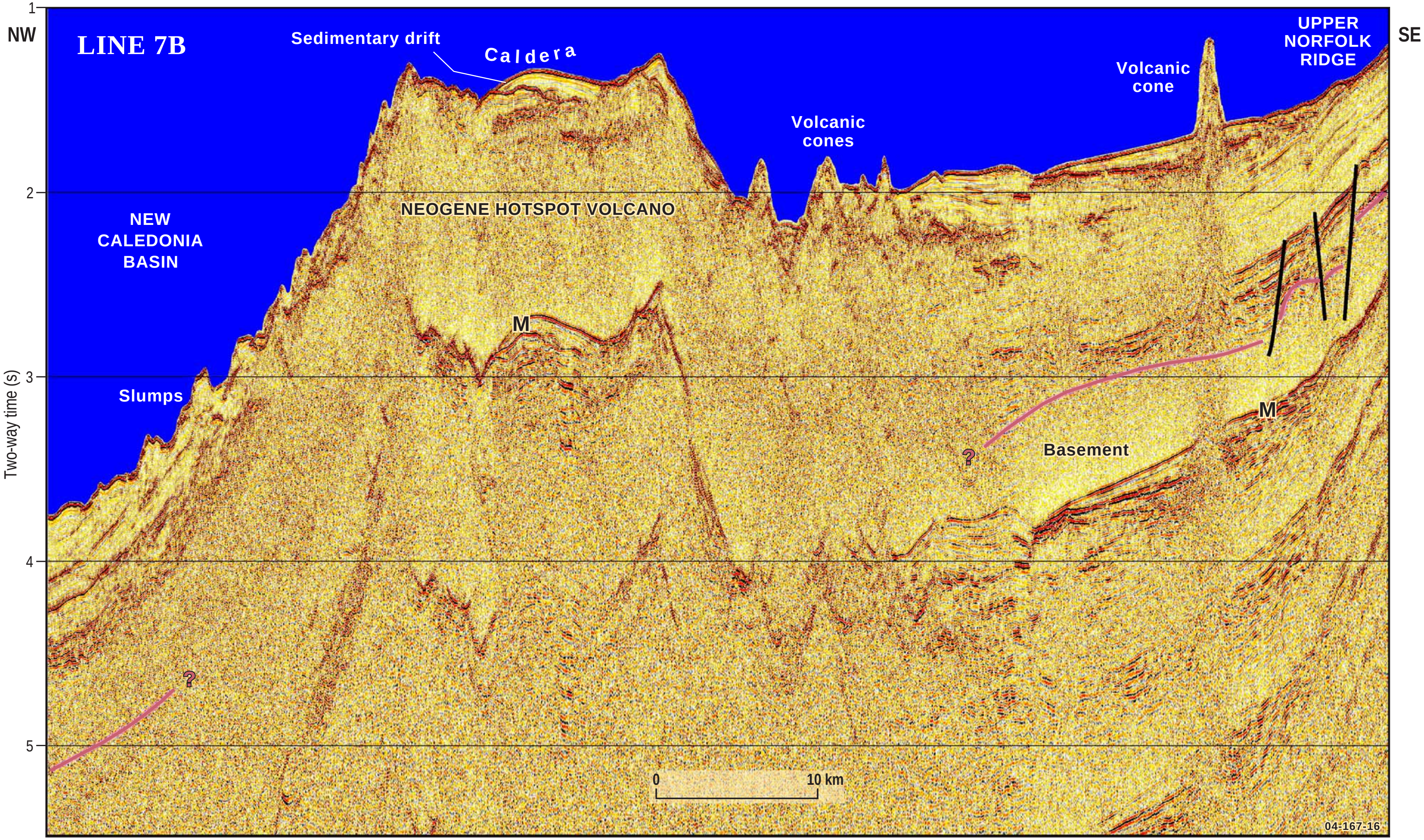

Figure 16. Detail of profile 232-7B on west flank of Norfolk Ridge

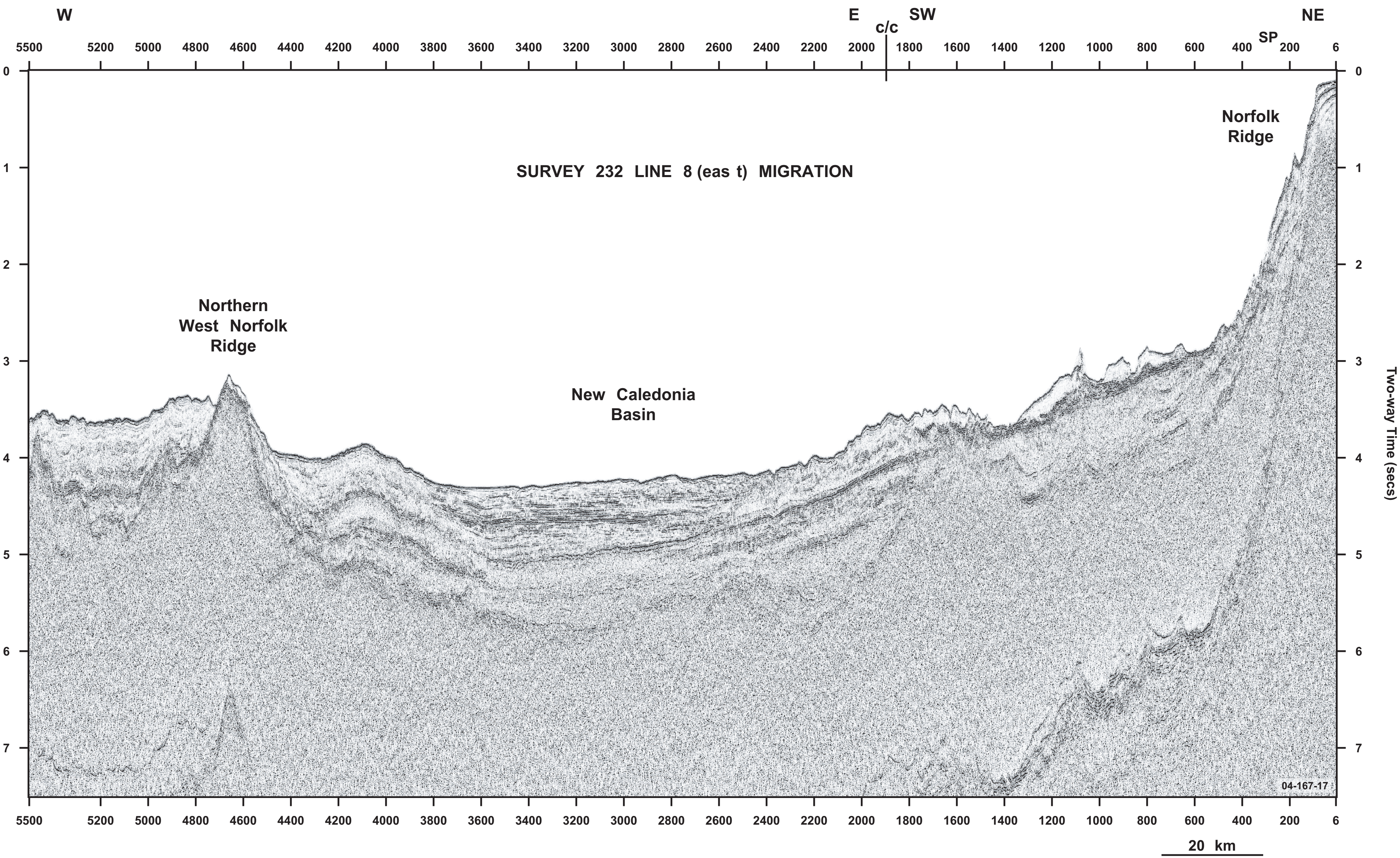

Figure 17. Seismic profile 232-8 (eastern part) crossing New Caledonia Basin

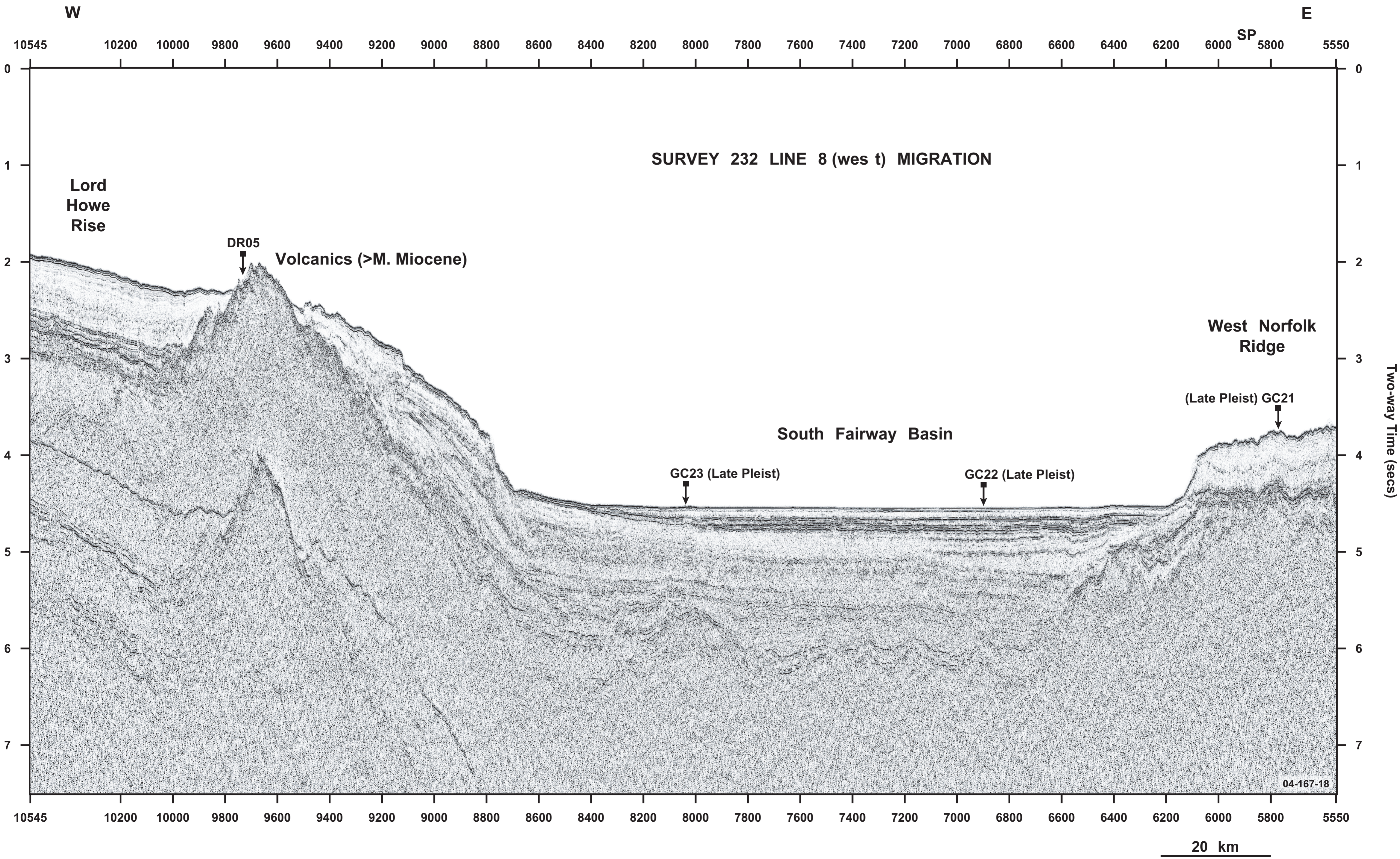

Figure 18. Seismic profile 232-8 (western part) crossing South Fairway Basin

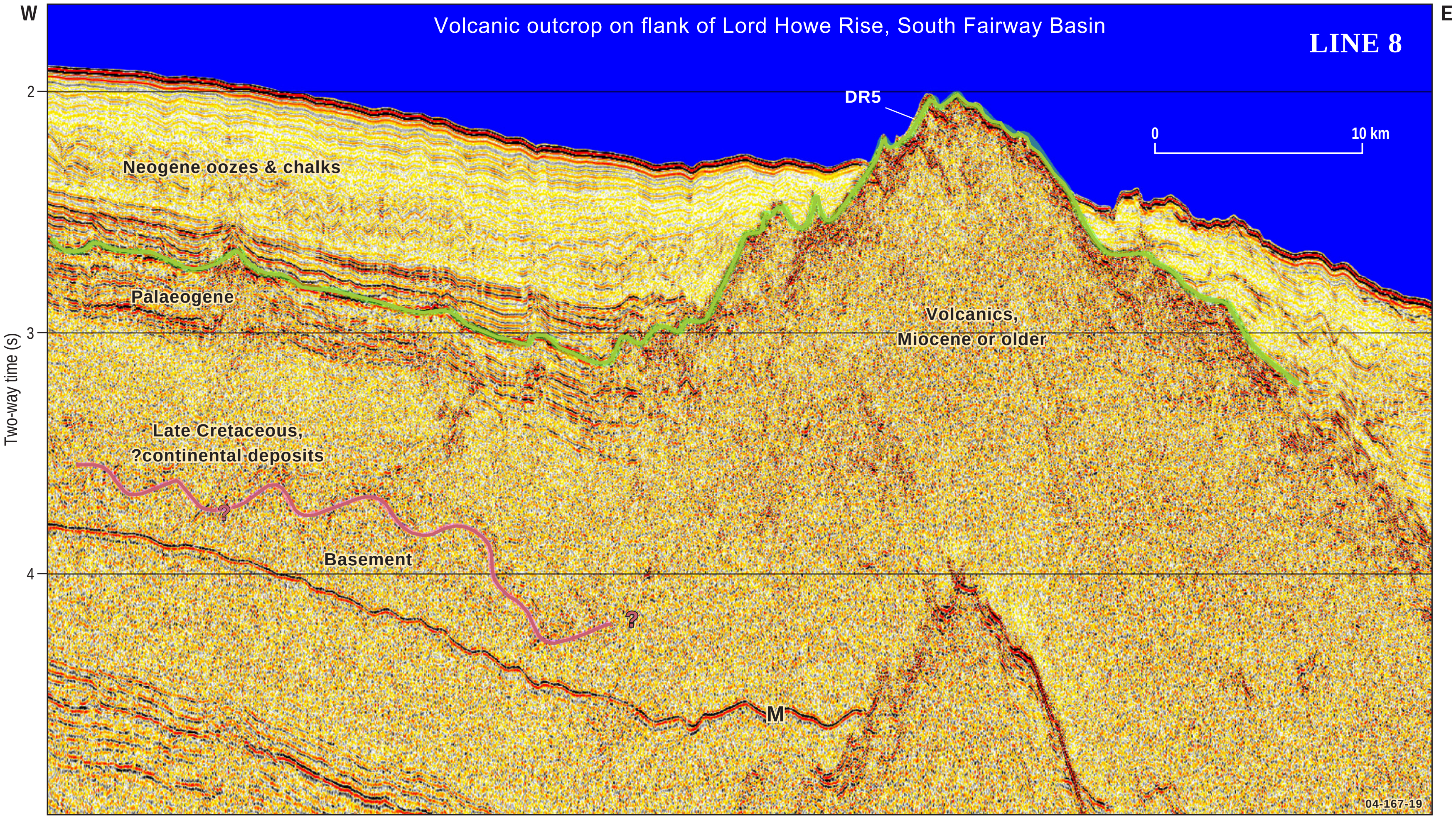

Figure 19. Detail of profile 232-8 on flank of Lord Howe Rise

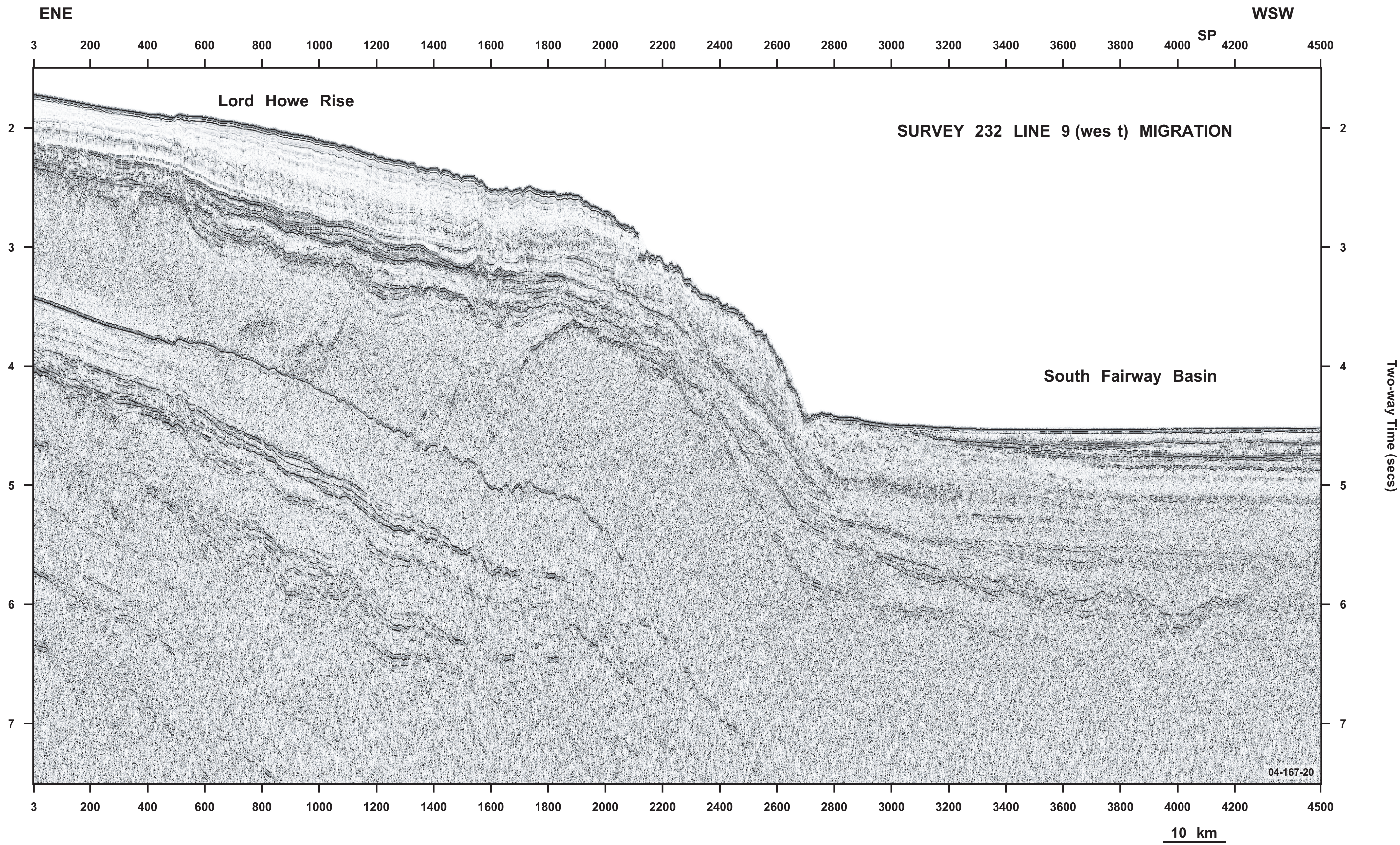

Figure 20. Seismic profile 232-9 (western part) crossing South Fairway Basin

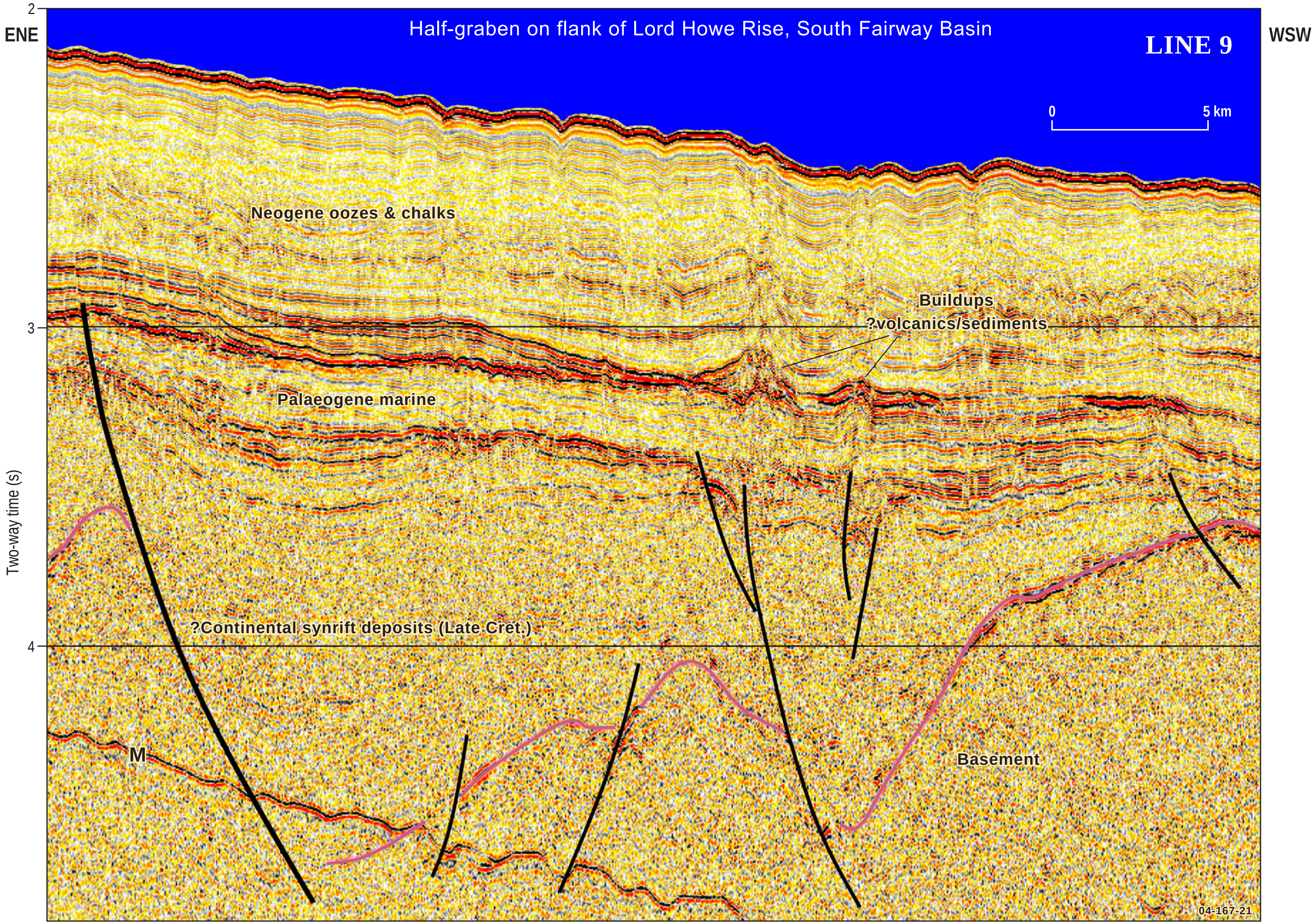

Figure 21. Detail of profile 232-9 on flank of Lord Howe Rise

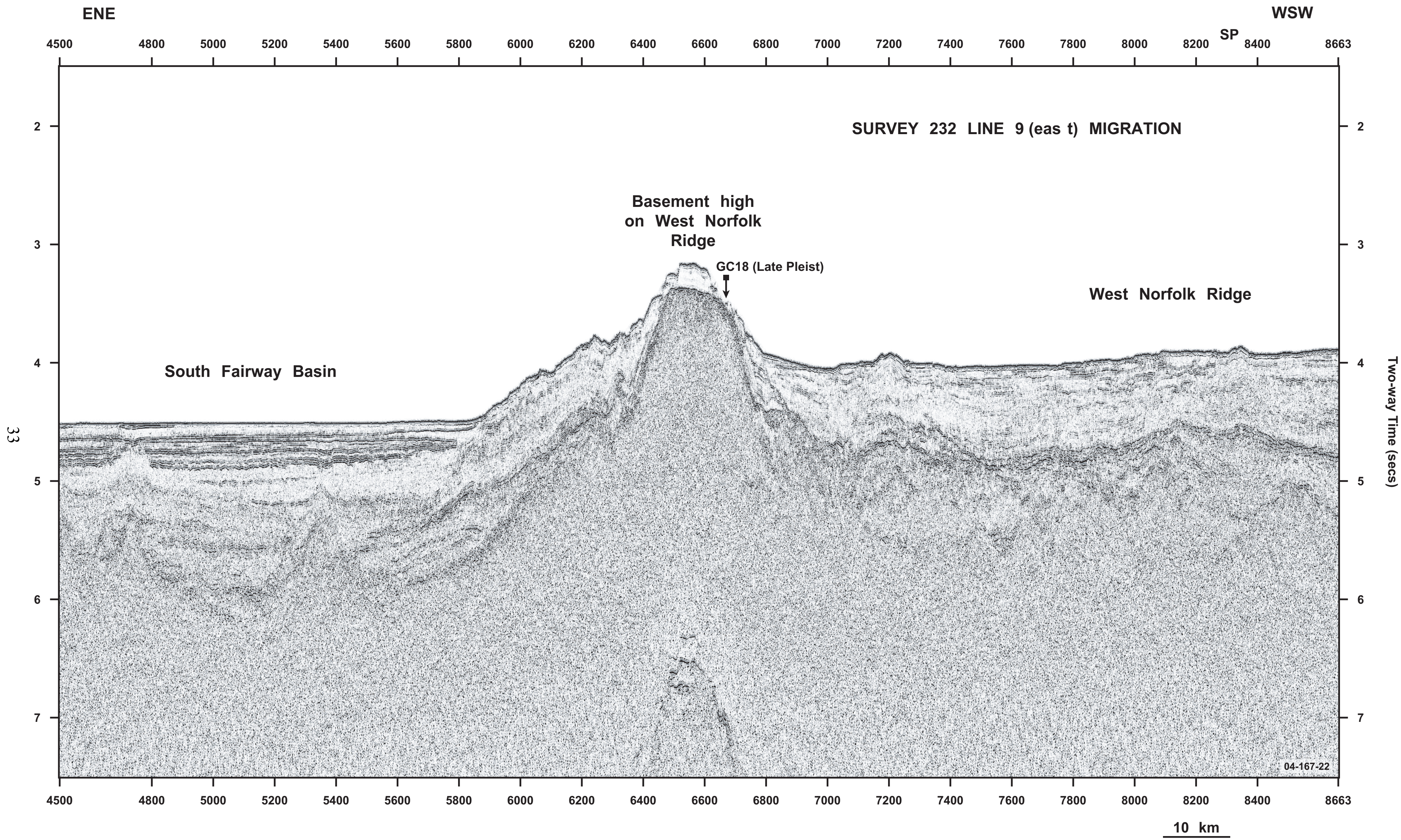

Figure 22. Seismic profile 232-9 (eastern part) crossing West Norfolk Ridge

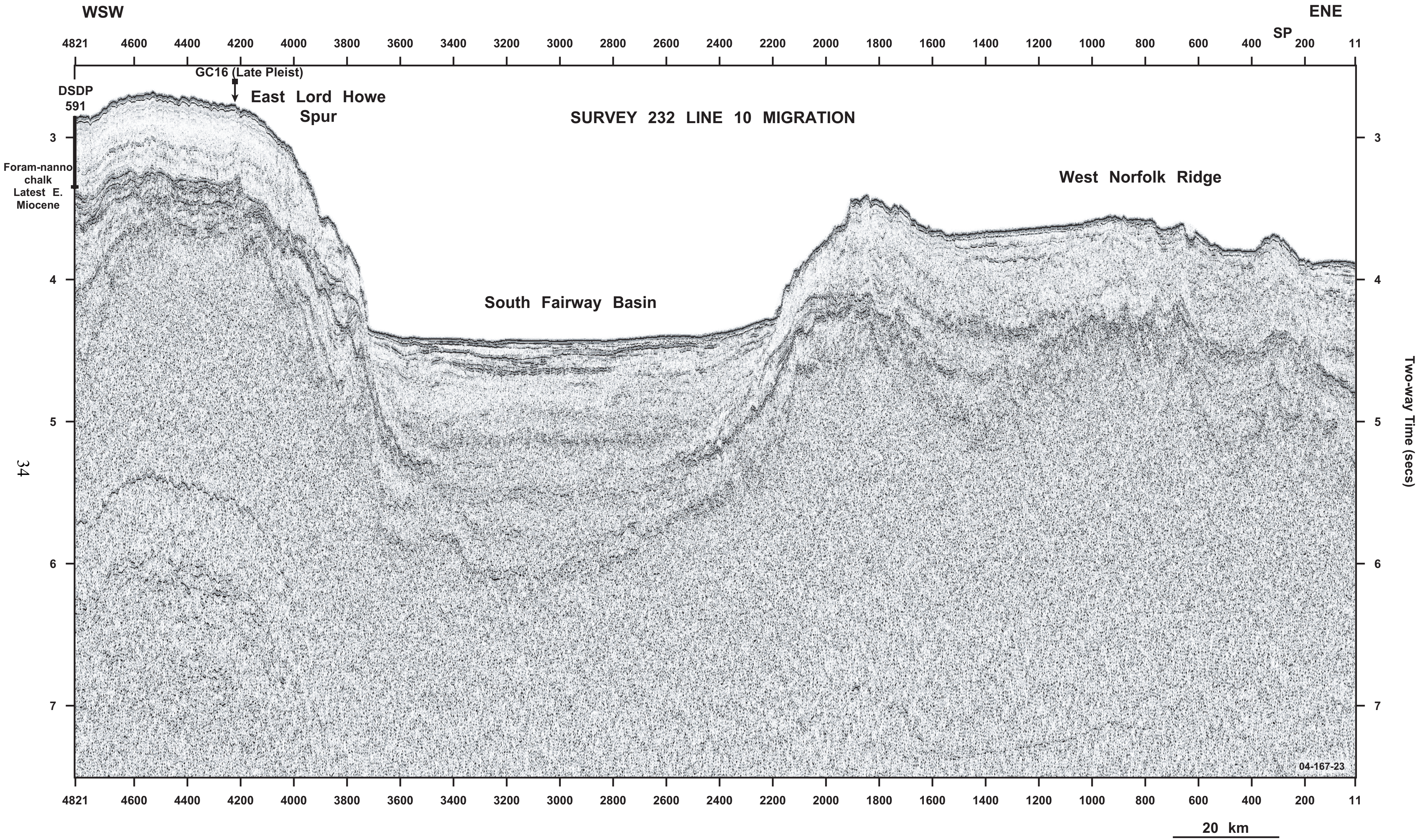

Figure 23. Seismic profile 232-10 crossing South Fairway Basin

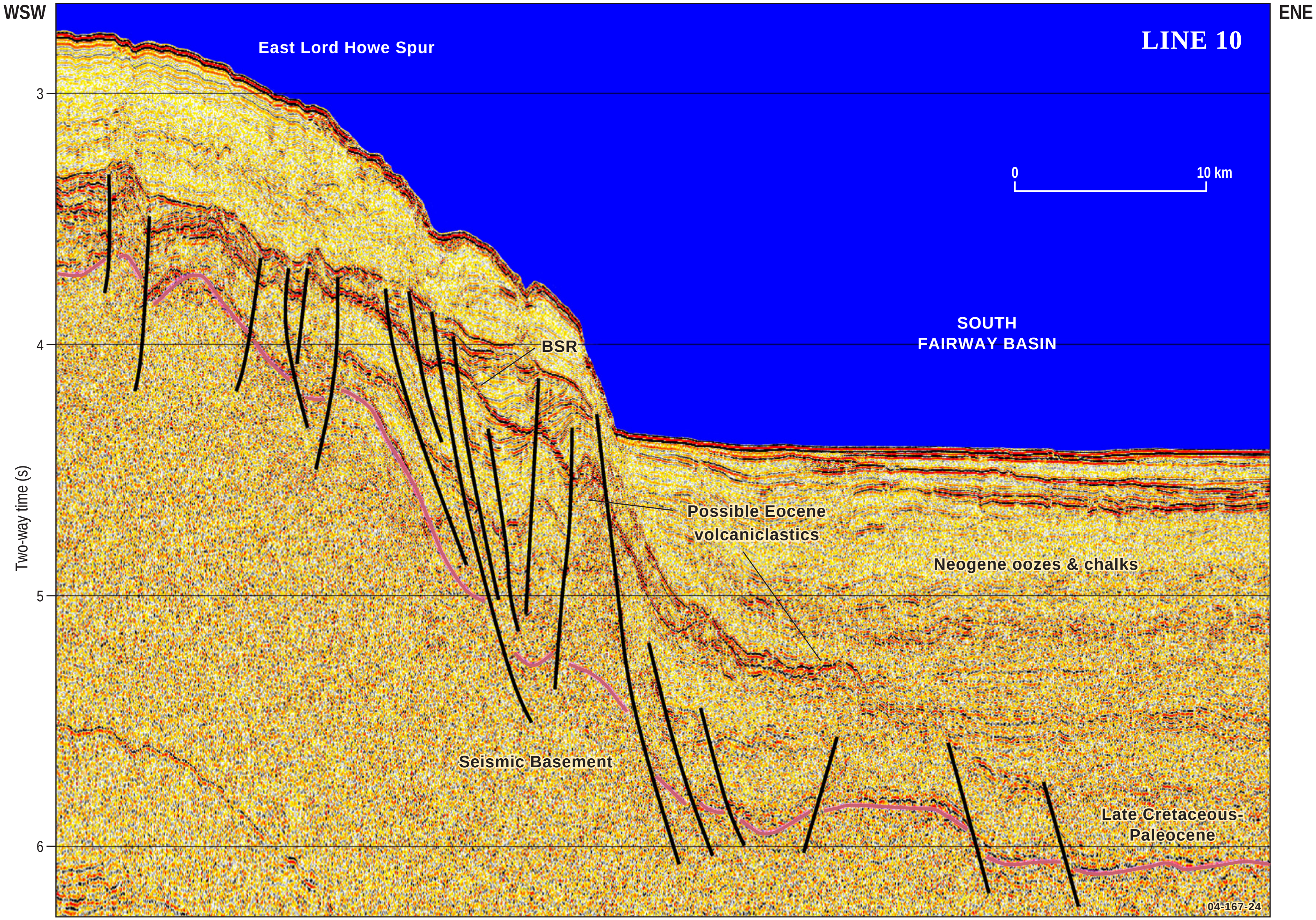

Figure 24. Detail of profile 232-10 in Fairway Basin

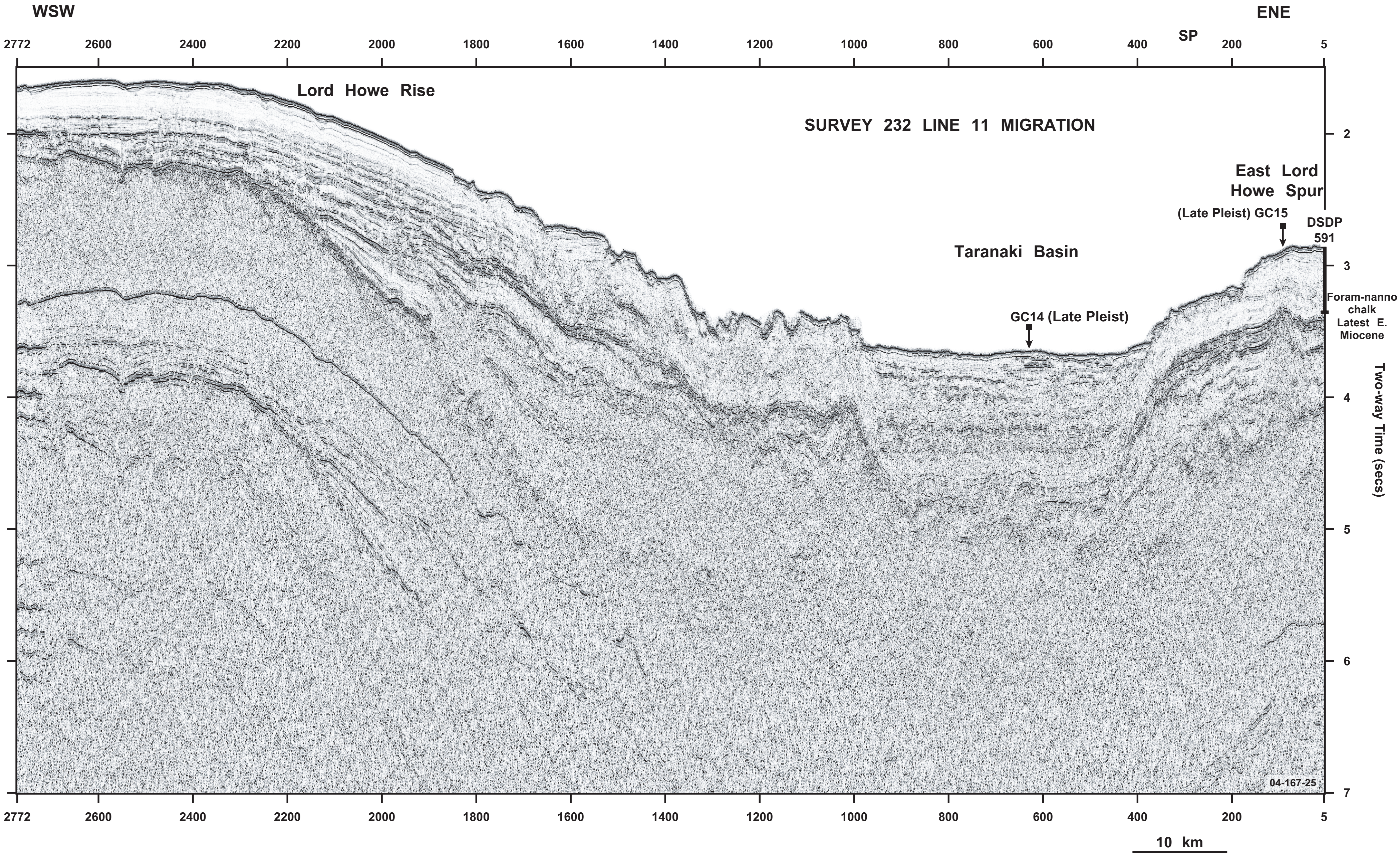

Figure 25. Seismic profile 232-11 crossing Taranaki Basin

(which joins the southern end of the largely subsurface, northwest-trending Fairway Ridge). The South Fairway Basin extends from 26°40'S to 31°30'S, and is 600 km long and 150 km wide. It is generally in water more than 3000 m deep. To the north it steps up along a probable east-west transform fault to the Central Fairway Basin. To the south it is limited by the generally high area between the East Lord Howe Spur and the West Norfolk Ridge. East of the subsurface ridge is the somewhat deeper New Caledonia Basin.

In the north (Figures 10-14) the Cainozoic sedimentary sequence, with up to 2500 m of section, looks much like that in the Central Fairway Basin. We interpret the basal section as consisting of 300-800 m of deformed Upper Cretaceous siliciclastic sediments including diapiric structures (Figure 10). Less deformed Palaeogene chalks, radiolarites, cherts and interbedded turbidites ~1000 m thick (Figure 12), derived from Lord Howe Rise, overlie the Cretaceous sequence. These are cut by a BSR in places (Figures 12 and 14). A seismically transparent sequence ~600 m thick is interpreted as Miocene and younger pelagic chalk and ooze. Igneous intrusions are common and diapirs reach into the Miocene sequence in places. Normal faults offset the basement by as much as ~700 m on the flank of the Lord Howe Rise (Figure 14). They diminish up-section, but some persist to the surface.

In the south (Figures 18-24) the sequence is generally similar. On the flank of the Lord Howe Rise the basal sequence is essentially transparent and 750-1000 m thick (Figures 19 and 21). It is less deformed that the equivalent sequence further north, and is assumed to consist of homogeneous Upper Cretaceous siliciclastic sediments. The overlying sequence is variably bedded and ~500 m thick, and is assumed to consist of Palaeogene chalk, radiolarite, chert and turbidites. The overlying sequence is transparent and undeformed Miocene and younger chalks and oozes ~500 m thick. Unlike the situation further north, the youngest part of the sequence in the deepwater part of the basin is strongly bedded, and probably consists of ooze interbedded with turbidites. The turbidites were probably derived from the southern margin, because they thicken southward and also because the western and eastern margins are draped with largely unaffected ooze.

In the south, igneous intrusions occur but diapirs are absent. A BSR is apparent on the eastern side of the East Lord Howe Spur (Figure 24). On the flanks of the Lord Howe Rise, faults displace the basement by as much as 1000 m (Figures 21 and 24) and diminish upward. They have lesser displacement in the deepwater part of the basin. Dredge 5 from the eastern Lord Howe Rise contains a volcanic breccia, which is at least as old as Middle Miocene age on foraminiferal evidence (Appendix 8). Small volcanic seamounts further northwest on the Lord Howe Rise are of Early Miocene age on the basis of foraminifera (Exon *et al*., 2004). Such volcanic eruptions might have provided much turbidite debris to the deepwater basin.

5.3. New Caledonia Basin

We define the structural New Caledonia Basin as consisting of a northern part 600 km long trending northwest, and a southern part 1000 km long trending north-south. It ends north of the Wanganella Ridge (Figure 5) and averages 150 km wide. According to Lafoy *et al*. (in prep.) the northern part is extended continental crust and the southern part is oceanic crust, and we support that view. Water depths are 3000-3500 m.

In the north, Line 2 (Figure 7) indicates that block faulting displaces (continental) basement by more than 1000 m. The sedimentary section is up to 2000 m thick and the sequences appear to be similar to those in the adjacent Fairway Basin. Transparent Upper Cretaceous siliciclastic sediments <500 m thick occur only in a half graben. The overlying, intermittently bedded sequence probably consists of interbedded Palaeogene chalk, radiolarite, chert and turbidites. In the graben it is <800 m thick, but the upper part of the sequence overflows the graben, in accordance with the regional picture of Eocene tectonism. The unconformably overlying, relatively transparent sediments are <500 m thick and little displaced by faulting, and probably consist of Neogene calcareous ooze and some turbidites.

The southern part of the New Caledonia Basin near Norfolk Island is bounded to the west by the West Norfolk Ridge, the east by the Norfolk Ridge, and the south by shallow basement between the West Norfolk and Norfolk Ridges. The true sediment thickness is unclear, because basement commonly was not reached by our low-powered seismic system (Figures 15 and 17), but it reaches 1500 m in places. The sedimentary section is flat-lying in general, with some areas of folding and diapirism. The generally seismically diffuse lower sequence, of probable Paleocene-Eocene age, contains rare strong reflectors. The upper sequence is transparent on both sides of the basin, but contains well-bedded sequences, probably turbidites, in the basin centre.

The Norfolk Ridge and West Norfolk Ridges are complex features that have continental crustal thicknesses (e.g. Herzer *et al.*, 1997). Herzer *et al.* (1999) describe marine Upper Cretaceous carbonaceous mudstones from the Norfolk Ridge. Mortimer *et al.* (1998) have described Triassic and Jurassic continental igneous rocks from the West Norfolk and Wanganella Ridges. The volcanic history of the Norfolk Ridge is poorly known. Mortimer *et al.* (1998) have Ar/Ar dated biotite from a volcanic breccia from the Norfolk Ridge south of Norfolk Island as latest Oligocene at 26 Ma. Jones and McDougall (1973) dated the intraplate alkaline lavas of Norfolk Island as much younger, Late Pliocene, using the K/Ar method. Our seismic profiles show that where the sea floor rises toward the Norfolk Ridge, basement is not always apparent (Figures 15 and 17), probably because of the masking effect of volcanic strata. Canyons cut into the young sediments below the sea floor, with some slumping of the upper sequence. These young sediments give way eastward, in 500 m water depth, to the hard volcanic outcrop of the pedestal of Norfolk Island. The pedestal is planated at about 75 m below sea level. Near the Norfolk Ridge (Figure 16) is a large free-standing volcano rising to within 900 m of the surface. Younger sediments partly fill its caldera, which is at least 17 km across. This volcano is part of a north-south chain apparent in satellite gravity data. Small satellite cones east of the main volcano give way to a sedimentary section ~1.2 seconds thick.

5.4. Southernmost area

In the southern region the situation is complex (Figures 5, 23 and 25). DSDP Site 206 (Table 1) is less than 100 km south of our seismic line 10 in the deepwater Taranaki Basin, and its stratigraphic section is likely to be similar to that in the deepwater basins revealed by seismic lines 10 and 11. At Site 206 (Burns, Andrews *et al.*, 1973) ~420 m of Miocene and younger calcareous ooze overlies 190 m of Oligocene chalk, which in turn overlies >120 m of Paleocene and Eocene radiolarian-rich chalk. Acoustic basement lies not far below the base of the site (734 m), so Cretaceous sediments are probably absent at this site on the flank of a local high.

The New Caledonia Basin was not surveyed, but shallows southward to a water depth of about 2000 m (Figure 5). The broad northern extension of the West Norfolk Ridge is 100 km across and about 2700 m deep, with irregular volcanic basement (Figure 23). Most of its sedimentary sequence (>1000 m thick) is seismically transparent, and is assumed to be Neogene calcareous ooze and chalk. A lower, moderately bedded sequence (<1000 m thick) may be Upper Cretaceous siliciclastics and Palaeogene radiolarian-rich chalk.

The western West Norfolk Ridge drops down into the 75 km wide southernmost part of the South Fairway Basin, which is about 3300 m deep. We regard this basin as giving way to the Taranaki Basin at a saddle a few tens of kilometres south of seismic profile 10 (Figure 5). In the southernmost South Fairway Basin the sedimentary section is up to 2000 m thick and largely transparent (Figure 24). Most of it is probably Neogene calcareous ooze and chalk, but there is assumed to be a Palaeogene chalk and radiolarite sequence, including a turbidite-rich Eocene sequence related to regional tectonism, and perhaps some Upper Cretaceous siliciclastic sediments. An upper, well-bedded, presumably turbidite-bearing section thickens into the basin to reach ~300 m thick. It is probably largely Quaternary and could be related to Quaternary volcanism like that on Norfolk Island (Jones and McDougall, 1973).

The broad East Lord Howe Spur extends SSE from the Lord Howe Rise, and is 75 km wide and ~2100 m deep. Basement lies ~1000 m below sea bed, and faults characterise its margins (Figures 24 and 25). There is major offsetting as high as the assumed Eocene level, suggesting that much of the displacement between the Spur and the bounding basins occurred during the regional Eocene tectonic event. The lower, well-bedded section is assumed to be Palaeogene chalks and radiolarites, with the major reflectors representing chert, and perhaps volcanogenic horizons. The upper section (<600 m thick) is transparent Neogene calcareous ooze, as shown by DSDP Site 591 (Table 1), which contains uppermost Lower Miocene chalk at total depth of 500 m.

West of the East Lord Howe Spur is a fault-bounded graben (Figure 25) trending NNW, which is the eastern part of a northwestern arm of the Taranaki Basin (Figure 5). It is 30 km wide and ~2700 m deep. The graben contains up to 2000 m of moderately bedded and generally flat-lying sedimentary section. On the evidence of DSDP Site 206, Miocene and younger calcareous ooze presumably overlies Oligocene chalk, Paleocene and Eocene radiolarian-rich chalk, and Cretaceous siliciclastics.

West of the graben, the Taranaki Basin extends about 45 km upslope toward the Lord Howe Rise (Figure 25). Basement, visible only in places, is up to 2500 m deep. The sedimentary section is largely transparent, with a bedded section ~1000 m thick. The older sequences onlap the rising basement westward, and the upper transparent sequence overlies planated basement. At 1650 m water depth, basement is up-thrown to 1500 metres below sea bed, and the Lord Howe Rise proper begins.

6. SEABED SAMPLING

The sampling results are summarised for New Caledonian territory in Table 4, and for Australian territory in Table 5. There were 22 successful Quaternary cores taken in water depths of 1297-3517 m, and key cores are figured in Appendix 2. The cores were described and sampled aboard for headspace gas, hydrocarbon isotopes and pore water. They recovered foram-bearing nannofossil ooze and nannofossil ooze. The southern cores - GC18, 22, 23, 25, 26 and 27 - show much more variation in colour and stronger colours than the others, suggesting more variation in redox conditions. Average recovery was 360 cm, and total recovery 80 m. One successful dredge (DR5) recovered Miocene volcaniclastic rocks and the other (DR1) Eocene radiolarian chalk.

6.1. Sampling in New Caledonian jurisdiction

Results are summarised in Table 4. Sample locations (Figure 4) were defined by 3.5 kHz echosounder and seismic data from the ZoNéCo 5 program (outlined in Auzende *et al*., 2000c) and by new FR9/01 seismic data (Table 3). The 11 core stations were in water 1297-3515 m deep, and the three dredge stations in water 2450-3300 m deep. A total of 41 metres of sediment were recovered from the cores, with no failures. Their length varies from 305 to 455 cm and averages 370 cm. Many are illustrated in Appendix 2. They consist largely of brownish to greyish foram-bearing nannofossil ooze. The three dredge hauls yielded Eocene radiolarian chalk in DR1, nothing in DR2, which snapped off on hard outcrop, and Quaternary ooze in DR3.

Table 4. Cores and dredges in New Caledonian jurisdiction

Core	Latitude	Longitude	Depth (m)	Recov. (cm) or (kg)	Description	Echofacies
GC01	25°18.67	163°04.75	1297	450	Pale foram-bearing nanno ooze; base E-M Pleistocene	N/A
GC02	25°03.71	163°40.02	2635	369	Pale brown foram-bearing nanno ooze; base E-M Pleistocene	1a
GC03	24°51.70	163°30.09	2522	339	Pale brown foram-bearing nanno ooze; base Late Pleistocene	DpBSR + 1b
GC04	24°48.18	163°29.99	2586	329	Pale foram-bearing nanno ooze; base Late Pleistocene	DS + 1b
GC05	24°54.98	163°46.75	2706	305	Pale brown foram-bearing nanno ooze; base Late Pleistocene	DpBSR + 1a
GC06	24°53.00	163°53.98	2764	338	Pale foram-bearing nanno ooze; base Late Pleistocene	DD + 1a
GC07	24°18.60	164°03.60	2835	N/A	Not attempted	DD + 1a + PM
GC08	25°08.10	164°13.50	2700	369	Pale foram-bearing nanno ooze (repeat section from 328 cm); base Late Pleistocene	DD + 1b + PM
GC09	25°03.71	164°30.05	2840	350	Pale brown foram-bearing nanno ooze; base Late Pleistocene	DpBSR + 1a
GC10	24°44.33	164°46.14	2580	445	Pale brown foram-bearing nanno ooze; base Late Pleistocene	
GC11	24°44.28	164°49.13	2820	350	Pale brown foram-bearing nanno ooze; base Late Pleistocene	
GC12	24°41.39	164°57.83	3517	455	Brown foram-bearing nanno ooze; base E-M Pleistocene	
DR01	25°11 25°11	165°02 165°01	3300- 3150	30 kg	Pale orange to white late Early Eocene chalky radiolarite; ooze, pumice.	
DR02	25°19	164°51	2450	0 kg	Lost dredge after strong bite (>4 tonnes)	
DR03	25°40.6	165°06.9	3130	3 kg	Quaternary ooze only	

Total recovery: 41 metres of core, so average is 370 cm

Seismic:
DS: sub-surface diapir
DpBSR: Diapir piercing the BSR
DD: Deep diapir

Echofacies (3.5 kHz):
1a: Layered, flat (long wave amplitude)
1b: Layered, wavy (short wave amplitude)
PM: possible pock mark

6.2. Sampling in Australian jurisdiction

The sampling was carried out from south (~31°50'S) to north (~27°15'S). Results are summarised in Table 5. The work was split into three areas based on the new seismic profiles. The Late Quaternary cores will allow a study of the composition, character and climate history of the region over nearly eight degrees of latitude including the New Caledonian cores. Many of the cores are figured in Appendix 2. Pale brown, yellow and pale grey colours dominate north of 28°S; darker grey, olive and white are interbedded with such colours south of 29°S. This suggests purely oxidising conditions in the north, but fluctuations in redox conditions in the south, probably related to variable inflow of bottom water through time. The only successful dredge (DR5) contains Miocene volcaniclastic rocks; the other four dredges contain only ooze.

Table 5. Cores and dredges in Australian jurisdiction

Core	Latitude (S)	Longitude (E)	Depth (m)	Recov. (cm) or (kg)	Description	Line/shot point	Target
GC13*	31° 53.0	163° 08.0	1188	10 cm	Pale olive muddy foram sand; base Late Pleistocene		PO
GC14	31° 39.35	164° 08.47	2720	519 cm	0-16 cm: pale brown foram-rich nanno ooze. 16-496: olive to white nanno ooze. 496-519: repeat 0-16; base Late Pleistocene	L11-615	PO
GC15	31° 35.59	164° 24.64	2140	246 cm	0-90 cm: pale brown & light grey nanno ooze. 90-246 cm: pale yellow & white nanno ooze; base Late Pleistocene	L11-85	DSDP 591 DD
GC16	31° 28.49	164° 44.53	2100	320 cm	0-29 cm: pale brown & light grey foram-rich nanno ooze. 29-320: light grey & pale olive nanno ooze; base Late Pleistocene	L10B-4207	MD, F, PM
GC17*	31° 17.94	165° 12.46	3320	None	Traces of foram sand	L10B-3240	PO
GC18	30° 26.87	165° 54.33	2590	240 cm	Interbedded v pale brown & light grey foram-bearing nanno ooze; base Late Pleistocene	L9C-6310	BR, WNR
GC19	29° 35.74	166° 13.33	2905	None	Fingers torn off core catcher	L8B- 3140	DD, NCB
GC20	29° 35.75	165° 57.65	2483	None	Bounced off hard rock, core cutter damaged. Ooze traces.	L8B-3722	BR
DR4	29° 35.75 29° 35.75	165° 57.00 165° 58.05	2565-2400	10 kg	Nibbles only. Pale grey foram nanno ooze with some pyritised forams. Very minor pumice.	L8B-3744-3707	BR W>E
GC21	29° 35.78	165° 28.60	2810	400 cm	0-290 cm: pale brown & yellow foram-bearing nanno ooze. 290-400 cm: repeat of top section; base Late Pleistocene	L8B-4800	DD, WNR
GC22	29° 35.86	164° 58.51	3405	445 cm	Multicoloured nanno ooze, with distinct beds 20-30 cm thick: white, pale yellow, pale & dark greenish grey; base Late Pleistocene	L8B-5916	DD
GC23	29° 35.88	164° 27.77	3392	433 cm	Multicoloured nanno ooze, with distinct beds 20-40 cm thick: yellow, yellowish brown, pale & dark greenish grey; base Late Pleistocene	L8B-8062	DD
DR5	29° 35.9	163° 42.3	~1700	5 kg	Basaltic volcaniclastic rocks: hyaloclastite, hyaloclastite breccia, minor basalt. Mn crusts to 3 cm thick. Late Miocene to Late Pliocene calcareous	L8-9744-9767	BR

					nannofossils and Early Pliocene forams in hyaloclastite infillings; Late Middle Miocene forams in Mn crust		
GC24	27° 52.02	165° 43.00	3450	266 cm	Pale brown & pale yellow nanno ooze; base Late Pleistocene	L7B-107	SB, DNS, BSR, NCB
DR6	27° 47.17 27° 46.98	165° 16.34 165° 15.18	3080-2840	5 kg	Very pale brown nanno ooze. Very minor pumice	L7-4654-4610	BR, WNR E>W
DR7	27° 47.36 27° 47.19	165° 17.36 165° 16.41	3280-3100	5 kg	Very pale brown nanno ooze	L7-4695-4660	BR, WNR E>W
GC25	27° 09.78	164° 36.54	3239	407 cm	0-359 cm: pale brown & pale yellow nanno ooze. 359-407: repeat section; base Late Pleistocene	L6-2510	DNS, SB
GC26	27° 13.74	164° 14.43	2935	377 cm	Pale yellow, pale brown & greenish grey nanno ooze; base E-M Pleistocene	L6-3350	DNS
GC27	27° 17.67	163° 52.50	1875	248 cm	Pale brown, pale yellow, light grey & white nanno ooze; base Late Pleistocene	L6-4150	SB, DNS

* Station repeated once.
Total recovery: 39 metres of core, so average is 354 cm

Seismic:

DNS: near-surface diapir
DpBSR: Diapir piercing the BSR
DD: Deep diapir
MD: Minor diapir
F: Fault
PO: palaeo-oceanography

SB: surface bulge
BSR: Bottom simulating reflector
WNR: West Norfolk Ridge
BR: basement ridge
WNCB: West New Caledonia Basin

Southern area

Cores GC13-17 (GC14-16 illustrated in Appendix 2) were taken on seismic Lines 11 and 10 (Figures 25 and 23), running ENE from the Lord Howe Rise. Core **GC13**, located on the eastern Lord Howe Rise at the end of seismic Line 11, recovered only 10 cm of foraminiferal sand in 1188 m of water, indicating current reworking of sediment at that depth. The seismic profile suggests firm bottom. Further ENE along Line 11, **GC14** was sited on a slight rise in the transparent sediments in the flat bottom of a 25 km wide half graben, which runs ESE from the flank of the Lord Howe Rise, southwest of the East Lord Howe Spur. The graben opens out southward, and is not part of the Fairway Basin. On seismic evidence the core site was above a shallow ‘flat spot’ and a deep diapir. It recovered 5.19 m of nannofossil ooze in 2726 m of water. **GC15**, on the western side of the East Lord Howe Spur, recovered 2.46 m of ooze from transparent strata in 2147 m of water. This was above a diapir that rises to ~0.3 seconds of the surface near ODP Site 591. **GC16**, also in transparent strata above a small diapir and fault on the eastern side of the same ridge, recovered 3.2 m of foram nannofossil ooze from 2089 m of water. **GC17**, in the flat base of the Fairway Basin, recovered only traces of foraminiferal sand and ooze from 3320 m of water. The seismic profile shows well-bedded sediments near the surface, suggesting that the corer was stopped by foraminiferal sand turbidites. These cores from south of 31ºS were more reduced than those recovered from New Caledonian territory north of 25ºS, with a brownish oxidised layer less than 1 m thick, above pale olive, brown and white oozes.

110 kilometres northeast of GC17, on Line 9 (Figure 22), lies a lightly sedimented basement high on the northern extension of the West Norfolk Ridge. **GC18** (figured in Appendix 2) recovered 240 cm of nannofossil ooze from the high in water 2590 m deep, but no basement rocks.

Central area

After a transit of 100 km to the north, a series of stations were taken along seismic Line 8 (Figure 18), from east to west, of which Cores GC21-23 are figured in Appendix 2. Core **GC19** was attempted in highly reflective bottom, in generally transparent sediments above a subsurface and seabed rise, in the flat southern New Caledonia Basin on Line 8. It failed when the tines of the core catcher sheared. Further west is a lightly sedimented basement high on the eastern flank of the northern extension of the West Norfolk Ridge, which was the subject of two failed stations (Figure 17). Core **GC20** skidded off outcrop on the western flank of the high in water 2483 m deep, with no recovery. Dredge **DR4**, taken up the western basement slope from water depths of 2580 to 2420 m, recovered only foram nannofossil ooze. Core **GC21** (Figure 18) was taken above a deep diapir in transparent ooze on the western part of the ridge, and recovered 400 cm of nannofossil ooze. Core **GC22** was located above a deep diapir in the flat bottom of the eastern part of the Fairway Basin. It was taken at 3405 m in a fairly reflective surface layer, and recovered 445 cm of pale grey nannofossil ooze. Core **GC23** was located in the flat bottom of the western part of the Fairway Basin. It was taken in water 3390 m deep, in a fairly reflective surface layer above a broad deep diapir, and recovered 433 cm of multicoloured nannofossil ooze. Dredge **DR5**, taken east to west on a rugged basement high, on the trend of the Vening-Meinesz Fracture Zone on the eastern edge of the Lord Howe Rise, recovered volcaniclastic rocks and manganese crust from water 1700 m deep. The rocks have been dated as Late Middle Miocene or older by foraminifera (Appendix 8). Ferromanganese crusts from dredge DR5 are up to 3 cm thick and are discussed in Appendix 6. In many respects they are quite like those from Christmas Island (Exon *et al*., 2002) and the Tasmanian region (Exon, 1997), but have higher contents of nickel and cobalt. These crusts are of no commercial interest.

Northern area

After a 270 km transit northeast, Core **GC24** was taken in moderately transparent sediment in the flat depression of the New Caledonia Basin on seismic Line 7 (Figure 15). This was on a bulge in the sea floor above a deep diapir and a BSR. It recovered 226 cm of pale brown and pale yellow nannofossil ooze from 3450 m water depth. Dredges **DR6** and **DR 7** were planned to sample the eastern slope of basement high on the northern West Norfolk Ridge (Figure 13). Dredge DR6 sampled the slope in water depths of 3080-2840 m and contained only nannofossil ooze. Dredge DR7 sampled the slope in water depths of 3280-3100 m and also contained only nannofossil ooze. Apparently the slopes were thinly blanketed in ooze.

After a transit of 145 km to the northwest to seismic Line 6, three cores (GC25-27) were taken westward along it (figured in Appendix 2). Core **GC25** (Figure 11) was taken in transparent sediments on a seafloor bulge rising 50 m above the generally flat seafloor of the eastern Fairway Basin. It is in water 3239 metres deep and above a diapir, which is at least 500 m across at depth and may reach the surface. It recovered 407 cm of nannofossil ooze. Core **GC26** was taken in water 2935 m deep, in transparent sediments in the Fairway Basin, at the base of the slope up to the Lord Howe Rise. It lies on a 50 m rise above sea bed, and above a near-seabed diapir at least 500 m across and fault-bounded to the west. It recovered 377 cm of nannofossil ooze. Core **GC27** was taken in water 1866 m deep, in weakly bedded sediments on the slope of the westernmost Fairway Basin. It lies above a near-surface diapir at least 300 m across. It recovered 248 cm of nannofossil ooze.

6.3. Quaternary sedimentation rates

The nannofossils (Section 7) show a clear relationship between location and age of the base of the cores. This suggests that there is a systematic variation in sedimentation rates, as most cores are of similar lengths (300-400 cm). The four oldest cores (GC1, 2, 12, 26) are in the north in very varied water depths, and their bases are Early to mid Pleistocene (CN13b/14a) in age. If one assumes an age of 1 Ma, average sedimentation rates are around 4 mm/1000 years. These older cores are on slopes, so may be subject to winnowing. Nine cores (GC4-11, 25, 27) whose bases are of intermediate age (Late Pleistocene, CN14b) are also in the north. Assuming an age of 400,000 years, average sedimentation rates are about 10 mm/1000 years. All the southern cores (GC14-24) have relatively young Late Pleistocene (CN15) bases. Assuming an age of 150,000 years, average sedimentation rates are about 25 mm/1000 years. In general, the northern cores have lower sedimentation rates than the southern cores, probably because productivity has been higher south of 26º45'S than further north.

7. CALCAREOUS NANNOFOSSIL BIOSTRATIGRAPHY OF CORE AND DREDGE SAMPLES FROM R.V. *FRANKLIN* CRUISE FR 9/01: EASTERN LORD HOWE RISE, TASMAN SEA

Richard W. Howe

7.1. Biostratigraphic Summary

Table 6. Biostratigraphic summary of calcareous nannofossil zonal assignments

SAMPLE	DEPTH (cm)	CN/CP ZONE	AGE
GC01	441-446	CN13b/14a (?CN14b)	Early to mid-Pleistocene (?Late Pleistocene)
GC02	354-360	CN13b/14a (?CN14b)	Early to mid-Pleistocene (?Late Pleistocene)
GC04	305-309	CN14b	Late Pleistocene
GC05	297-300	CN14b	Late Pleistocene
GC06	318-323	CN14b	Late Pleistocene
GC08	320-325	CN14b	Late Pleistocene
GC09	330-335	CN14b	Late Pleistocene
GC10	433-438	CN14b	Late Pleistocene
GC11	338-343	CN14b	Late Pleistocene
GC12	419-425	CN13b/14a	Early to mid-Pleistocene
GC14	485-490	CN15	Late Pleistocene
GC15	232-236	lower CN15	Late Pleistocene
GC16	285-290	CN15	Late Pleistocene
GC18	205-210	CN15	Late Pleistocene
GC21	275-280	CN15	Late Pleistocene
GC22	430-435	CN15	Late Pleistocene
GC23	418-424	CN15	Late Pleistocene
GC24	235-240	CN15	Late Pleistocene
GC25	318-325	CN14b	Late Pleistocene
GC26	334-340	CN13b/14a	Early to mid-Pleistocene
GC27	219-225	CN14b	Late Pleistocene
DR1A1	-	-	-
DR1B1	-	CP12	Late Early to earliest Middle Eocene
DR5A6	-	CN6-12b (?CN9b)	Late Miocene to Early Late Pliocene (?late Late Miocene)

7.2. Introduction

Twenty-one gravity core and three dredge samples from the Eastern Lord Howe Rise were examined for their calcareous nannofossil content. Nannofossil smear slides (see Bown & Young, 1998) were supplied ready-made by Geoscience Australia and examined with a Jenaval transmitted light microscope equipped with cross-polarising facilities at a magnification of 1250x. Generic and species assignments follow Perch-Nielsen (1985), Weaver (1993), Young (1998), and Hine & Weaver (1998). The ages of the samples have been determined using the Neogene CN and Palaeogene CP zonations of Okada & Bukry (1980), (Figure 26), as correlated by Berggren et al. (1995a). The zonal assignment and age of each sample are summarised in Table 6 (above), and discussed below, with the nannofossil assemblages detailed on Table 7.

Quantitative counts of at least 100 specimens of *Emiliania huxleyi, Gephyrocapsa* spp. (not including *G. oceanica/parallela*) and *Pseudoemiliania lacunosa* were made on each sample. Semi-quantitative estimates were made of the abundances of other species as VH = very high, >100 specimens per field of view (FOV); H = high, 50–100 specimens per FOV; M = moderate 10–50 specimens per FOV; L = low, 1–10 specimens per FOV; VL = very low, 1 specimen per 1–10 FOV's. Individual species abundances were recorded as follows: A = abundant, >100 specimens per FOV; C = common, 11–100 specimens per FOV; F = few, 1–10 specimens per FOV; R = rare, 1 specimen in 10 FOV's; S = single, only a single specimen observed. As the nannofossil assemblage in a sample can show overgrowth of some species, and dissolution of others, only the overall preservation state of the assemblage is recorded here as G = good, whole assemblage is well preserved, with the diagnostic features of most species preserved; M = moderate, with some dissolution and/or overgrowth, but most species still identifiable, P = poor, severe dissolution and/or overgrowth, with only a few species identifiable to species level. Nannofossil assemblages were generally of high abundance and good preservation.

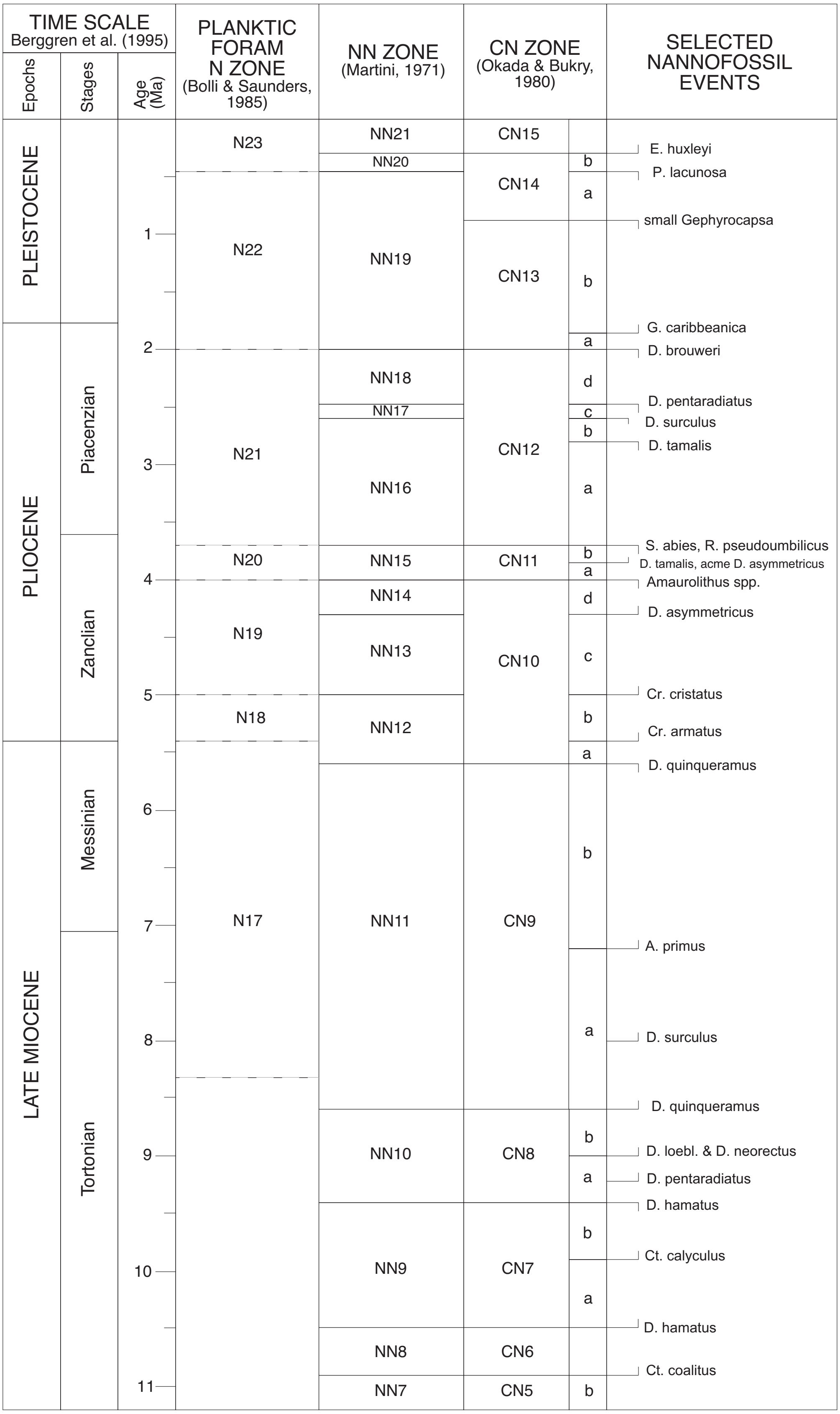

Figure 26. Late Neogene CN nannofossil zonation of Okada & Bukry (1980) and NN zonation of Martini (1971), modified by Young (1998). Approximate correlations are given to the N planktonic foraminiferal zonation of Bolli & Saunders (1985).

Table 7. Details of nannofossil assemblages

	Sample	Core	Depth (cm)	Nannofossil abundance	Nannofossil preservation	1 *Amaurolithus amplificus*	2 *Amaurolithus primus*	3 *Calcidiscus leptoporus*	4 *Calcidiscus macintyrei*	5 *Ceratolithus cristatus*	6 *Chiasmolithus grandis*	7 *Chiasmolithus solitus*	8 *Clausicoccus fenestratus*	9 *Coccolithus formosus*	10 *Coccolithus pelagicus*	11 *Cyclicargolithus floridanus*	12 *Discoaster brouweri*	13 *Discoaster deflandrei*	14 *Discoaster exilis*	15 *Discoaster kuepperi*	16 *Discoaster lodoensis*	17 *Discoaster pentaradiatus*	18 *Discoaster quinqueramus*	19 *Discoaster* sp. 5 ray	20 *Discoaster* sp. 6 ray	21 *Discoaster* sp. 9 ray	22 *Discoaster sublodoensis*	23 *Discoaster surculus*	24 *Discoaster variabilis*
1	6406564	GC01	441-446	VH	G	.	.	C	.	R	.	.	.	.	F	.	.	.	R	.	.	.	.	.	.	.	.	.	.
2	6406565	GC02	354-360	H	G	.	.	C	.	R	.	.	.	.	F	.	.	.	.	.	.	.	.	.	.	.	.	.	.
3	6406566	GC04	305-309	VH	VG	.	.	C	.	.	.	.	.	.	F	.	.	.	.	.	.	.	.	.	.	.	.	.	.
4	6406567	GC05	297-300	VH	VG	.	.	F	.	R	.	.	.	.	R	.	.	.	.	.	.	.	.	.	.	.	.	.	.
5	6406568	GC06	318-323	VH	VG	.	.	C	.	.	.	.	.	.	R	.	.	.	.	.	.	.	.	.	.	.	.	.	.
6	6406569	GC08	320-325	VH	VG	.	.	C	.	R	.	.	.	.	R	.	.	.	.	.	.	.	.	.	.	.	.	.	.
7	6406570	GC09	330-335	VH	VG	.	.	C	.	R	.	.	.	.	R	.	.	.	.	.	.	.	.	.	.	.	.	.	.
8	6406573	GC10	433-438	H	M-G	.	.	C	.	S	.	.	.	.	F	.	.	.	.	.	.	.	.	S	.	.	.	.	.
9	6406572	GC11	338-343	VH	VG	.	.	C	.	.	.	.	.	.	R	.	.	.	.	.	.	.	.	.	.	.	.	.	.
10	6406571	GC12	419-425	VH	M-G	.	.	C	R	R	.	.	.	.	F	R	.	R	.	.	.	R	R	.	R	.	.	.	R
11	6406575	GC14	485-490	H	M-G	.	.	C	.	.	.	.	.	.	F	S	.	.	.	.	.	.	.	.	.	.	.	.	.
12	6406574	GC15	232-236	H	M-G	.	.	C	.	R	.	.	.	.	F	.	.	.	.	.	.	.	.	.	.	.	.	.	.
13	6406576	GC16	285-290	H	M-G	.	.	C	.	.	.	.	.	.	F	.	.	.	.	.	.	.	.	.	.	.	.	.	.
14	6406577	GC18	205-210	H	M-G	.	.	C	.	.	.	.	.	.	F	.	.	.	.	.	.	.	.	.	.	.	.	.	.
15	6406578	GC21	275-280	VH	M-G	.	.	C	.	.	.	.	.	.	F	.	.	.	.	.	.	.	.	.	.	.	.	.	.
16	6406579	GC22	430-435	VH	G	.	.	C	.	R	.	.	.	.	F	.	.	.	.	.	.	.	.	.	.	.	.	.	.
17	6406580	GC23	418-424	VH	G	.	.	C	.	.	.	.	.	.	F	.	.	.	.	.	.	.	.	.	.	.	.	.	.
18	6406581	GC24	235-240	VH	G	.	.	C	.	R	.	.	.	.	F	.	.	.	.	.	.	.	.	.	.	.	.	.	.
19	6406582	GC25	318-325	VH	G	.	.	C	R	R	.	.	.	.	F	.	R	.	.	.	.	R	.	.	.	.	.	.	.
20	6406583	GC26	334-340	VH	G	.	.	C	.	.	.	.	.	.	F	.	.	.	.	.	.	.	.	.	.	.	.	.	.
21	6406584	GC27	219-225	H	G	.	.	C	.	.	.	.	.	.	F	.	.	.	.	.	.	.	.	.	.	.	.	.	.
22	6406587	DR1A1	-	B	-	.	.	.	.	.	.	.	.	.	.	.	.	.	.	.	.	.	.	.	.	.	.	.	.
23	6406586	DR1B1	-	H	M-G	.	.	.	.	.	R	F	F	C	C	.	.	.	.	F	F	.	.	.	.	R	R	.	.
24	6406585	DR5A6	-	M-H	P	S	S	C	F	.	.	.	.	.	F	.	.	.	.	.	.	R	.	R	F	.	.	.	R

	25 *Emiliania huxleyi*	26 *Gephyrocapsa aperta/ericsonii*	27 *Gephyrocapsa caribbeanica*	28 *Gephyrocapsa muellerae*	29 *Gephyrocapsa oceanica/parallela*	30 *Helicosphaera carteri*	31 *Helicosphaera inversa*	32 *Helicosphaera lophota*	33 *Neococcolithes dubius*	34 *Neococcolithes minutus*	35 *Oolithotus fragilis*	36 *Pontosphaera* spp.	37 *Pseudoemiliania lacunosa*	38 *Reticulofenestra asanoi*	39 *Reticulofenestra bisecta*	40 *Reticulofenestra dictyoda*	41 *Reticulofenestra gelida*	42 *Reticulofenestra pseudoumbilicus*	43 *Reticulofenestra* small spp.	44 *Rhabdosphaera claviger*	45 *Scapholithus fossilis*	46 *Scyphosphaera* spp.	47 *Scyphosphaera tubifera*	48 *Sphenolithus abies*	49 *Sphenolithus heteromorphus*	50 *Sphenolithus moriformis*	51 *Sphenolithus radians*	52 *Syracosphaera* spp. indet.	53 *Tetralithoides quadrilaminatus*	54 *Toweius crassus*	55 *Umbellosphaera* spp.	56 *Umbilicosphaera rotula*	57 *Umbilicosphaera* spp.	58 *Zygrhabilithus bijugatus*
1	.	25	30	55	C	F	R	.	.	.	.	F	2	.	.	.	.	.	.	F	R	.	.	.	.	.	.	F	.	.	F	.	F	.
2	.	62	23	53	C	F	R	.	.	.	.	F	2	.	.	.	.	.	.	F	R	.	.	.	.	.	.	F	.	.	F	.	F	.
3	.	10	60	61	C	F	R	.	.	.	.	F	.	.	.	.	.	.	.	F	R	.	.	.	.	.	.	C	.	.	F	.	F	.
4	.	.	123	65	C	F	R	.	.	.	.	F	.	.	.	.	.	.	.	F	R	.	.	.	.	.	.	F	.	.	F	.	F	.
5	.	25	83	71	C	F	R	.	.	.	.	F	.	.	.	.	.	.	.	F	R	.	.	.	.	.	.	C	.	.	F	.	F	.
6	.	27	85	92	C	F	.	.	.	.	.	F	.	.	.	.	.	.	.	F	R	.	.	.	.	.	.	C	.	.	F	.	F	.
7	.	19	25	87	C	F	R	.	.	.	.	F	.	.	.	.	.	.	.	F	R	.	.	.	.	.	.	C	.	.	F	.	F	.
8	.	27	48	82	C	C	.	.	.	.	.	F	.	.	.	.	.	.	.	F	R	.	.	.	.	.	.	F	.	.	F	.	F	.
9	.	21	52	104	C	F	R	.	.	.	.	R	.	.	.	.	.	.	.	F	R	.	.	.	.	.	.	F	.	.	F	.	F	.
10	.	10	71	68	C	C	.	.	.	.	.	R	16	.	.	.	R	R	F	F	R	.	.	R	.	.	.	C	S	.	F	R	F	.
11	60	52	18	25	C	C	.	.	.	.	.	F	.	.	S	.	R	.	.	F	R	.	.	.	.	.	.	C	.	.	F	.	F	.
12	15	57	39	33	C	C	R	.	.	.	.	.	.	.	.	.	.	.	.	F	R	.	.	.	.	.	.	F	.	.	F	.	F	.
13	93	38	28	24	C	C	.	.	.	.	.	F	2	.	.	.	.	.	.	F	R	.	.	.	.	.	.	C	.	.	F	.	F	.
14	52	28	19	23	C	C	.	.	.	.	.	F	2	.	.	.	.	.	.	F	R	.	.	.	.	.	.	C	.	.	F	.	F	.
15	41	39	30	29	C	C	.	.	.	.	.	F	.	.	.	.	.	.	.	F	R	.	.	.	.	.	.	C	.	.	F	.	F	.
16	6	76	6	47	C	C	.	.	.	.	.	F	.	.	.	.	.	.	.	F	R	.	.	.	.	.	.	C	.	.	F	.	F	.
17	28	58	30	22	C	C	.	.	.	.	.	F	.	.	.	.	.	.	.	F	R	.	.	.	.	.	.	C	.	.	F	.	F	.
18	13	41	36	42	C	C	.	.	.	.	.	F	.	.	.	.	.	.	.	F	R	.	.	.	.	.	.	C	.	.	F	.	F	.
19	.	11	48	91	.	C	.	.	.	.	.	R	.	.	.	.	R	.	.	F	R	.	.	S	.	.	.	C	.	.	R	.	F	.
20	.	84	86	.	C	C	.	.	.	.	.	F	37	.	.	.	.	.	.	F	R	.	.	.	.	.	.	C	.	.	F	.	F	.
21	.	28	46	57	C	C	.	.	.	.	.	F	.	.	.	.	.	.	.	F	R	.	.	.	.	.	.	C	.	.	F	.	F	.
22	.	.	.	.	.	.	.	.	.	.	.	.	.	.	.	.	.	.	.	.	.	.	.	.	.	.	.	.	.	.	.	.	.	.
23	.	.	.	.	.	.	.	F	R	R	.	.	.	.	.	C	.	.	.	.	.	.	.	.	.	R	R	.	.	R	.	.	.	F
24	.	.	C	.	.	.	.	.	.	.	.	F	.	.	.	.	C	.	A	F	.	R	R	F	S	F	.	F	.	.	.	F	.	.

	Total Counted	Total *Gephyrocapsa* spp. (excl. *G. oceanica*) + *E. huxleyi* + *P. lacunosa*	%*E. huxleyi*	%*G. aperta/ericsonii*	%*G. caribbeanica*	%*G. muellerae*	%*P. lacunosa*	CN/CP ZONE (Okada & Bukry, 1980)
			Quaternary nannofossil abundances					
1	112	112	0.0	22.3	26.8	49.1	1.8	CN13b/14a (?CN14b
2	140	140	0.0	44.3	16.4	37.9	1.4	CN13b/14a (?CN14b
3	131	131	0.0	7.6	45.8	46.6	0.0	CN14b
4	188	188	0.0	0.0	65.4	34.6	0.0	CN14b
5	179	179	0.0	14.0	46.4	39.7	0.0	CN14b
6	204	204	0.0	13.2	41.7	45.1	0.0	CN14b
7	131	131	0.0	14.5	19.1	66.4	0.0	CN14b
8	157	157	0.0	17.2	30.6	52.2	0.0	CN14b
9	177	177	0.0	11.9	29.4	58.8	0.0	CN14b
10	165	165	0.0	6.1	43.0	41.2	9.7	CN13b/14a
11	155	155	38.7	33.5	11.6	16.1	0.0	CN15
12	144	144	10.4	39.6	27.1	22.9	0.0	lower CN15
13	185	185	50.3	20.5	15.1	13.0	1.1	CN15
14	124	124	41.9	22.6	15.3	18.5	1.6	CN15
15	139	139	29.5	28.1	21.6	20.9	0.0	CN15
16	135	135	4.4	56.3	4.4	34.8	0.0	CN15
17	138	138	20.3	42.0	21.7	15.9	0.0	CN15
18	132	132	9.8	31.1	27.3	31.8	0.0	CN15
19	150	150	0.0	7.3	32.0	60.7	0.0	CN14b
20	207	207	0.0	40.6	41.5	0.0	17.9	CN13b/14a
21	131	131	0.0	21.4	35.1	43.5	0.0	CN14b
22	-	-	-	-	-	-	-	-
23	-	-	-	-	-	-	-	CP12
24	-	-	-	-	-	-	-	CN6-12b (?CN9b)

7.3. Calcareous nannofossil biostratigraphy

GC01 441-446 cm
Index nannofossil species
This zonal assignment is based on the presence of *Pseudoemiliania lacunosa,* the HO (highest occurrence) of which marks the top of Subzone CN14a, and the absence of *Calcidiscus macintyrei,* the HO of which marks the base of Subzone CN13b. This sample contains rare *Discoaster exilis,* an Early to Middle Miocene species, which is interpreted to be reworked. *P. lacunosa* is also rare in this sample, suggesting that it too may be reworked and that the sample may belong to Subzone CN14b.
Zone
CN13b/14a (?CN14b)
Age
Early to mid-Pleistocene (?Late Pleistocene)

GC02 354-360 cm
Index nannofossil species
This zonal assignment is based on the presence of *Pseudoemiliania lacunosa,* the HO of which marks the top of Subzone CN14a, and the absence of *Calcidiscus macintyrei,* the HO of which marks the base of Subzone CN13b. *P. lacunosa* is rare in this sample, suggesting that it may be reworked and that the sample may belong to Subzone CN14b.
Zone
CN13b/14a (?CN14b)
Age
Early to mid-Pleistocene (?Late Pleistocene)

GC04, 305-309 cm
Index nannofossil species
This zonal assignment is based on the absence of Pseudoemiliania lacunosa, the HO of which marks the top of Subzone CN14a, and the absence of Emiliania huxleyi, the LO (lowest occurrence) of which marks the base of Zone CN15.
Zone
CN14b
Age
Late Pleistocene

GC05 297-300 cm
Index nannofossil species
This zonal assignment is based on the absence of *Pseudoemiliania lacunosa,* the HO of which marks the top of Subzone CN14a, and the absence of *Emiliania huxleyi,* the LO of which marks the base of Zone CN15.
Zone
CN14b
Age
Late Pleistocence

GC06 318-323 cm
Index nannofossil species
This zonal assignment is based on the absence of *Pseudoemiliania lacunosa,* the HO of which marks the top of Subzone CN14a, and the absence of *Emiliania huxleyi,* the LO of which marks the base of Zone CN15.

Zone
CN14b
Age
Late Pleistocene

GC08 320-325 cm
Index nannofossil species
This zonal assignment is based on the absence of *Pseudoemiliania lacunosa,* the HO of which marks the top of Subzone CN14a, and the absence of *Emiliania huxleyi,* the LO of which marks the base of Zone CN15.
Zone
CN14b
Age
Late Pleistocene

GC09 330-335 cm
Index nannofossil species
This zonal assignment is based on the absence of *Pseudoemiliania lacunosa,* the HO of which marks the top of Subzone CN14a, and the absence of *Emiliania huxleyi,* the LO of which marks the base of Zone CN15.
Zone
CN14b
Age
Late Pleistocene

GC10 433-438 cm
Index nannofossil species
This zonal assignment is based on the absence of *Pseudoemiliania lacunosa,* the HO of which marks the top of Subzone CN14a, and the absence of *Emiliania huxleyi,* the LO of which marks the base of Zone CN15.
Zone
CN14b
Age
Late Pleistocene

GC11 338-343 cm
Index nannofossil species
This zonal assignment is based on the absence of *Pseudoemiliania lacunosa,* the HO of which marks the top of Subzone CN14a, and the absence of *Emiliania huxleyi,* the LO of which marks the base of Zone CN15.
Zone
CN14b
Age
Late Pleistocene

GC12 419-425 cm
Index nannofossil species
This zonal assignment is based on the presence of *Pseudoemiliania lacunosa,* the HO of which marks the top of Subzone CN14a, and the absence of *Calcidiscus macintyrei,* the HO of which marks the base of Subzone CN13b. This sample contains rare Miocene to Early Pliocene species such as *Cycliargolithus floridanus, Discoaster deflandrei, D. pentaradiatus, D. quinqueramus,* which are interpreted to be reworked. The reworked specimens are poorly preserved, in contrast to

the Pleistocene assemblage, which is well preserved. *Calcidiscus macintyrei* is present in the sample, but all specimens of *C. macintyrei* observed are in the same poor state of preservation as the reworked Miocene/Pliocene specimens, so they are also interpreted to be reworked.

Zone

CN13b/14a

Age

Early to mid-Pleistocene

GC14 485-490 cm

Index nannofossil species

This zonal assignment is based on the presence of *Emiliana huxleyi,* the LO of which marks the base of Zone CN15.

Zone

CN15

Age

Late Pleistocenc

GC15 232-236 cm

Index nannofossil species

This zonal assignment is based on the presence of *Emiliana huxleyi,* the LO of which marks the base of Zone CN15, and the HO of *Helicosphaera inversa,* which occurs midway through Zone CN15.

Zone

Lower CN15

Age

Late Pleistocene

GC16 285-290 cm

Index nannofossil species

This zonal assignment is based on the presence of *Emiliana huxleyi,* the LO of which marks the base of Zone CN15. Rare *Pseudoemiliania lacunosa* are present, which are interpreted as reworked.

Zone

CN15

Age

Late Pleistocene

GC18 205-210 cm

Index nannofossil species

This zonal assignment is based on the presence of *Emiliana huxleyi,* the LO of which marks the base of Zone CN15. Rare *Pseudoemiliania lacunosa* are present, which are interpreted as reworked.

Zone

CN15

Age

Late Pleistocene

GC21 275-280 cm
Index nannofossil species
This zonal assignment is based on the presence of *Emiliana huxleyi,* the LO of which marks the base of Zone CN15.
Zone
CN15
Age
Late Pleistocene

GC22 430-435 cm
Index nannofossil species
This zonal assignment is based on the presence of *Emiliana huxleyi,* the LO of which marks the base of Zone CN15.
Zone
CN15
Age
Late Pleistocene

GC23 418-424 cm
Index nannofossil species
This zonal assignment is based on the presence of *Emiliana huxleyi,* the LO of which marks the base of Zone CN15.
Zone
CN15
Age
Late Pleistocene

GC24 235-240 cm
Index nannofossil species
This zonal assignment is based on the presence of *Emiliana huxleyi,* the LO of which marks the base of Zone CN15.
Zone
CN15
Age
Late Pleistocene

GC25 318-325 cm
Index nannofossil species
This zonal assignment is based on the absence of *Pseudoemiliania lacunosa,* the HO of which marks the top of Subzone CN14a, and the absence of *Emiliania huxleyi,* the LO of which marks the base of Zone CN15.
Zone
CN14b
Age
Late Pleistocene

GC26 334-340 cm
Index nannofossil species
This zonal assignment is based on the presence of *Pseudoemiliania lacunosa,* the HO of which marks the top of Subzone CN14a, and the absence of *Calcidiscus macintyrei,* the HO of which marks the base of Subzone CN13b.

Zone
CN13b/14a
Age
Early to mid-Pleistocene

GC27 219-225 cm
Index nannofossil species
This zonal assignment is based on the absence of *Pseudoemiliania lacunosa,* the HO of which marks the top of Subzone CN14a, and the absence of *Emiliania huxleyi,* the LO of which marks the base of Zone CN15.
Zone
CN14b
Age
Late Pleistocene

DR1A1
Barren of nannofossils.

DR1B1
Index nannofossil species
This zonal assignment is based on the presence of *Discoaster kuepperi,* the HO of which marks the top of Zone CP12, and the presence of *D. sublodoensis,* the LO of which marks the base of Zone CP12.
Zone
CP12
Age
Late Early to earliest Middle Eocene

DR5A6
Index nannofossil species
Preservation in this sample is poor from this soft micrite infilling in a hyaloclastite, so zonal assignment is tentative. The presence of Neogene discoasters with 5 rays (none of which were observed to be asymmetric) suggests that the sample belongs to Zones CN6-CN12b. The presence of single specimens of *Amaurolithus amplificus* (which ranges within CN9b) and *A. primus* (which ranges from within CN9b to CN10) suggest that the sample belongs to Zone CN9b. The presence of the Lower Miocene *Sphenolithus heteromorphus* suggests that some reworked material is present in the sample.
Zone
CN6-12b (?CN9b)
Age
Late Miocene to Early Late Pliocene (?late Late Miocene)

8. PLANKTIC FORAMINIFERAL BIOSTRATIGRAPHY OF SAMPLES FROM *FRANKLIN* FR9/01 SAMPLES

George C. Chaproniere

8.1. Introduction

Twenty-four samples (21 from low in cores; 3 from dredges) from R/V *Franklin* Cruise FR9/01 have been examined for planktic foraminiferal biostratigraphic determinations. Washed residues were supplied by Geoscience Australia. All core samples contain abundant and well preserved Pleistocene planktic foraminiferal faunas; two of the dredge samples contain poorly preserved foraminiferal assemblages, and the assemblage of the third is siliceous and made up mainly of radiolaria with some diatoms. The planktic foraminiferal biostratigraphic results are summarised in Table 8, using the tropical zonal scheme of Berggren et al. (1995a, b) and the temperate scheme of Jenkins (1985, 1993a, b). For the Quaternary, the scheme adopted is that of Chaproniere (1991). Species occurrence is recorded in Table 9. Overall the planktic assemblages in the cores are similar to those reported on from the Coral Sea (Chaproniere, 1991, 1996) and from the Lau Basin (Chaproniere et al., 1994), although temperate water species are more abundant in these samples, reflecting their more southern location. Two late Early Eocene samples, one with numerous radiolaria, were also identified from one dredge haul. Another dredge haul contains an Early Pliocene assemblage in micrite within a volcanic breccia.

The planktic assemblages found in the core samples are typically subtropical to warm temperate, and tend to be dominated either by the *Globorotalia (Truncorotalia)* or the *Gr. inflata* groups.

8.2. Sample descriptions

CORES

Sample: 6406564 GC01, 441-446 cm
The planktic foraminiferal assemblage is very well preserved, and of moderately high diversity. The presence of *Globorotalia truncatulinoides,* with *Gr. hessi, Bolliella praeadamsi* and *Pulleniatina finalis* (very rare), but without *Globigerinella calida*, indicates Zone N.22, *Bolliella praeadamsi* Subzone; pink *Globigerinoides ruber* is also present, indicating ages older than 120,000 years. The *Gr. inflata* group dominates the assemblage. The presence of specimens of *Gr. inflata* and dextral *Neogloboquadrina pachyderma* and rare *Sphaeroidinella dehiscens* suggests a greater influence of the temperate water masses than of the tropical. The absence of pteropods, preservation of the fauna (fragmentation very low), the presence of the solution susceptible *Hastigerina pelagica* and the proportion of benthic foraminiferids (<5%) are consistent with the water depths existing at this site (1297m) at present, although the aragonite compensation depth (ACD) may have been shallow in this area.

Table 8. Summary of planktic foraminiferal biostratigraphy

Number	Sample	Zone	Subzone	Comments
6406564	GC01, 441-446cm	N.22	*Bolliella praeadamsi*	*Gr. inflata* group dominant.
6406565	GC02, 356-360cm	N.22	*Bolliella praeadamsi*	*Gr. inflata* group dominant.
6406566	GC04, 305-309cm	N.23	*Globigerinella calida*	*Gr. (Truncorotalia)* group dominant.
6406567	GC05, 297-300cm	N.22	*Bolliella praeadamsi*	*Gr. (Truncorotalia)* group dominant.
6406568	GC06, 318-323cm	N.22	*Globorotalia hessi*	*Gr. (Truncorotalia)* group dominant.

(table continued overleaf)

6406569	GC08, 320-325cm	N.22	*Bolliella praeadamsi*	Both groups equal.
6406570	GC09, 330-335cm	N.22	*Bolliella praeadamsi*	*Gr. (Truncorotalia)* group dominant.
6406573	GC10, 433-438cm	N.22	*Bolliella praeadamsi*	*Gr. (Truncorotalia)* group dominant.
6406572	GC11, 338-343cm	N.22	*Globorotalia hessi*	*Gr. (Truncorotalia)* group dominant.
6406571	GC12, 419-425cm	N.22	*Globorotalia hessi*	*Gr. (Truncorotalia)* group dominant.
6406575	GC14, 485-490cm	N.22	*Bolliella praeadamsi*	*Gr. inflata* group dominant.
6406574	GC15, 232-236cm	N.22	*Bolliella praeadamsi*	*Gr. inflata* group dominant.
6406576	GC16, 285-290cm	N.22	*Bolliella praeadamsi*	*Gr. inflata* group dominant.
6406577	GC18, 205-210cm	N.22	*Bolliella praeadamsi*	*Gr. inflata* group dominant.
6406578	GC21, 275-280cm	N.23	*Globigerinella calida*	*Gr. inflata* group dominant.
6406579	GC22, 430-435cm	N.22	*Bolliella praeadamsi*	*Gr. (Truncorotalia)* group dominant.
6406580	GC23, 418-424cm	N.22	*Bolliella praeadamsi*	*Gr. inflata* group dominant.
6406581	GC24, 235-240cm	N.22	*Bolliella praeadamsi*	*Gr. inflata* group dominant.
6406582	GC25, 318-325cm	N.22	*Globorotalia hessi*	*Gr. (Truncorotalia)* group dominant.
6406583	GC26, 334-340cm	N.22	*Globorotalia hessi*	*Gr. (Truncorotalia)* group dominant.
6406584	GC27, 219-225cm	N.22	*Globorotalia hessi*	*Gr. (Truncorotalia)* group dominant.
6406587	DR01A1	P9; SP7		Dominated by radiolarians
6406588	DR01B1	P9; SP7		Poor preservation
6406589	DR05A6	N.19; SN12	SN12a, *Gr. pliozea*	Warm temperate assemblage

Note for non-specialists: The *Globigerinella callida* subzone is the youngest, the *Bolliella praeadamsi* subzone lies between, and the *Globorotalia hessi* subzone is the oldest.

Sample: 6406565 GC02, 354-360 cm

The planktic foraminiferal assemblage is very well preserved, and of moderately high diversity. The presence of *Globorotalia truncatulinoides,* with *Gr. hessi*, *Bolliella praeadamsi* and *Pulleniatina finalis* (very rare), but without *Globigerinella calida,* indicates Zone N.22, *Bolliella praeadamsi* Subzone; pink *Globigerinoides ruber* is also present indicating ages older than 120,000 years. The *Gr. inflata* group dominates the assemblage. The presence of specimens of *Gr. inflata* and rare *Sphaeroidinella dehiscens* suggests a greater influence of the temperate water masses than of the tropical. The absence of pteropods, preservation of the fauna (fragmentation low) and the proportion of benthic foraminiferids (<5%) are consistent with the water depths existing at this site (2635m).

Sample: 6406566 GC04, 305-309 cm

The planktic foraminiferal assemblage is very well preserved, and of moderately high diversity. The presence of *Globorotalia truncatulinoides,* with *Gr. hessi, Bolliella praeadamsi, Pulleniatina finalis* (very rare) and *Globigerinella calida,* indicates Zone N.23, *Globigerinella calida* Subzone; pink *Globigerinoides ruber* is also present indicating ages older than 120,000 years, that is in the lower part of the subzone. The *Globorotalia (Truncorotalia)* group dominates the *Gr. inflata* group in this assemblage. The presence of specimens of *Gr. inflata* and rare *Sphaeroidinella dehiscens* suggests the influence of both temperate and tropical water masses. The absence of pteropods, preservation of the fauna (fragmentation low) and the proportion of benthic foraminiferids (<5%) are consistent with the water depths existing at this site (2586m).

Sample: 6406567 GC05, 297-300 cm
The planktic foraminiferal assemblage is very well preserved, and of moderately high diversity. The presence of *Globorotalia truncatulinoides,* with *Gr. hessi, Bolliella praeadamsi* and *Pulleniatina finalis* (very rare), but without *Globigerinella calida,* indicates Zone N.22, *Bolliella praeadamsi* Subzone; pink *Globigerinoides ruber* is also present indicating ages older than 120,000 years. The *Globorotalia (Truncorotalia)* group dominates the *Gr. inflata* group in this assemblage. The presence of specimens of *Gr. inflata,* which are of smaller size and are rarer than in other samples, *Neogloboquadrina pachyderma* (dextral) and rare *Sphaeroidinella dehiscens* suggests the influence of both temperate and tropical water masses. The absence of pteropods, preservation of the fauna (fragmentation low) and the proportion of benthic foraminiferids (<5%) are consistent with the water depths existing at this site (2706m).

Sample: 6406568 GC06, 318-323 cm
The planktic foraminiferal assemblage is very well preserved, and of moderately high diversity. The presence of *Globorotalia truncatulinoides,* with *Gr. hessi,* but without *Bolliella praeadamsi* and *Pulleniatina finalis* indicates Zone N.22, *Globorotalia hessi* Subzone; pink *Globigerinoides ruber* is also present indicating ages older than 120,000 years. The *Globorotalia (Truncorotalia)* and *Gr. cultrata* groups dominate the assemblage. The presence of specimens of *Gr. inflata* and rare *Sphaeroidinella dehiscens* suggests the influence of both temperate and tropical water masses. The absence of pteropods, preservation of the fauna (fragmentation moderate in the -125µm fraction) and the proportion of benthic foraminiferids (<5%) are consistent with the water depths existing at this site (2764m).

Sample: 6406569 GC08, 320-325 cm
The planktic foraminiferal assemblage is very well preserved, and of moderately high diversity. The presence of *Globorotalia truncatulinoides,* with *Gr. hessi, Bolliella praeadamsi* and *Pulleniatina finalis* (very rare), but without *Globigerinella calida,* indicates Zone N.22, *Bolliella praeadamsi* Subzone; pink *Globigerinoides ruber* is also present indicating ages older than 120,000 years. The *Globorotalia (Truncorotalia)* and *Gr. inflata* groups equally dominate the assemblage. The presence of specimens of *Gr. inflata, Neogloboquadrina pachyderma* (dextral) and rare *Globorotalia tumida*, *Sphaeroidinella dehiscens* suggests the influence of both temperate and tropical water masses. The absence of pteropods, preservation of the fauna (fragmentation low) and the proportion of benthic foraminiferids (<5%) are consistent with the water depths existing at this site (2700m).

Sample: 6406570 GC09, 330-335 cm
The planktic foraminiferal assemblage is very well preserved, and of moderately high diversity. The presence of *Globorotalia truncatulinoides,* with *Gr. hessi, Bolliella praeadamsi* and *Pulleniatina finalis* (very rare), but without *Globigerinella calida,* indicates Zone N.22, *Bolliella praeadamsi* Subzone; pink *Globigerinoides ruber* is also present, indicating ages older than 120,000 years. The *Globorotalia (Truncorotalia)* group dominates the assemblage. The presence of rare specimens of *Gr. inflata, Gr. flexuosa* and *Sphaeroidinella dehiscens* suggests the influence of both temperate and tropical water masses. The absence of pteropods, preservation of the fauna (fragmentation low) and the proportion of benthic foraminiferids (<5%) are consistent with the water depths existing at this site (2840m).

Sample: 6406573 GC10, 433-438 cm
The planktic foraminiferal assemblage is very well preserved, and of moderately high diversity. The presence of *Globorotalia truncatulinoides,* with *Gr. hessi, Bolliella praeadamsi* and *Pulleniatina finalis* (very rare), but without *Globigerinella calida,* indicates Zone N.22, *Bolliella praeadamsi*

Subzone; pink *Globigerinoides ruber* is also present indicating ages older than 120,000 years. The *Globorotalia (Truncorotalia)* group dominates the assemblage. The presence of rare specimens of *Gr. inflata,* and *Sphaeroidinella dehiscens* suggests the influence of both temperate and tropical water masses. The presence of a single, brown-stained specimen of *Globorotalia limbata* (Middle Miocene to Pliocene) suggests some reworking from older beds The absence of pteropods, preservation of the fauna (fragmentation low), presence of *Hastigerina pelagica* and the proportion of benthic foraminiferids (<5%) suggest water depths shallower than currently existing at this site (2580m).

Sample: 6406572 GC11, 338-343 cm
The planktic foraminiferal assemblage is very well preserved, and of moderately high diversity. The presence of *Globorotalia truncatulinoides,* with *Gr. hessi,* without *Bolliella praeadamsi* and *Pulleniatina finalis,* indicates Zone N.22, *Globorotalia hessi* Subzone; pink *Globigerinoides ruber* is also present indicating ages older than 120,000 years. The specimens of *Gr. hessi* show weak spiral side concavity; this together with the presence of the ancestral form, *Gr. ronda*, may suggest a level low in the subzone. The *Globorotalia (Truncorotalia)* and *Gr. cultrata* groups dominate the assemblage. The presence of specimens of *Gr. inflata* and rare *Gr. tumida* and *Sphaeroidinella dehiscens* suggests the influence of both temperate and tropical water masses. The absence of pteropods, preservation of the fauna (fragmentation low) and the proportion of benthic foraminiferids (<5%) are consistent with the water depths existing at this site (2820m).

Sample: 6406571 GC12, 419-425 cm
The planktic foraminiferal assemblage is very well preserved, and of moderately high diversity. The presence of *Globorotalia truncatulinoides,* with *Gr. hessi,* but without *Bolliella praeadamsi* and *Pulleniatina finalis* indicates Zone N.22, *Globorotalia hessi* Subzone; pink *Globigerinoides ruber* is absent. The presence of very rare *Gr. tosaensis* suggests a level low in the subzone. The *Globorotalia (Truncorotalia)* and *Gr. cultrata* groups dominate the assemblage. The presence of specimens of *Gr. inflata* and *Gr. tumida* (dominant menardiform) and *Sphaeroidinella dehiscens* suggests the influence of both temperate and tropical water masses. The absence of pteropods, preservation of the fauna (fragmentation moderate) and the proportion of benthic foraminiferids (<5%) are consistent with the water depths existing at this site (3517m).

Sample: 6406575 GC14, 485-490 cm
The planktic foraminiferal assemblage is very well preserved, and of moderately high diversity. The presence of *Globorotalia truncatulinoides,* with *Gr. hessi, Bolliella praeadamsi* and *Pulleniatina finalis* (very rare), without *Globigerinella calida,* indicates Zone N.22, *Bolliella praeadamsi* Subzone; pink *Globigerinoides ruber* is absent. The *Globorotalia (Truncorotalia)* group is rare, with *Gr. inflata* dominating the assemblage. The presence of *Gr. inflata, Globigerina bulloides* (common) and *Neogloboquadrina pachyderma* with *Sphaeroidinella dehiscens* suggests a greater influence of temperate water masses than of the tropical. The absence of pteropods, preservation of the fauna (fragmentation low) and the proportion of benthic foraminiferids (<5%) suggest water depths shallower than currently existing at this site (2720m).

Sample: 6406574 GC15, 232-236 cm
The planktic foraminiferal assemblage is very well preserved, and of moderately high diversity. The presence of *Globorotalia truncatulinoides,* with *Gr. hessi*, *Bolliella praeadamsi* and *Pulleniatina finalis* (very rare), but without *Globigerinella calida,* indicates Zone N.22, *Bolliella praeadamsi* Subzone; pink *Globigerinoides ruber* is also present indicating ages older than 120,000 years. The *Globorotalia inflata* group dominates the assemblage. The presence of specimens of *Gr. inflata,* common *Globigerina bulloides* and dextral *Neogloboquadrina pachyderma* and rare *Sphaeroidinella dehiscens* suggests a greater influence of temperate water masses than of the

tropical. The absence of pteropods, preservation of the fauna (fragmentation low) and the proportion of benthic foraminiferids (<5%) are consistent with the water depths existing at this site (2140m) at present.

Sample: 6406576 GC16, 285-290 cm
The planktic foraminiferal assemblage is very well preserved, and of moderately high diversity. The presence of *Globorotalia truncatulinoides,* with *Gr. hessi, Bolliella praeadamsi* and *Pulleniatina finalis* (very rare), but without *Globigerinella calida,* indicates Zone N.22, *Bolliella praeadamsi* Subzone; pink *Globigerinoides ruber* is also present indicating ages older than 120,000 years. The *Globorotalia inflata* group dominates the assemblage. The presence of specimens of *Gr. inflata, Globigerina bulloides* and dextral *Neogloboquadrina pachyderma* and rare *Sphaeroidinella dehiscens* suggests a greater influence of temperate water masses than of the tropical. The absence of pteropods, preservation of the fauna (fragmentation low) and the proportion of benthic foraminiferids (<5%) are consistent with the water depths existing at this site (2100m) at present.

Sample: 6406577 GC18, 205-210 cm
The planktic foraminiferal assemblage is very well preserved, and of moderately high diversity. The presence of *Globorotalia truncatulinoides,* with *Gr. hessi, Bolliella praeadamsi* and *Pulleniatina finalis* (very rare), but without *Globigerinella calida,* indicates Zone N.22, *Bolliella praeadamsi* Subzone; pink *Globigerinoides ruber* is also present, indicating ages older than 120,000 years. The *Globorotalia inflata* group dominates the assemblage. The presence of specimens of *Gr. inflata,* common *Globigerina bulloides* and dextral *Neogloboquadrina pachyderma* and rare *Sphaeroidinella dehiscens* suggests a greater influence of temperate water masses than of the tropical. The absence of pteropods, preservation of the fauna (fragmentation low) and the proportion of benthic foraminiferids (<5%) are consistent with the water depths existing at this site (2590m) at present.

Sample: 6406578 GC21, 275-280 cm
The planktic foraminiferal assemblage is very well preserved, and of moderately high diversity. The presence of *Globorotalia truncatulinoides,* with *Gr. hessi, Bolliella praeadamsi, Pulleniatina finalis* (very rare) and *Globigerinella calida,* indicates Zone N.23, *Globigerinella calida* Subzone; pink *Globigerinoides ruber* is also present indicating ages older than 120,000 years, that is in the lower part of the subzone. The *Globorotalia inflata* group dominates the assemblage. The presence of *Gr. inflata* and rare *Sphaeroidinella dehiscens* suggests the influence of both temperate and tropical water masses. The absence of pteropods, preservation of the fauna (fragmentation low) and the proportion of benthic foraminiferids (<5%) are consistent with the water depths existing at this site (2810m).

Sample: 6406579 GC22, 430-435 cm
The planktic foraminiferal assemblage is very well preserved, and of moderately high diversity. The presence of *Globorotalia truncatulinoides,* with *Gr. hessi, Bolliella praeadamsi* and *Pulleniatina finalis*, but without *Globigerinella calida,* indicates Zone N.22, *Bolliella praeadamsi* Subzone; pink *Globigerinoides ruber* is very rare and indicates ages older than 120,000 years. The *Globorotalia (Truncorotalia)* group dominates the *Gr. inflata* group in this assemblage. The presence of specimens of *Gr. inflata* and *Globigerina bulloides* with *Sphaeroidinella dehiscens* suggests the influence of both temperate and tropical water masses. The absence of pteropods, preservation of the fauna (fragmentation low) and the proportion of benthic foraminiferids (<5%) may suggest shallower water depths to those existing presently at this site (3405m).

Sample: 6406580 GC23, 418-424 cm
The planktic foraminiferal assemblage is very well preserved, and of moderately high diversity. The presence of *Globorotalia truncatulinoides,* with *Gr. hessi, Bolliella praeadamsi* and *Pulleniatina*

finalis, but without *Globigerinella calida,* indicates Zone N.22, *Bolliella praeadamsi* Subzone; pink *Globigerinoides ruber* indicates ages older than 120,000 years. The *Gr. inflata* group dominates the very rare *Globorotalia (Truncorotalia)* group in this assemblage. The presence of specimens of *Gr. inflata, Neogloboquadrina pachyderma* and *Globigerina bulloides* with *Sphaeroidinella dehiscens* suggests the temperate water mass has a greater influence on the assemblages than the tropical water mass. The absence of pteropods, preservation of the fauna (fragmentation low) and the proportion of benthic foraminiferids (<5%) are consistent with the water depths existing at this site (3392m).

Sample: 6406581 GC24, 235-240 cm
The planktic foraminiferal assemblage is very well preserved, and of moderately high diversity. The presence of *Globorotalia truncatulinoides,* with *Gr. hessi, Bolliella praeadamsi* and *Pulleniatina finalis*, but without *Globigerinella calida,* indicates Zone N.22, *Bolliella praeadamsi* Subzone; pink *Globigerinoides ruber* is very rare and indicates ages older than 120,000 years. The *Gr. inflata* group dominates the rare *Globorotalia (Truncorotalia)* group in this assemblage. The presence of specimens of *Gr. inflata, Neogloboquadrina pachyderma* and *Globigerina bulloides* with *Sphaeroidinella dehiscens* suggests the temperate water mass has a greater influence on the assemblages than the tropical water mass. The absence of pteropods, preservation of the fauna (fragmentation low) and the proportion of benthic foraminiferids (<5%) are consistent with the water depths existing at this site (3450m).

Sample: 6406582 GC25, 318-325 cm
The planktic foraminiferal assemblage is very well preserved, and of moderately high diversity. The presence of *Globorotalia truncatulinoides,* with *Gr. hessi,* but without *Bolliella praeadamsi* and *Pulleniatina finalis,* indicates Zone N.22, *Globorotalia hessi* Subzone; the presence of questionable specimens of *Gr. tosaensis* (broken) may indicate a level low in the subzone. Pink *Globigerinoides ruber* is very rare. The *Globorotalia (Truncorotalia)* and *Gr. cultrata* groups dominate the assemblage. The presence of specimens of *Gr. inflata, Neogloboquadrina pachyderma* and *Sphaeroidinella dehiscens* suggests the influence of both temperate and tropical water masses. The absence of pteropods, preservation of the fauna (fragmentation moderate) and the proportion of benthic foraminiferids (<5%) are consistent with the water depths existing at this site (3239m).

Sample: 6406583 GC26, 334-340 cm
The planktic foraminiferal assemblage is very well preserved, and of moderately high diversity. The presence of *Globorotalia truncatulinoides,* with *Gr. hessi,* but without *Bolliella praeadamsi* and *Pulleniatina finalis,* indicates Zone N.22, *Globorotalia hessi* Subzone; pink *Globigerinoides ruber* is absent. The *Globorotalia (Truncorotalia)* and *Gr. cultrata* groups dominate the assemblage. The presence of specimens of *Gr. inflata, Neogloboquadrina pachyderma* and *Gr. ronda* and *Sphaeroidinella dehiscens* suggests the influence of both temperate and tropical water masses. The absence of pteropods, preservation of the fauna (fragmentation moderate) and the proportion of benthic foraminiferids (<5%) are consistent with the water depths existing at this site (2935m).

Sample: 6406584 GC27, 219-225 cm
The planktic foraminiferal assemblage is very well preserved, and of moderately high diversity. The presence of *Globorotalia truncatulinoides,* with *Gr. hessi,* but without *Bolliella praeadamsi* and *Pulleniatina finalis,* indicates Zone N.22, *Globorotalia hessi* Subzone; pink *Globigerinoides ruber* is present. The *Globorotalia (Truncorotalia)* group dominates the assemblage. The presence of specimens of *Gr. inflata, Ga. bulloides* with *Gr. ronda* and *Sphaeroidinella dehiscens* suggests the influence of both temperate and tropical water masses. The absence of pteropods, preservation of the fauna (fragmentation low) and the proportion of benthic foraminiferids (<5%) are consistent with the water depths existing at this site (1875m).

DREDGES

Sample: 6406587 DR01A1

The assemblage is difficult to study because the degree of cementation makes study of specimens difficult. For this reason it is not possible to make a palaeoenvironmental assessment. However, sufficient key species have been identified for dating purposes. The overlap of *Morozovella crater* (= *M. caucasica*) with *Acarinina primitiva* and *Ac. spinuloinflata* indicates subtropical/tropical Zone P9, and within the temperate *Morozovella crater* Zone. The age is thus late Early Eocene.

Sample: 6406588 DR01B1

This sample has a very high siliceous faunal component – it is dominated by radiolaria, and rare diatoms are also present. Well preserved planktic foraminiferids are present, but because of their dilution by the siliceous groups, no palaeoenvironmental analysis has been attempted. The foraminiferal assemblage is very similar to that from DR01A1, but is more diverse. The overlap of *Morozovella crater* (= *M. caucasica*) with *Acarinina primitiva, Ac. soldadoensis* and *Ac. spinuloinflata* indicates subtropical/tropical Zone P9, and within the temperate *Morozovella crater* Zone. The age is late Early Eocene.

Sample: 6406589 DR05A6

The assemblage of this sample is generally poorly preserved, with many specimens coated by cements, making identification difficult. However some specimens have better preservation, permitting good identification and biostratigraphic assessment. The overall poor preservation means that palaeoenvironmental assessment cannot be made. The overlap of *Globorotalia pliozea* with *Gr. puncticulata* indicates temperate Zone SN12, SN12a *Gr. pliozea* Subzone. Also, the overlap of *Gr. margaritae* with *Gr. cibaoensis* and *Gr. crassula* without *Gr. crassaformis* indicates tropical/subtropical Zone N19. The age is thus middle Early Pliocene. This fauna is a mix of subtropical and temperate species suggesting a warm water influence in this area at the time.

8.3. Comments and recommendations

The distribution of warm and cool water indicators in the suite of core samples is interesting. It would be expected that the northern samples would consistently tend to contain more warm water forms (*Gr. tumida*, *Gr. ronda*) than cool water forms (*Ne. pachyderma*, *Ga. bulloides*). Though *Gr. inflata* is present in most samples, its numerical relationship to the *Globorotalia (Truncorotalia)* group would be expected to be related to location – the *Gr. inflata* group should dominate the southern assemblages. However, this is not always the case. Instead the warm water forms dominate in all samples from the *Globorotalia hessi* Subzone of Zone N22, be they northern or southern. Of the 13 samples from the younger *Bolliella praeadamsi* Subzone, only in four is the *Gr. (Truncorotalia)* group dominant; three of these (GC05, 09, 10) are northern, one (GC22) is southern. Of the two from the (youngest) *Globigerinella calida* Subzone, one (GC21) is dominated by *Gr. inflata*, and the other (GC04) dominated by the *Gr. (Truncorotalia)* group, which is what should be expected. Examination of surface sediment samples would be expected to show this same trend, and they should also be studied. The patterns observed may well be reflecting movements in oceanic fronts controlled by climatic variation. This changing relationship between warmer and cooler forms is obviously chronologic rather than geographic (spatial). In order to investigate this relationship, it is recommended that a more detailed study of the cores penetrating into the older section (in particular the longer ones GC12, from the north, and GC25, from further south, and GC22 a multicoloured core from the south) should be made. Selected surface samples should also be studied, perhaps the core-top samples, although much of the modern sediment may have been lost during the coring operation.

Table 9. Chart showing distribution of planktic foraminiferids in the studied samples.

Sample Depth	*Acarinina bullbrooki*	*Acarinina primitiva*	*Acarinina soldadoensis*	*Acarinina spinuloinflata*	*Beella digitata*	*Bolliella praeadamsi*	*Candeina nitida*	*Dentoglobigerina altispira*	*Globigerina bulloides*	*Globigerina falconensis*	*Globigerina quinqueloba*	*Globigerinella aequilateralis*	*Globigerinella calida*	*Globigerinella obesa*	*Globigerinella praecalida*	*Globigerinita glutinata*	*Globigerinita uvula*	*Globigerinoides conglobatus*	*Globigerinoides elongatus*	*Globigerinoides extremus*	*Globigerinoides immaturus*
Fr09/01-DR1A1	X	X		X																	
Fr09/01-DR1B1			X	X														X			
Fr09/01-DR5A6								X	X		X					X				X	
Fr09/01-GC01, 441-446						X	X			X	X	X				X		X	X		X
Fr09/01-GC02, 354-360					X					X	X	X			X	X		X	X		X
Fr09/01-GC04, 305-309					X	X			X				X		X			X	X		
Fr09/01-GC05, 297-300						X			X		X	X	?		X	X		X	X		X
Fr09/01-GC06, 318-323							X		X		X	X			X	X		X	X		X
Fr09/01-GC08, 320-325					X	X	X		X	X	X	X			X	X		X	X		X
Fr09/01-GC09, 330-335						X	X		X	X	X	X	?		X			X	X		X
Fr09/01-GC10, 433-438					X	X	X		X	X	X	X		X	X	X		X	X		
Fr09/01-GC11, 338-343					X				X	X	X	X			X	X		X	X		
Fr09/01-GC12, 419-425					X		X		X		X	X		X	X	X		X	X		X
Fr09/01-GC14, 485-490					X	X			X	X	X	X			X	X	X	X	X		
Fr09/01-GC15, 232-236					X	X			X	X	X	X			X	X		X	X		
Fr09/01-GC16, 285-290					X	X			X	X	X	X			X	X			X		
Fr09/01-GC18, 205-210						X			X	X	X	X		X	X			X	X		
Fr09/01-GC21, 275-280					X	X			X	X	X	X	X		X	X		X	X		
Fr09/01-GC22, 430-435					X	X			X		X	X			X	X		X	X		X
Fr09/01-GC23, 418-424					X	X			X		X	X			X	X		X	X		X
Fr09/01-GC24, 235-240					X	X			X	X	X	X			X	X		X	X		X
Fr09/01-GC25, 318-325					X	?			X		X	X			X	X		X	X		
Fr09/01-GC26, 334-340					X	?			X	X		X			X	X		X	X		X
Fr09/01-GC27, 219-225					X		X		X	X		X			X	X		X	X		X

Sample Depth	*Globigerinoides ruber* pink	*Globigerinoides ruber* white	*Globigerinoides sacculifer*	*Globorotalia bermudezi*	*Globorotalia cibaoensis*	*Globorotalia crassaconica*	*Globorotalia crassaformis* (dex)	*Globorotalia crassaformis* (sin)	*Globorotalia crassula*	*Globorotalia cultrata*	*Globorotalia fimbriata*	*Globorotalia flexuosa*	*Globorotalia hessi*	*Globorotalia inflata* (sin)	*Globorotalia limbata*	*Globorotalia margaritae*	*Globorotalia menardii*	*Globorotalia neoflexuosa*	*Globorotalia pliozea*	*Globorotalia puncticulata*	*Globorotalia ronda*
Fr09/01-DR1A1																					
Fr09/01-DR1B1																					
Fr09/01-DR5A6					X				X						X	X	X		X	X	
Fr09/01-GC01, 441-446	X	X	X				X	X	X	X			X	X			X	X			
Fr09/01-GC02, 354-360	X	X	X				X	X	X	X			X	X			X	X			
Fr09/01-GC04, 305-309	X	X	X				X	X		X			X	X			X				
Fr09/01-GC05, 297-300	X	X	X					X	X				X	X			X	X			
Fr09/01-GC06, 318-323	X	X	X				X			X	?		X	X			X	X			?
Fr09/01-GC08, 320-325	X	X	X				X	X		X			X	X			X	X			X
Fr09/01-GC09, 330-335	X		X				X	X		X		X	X	X			X	X			?
Fr09/01-GC10, 433-438	X	X	X	X			X			X			X	X	r		X	X			
Fr09/01-GC11, 338-343	X	X	X			X	X	X		X			X	X			X	X			X
Fr09/01-GC12, 419-425		X	X					X				X	X	X			X				
Fr09/01-GC14, 485-490		X	X				X						X	X			X				
Fr09/01-GC15, 232-236	X	X	X				X	X					X	X			X				
Fr09/01-GC16, 285-290	X	X	X				X	X					X	X			X	X			
Fr09/01-GC18, 205-210	X	X				X	X						X	X			X	X			
Fr09/01-GC21, 275-280	X	X	X	X		X	X						X	X			X	X			
Fr09/01-GC22, 430-435	X	X	X			X	X						X	X			X				
Fr09/01-GC23, 418-424	X	X	X				X		X				X	X			X	X			
Fr09/01-GC24, 235-240	X	X	X				X						X	X			X				
Fr09/01-GC25, 318-325		X	X			X	X		X					X				X			
Fr09/01-GC26, 334-340		X	X										X	X			X	X			X
Fr09/01-GC27, 219-225	X	X	X				X		X				X	X			X				

Sample Depth	*Globorotalia scitula*	*Globorotalia tosaensis*	*Globorotalia truncatulinoides*	*Globorotalia tumida*	*Globorotalia viola*	*Globoturborotalita apertura*	*Globoturborotalita decoraperta*	*Globoturborotalita nepenthes*	*Globoturborotalita rubescens* p	*Globoturborotalita rubescens* w	*Globoturborotalita tenellus*	*Hastigerina pelagica*	*Morozovella caucasica*	*Morozovella crater*	*Morozovella spinulosa*	*Neogloboquadrina dutertrei*	*Neogloboquadrina humerosa*	*Neogloboquadrina pachyderma* dext	*Orbulina universa*	*Pulleniatina finalis*	*Pulleniatina obliquiloculata* dext
Fr09/01-DR1A1													X	X							
Fr09/01-DR1B1													?	X	X						
Fr09/01-DR5A6	X			X		X	X	X		X							X		X		
Fr09/01-GC01, 441-446	X		X						X	X	X	X						X	X		X
Fr09/01-GC02, 354-360									X	X						X			X	X	X
Fr09/01-GC04, 305-309			X						X	X						X			X		X
Fr09/01-GC05, 297-300			X						X	X						X		X	X	X	X
Fr09/01-GC06, 318-323				X					X	X						X			X		X
Fr09/01-GC08, 320-325			X	X					X	X	X					X		X	X	?	X
Fr09/01-GC09, 330-335	X		X	X					X	X	X	X				X			X	X	X
Fr09/01-GC10, 433-438	X				X				X	X	X	X				X			X	X	X
Fr09/01-GC11, 338-343			X	X					X	X	X					X			X		X
Fr09/01-GC12, 419-425		X	X	X												X			X		X
Fr09/01-GC14, 485-490			X		X					X						X		X	X	X	X
Fr09/01-GC15, 232-236	X		X						X	X	X					X		X	X		
Fr09/01-GC16, 285-290	X		X						X	X	X					X		X	X	?	X
Fr09/01-GC18, 205-210	X		X						X	X	X					X		X	X	X	X
Fr09/01-GC21, 275-280	X		X		X				X	X						X		X	X	X	X
Fr09/01-GC22, 430-435	X		X						X	X	X					X			X	X	X
Fr09/01-GC23, 418-424	X		X						X	X						X		X	X	X	X
Fr09/01-GC24, 235-240	X								X	X	X					X		X	X	X	X
Fr09/01-GC25, 318-325		?	X	X						X						X		X	X		X
Fr09/01-GC26, 334-340	X		X							X	X					X		X	X		X
Fr09/01-GC27, 219-225	X		X						X	X	X					X			X		X

Sample Depth	*Pulleniatina praecursor*	*Sphaeroidinella dehiscens*	*Sphaeroidinellopsis seminulina*	*Subbotina eocaena*	*Subbotina linaperta*	*Tenuitella anfracta*	*Tenuitella iota*	*Turborotalita humilis*	indeterminable miliolines	indeterminable rotalines	indeterminable textularines	Barnacles unident	Bivalves unident	Brachiopods unident	Bryozoa unident	Echinoids unident	Fish teeth unident	Ostracods unident	Radiolaria indet	Sponge spicules unident
Fr09/01-DR1A1					X					X			?	?						
Fr09/01-DR1B1				X	X					X						X		X	X	
Fr09/01-DR5A6			X														X	X		
Fr09/01-GC01, 441-446		X				X	X		X	X	X							X	X	X
Fr09/01-GC02, 354-360		X					X		X	X								X		
Fr09/01-GC04, 305-309		X				X	X		X	X										
Fr09/01-GC05, 297-300		X					X		X	X						X		X		
Fr09/01-GC06, 318-323		X					X		X	X	X					X		X		
Fr09/01-GC08, 320-325		X							X	X	X									
Fr09/01-GC09, 330-335		X					X		X	X	X					X		?		
Fr09/01-GC10, 433-438		X					X		X	X	X					X		X		
Fr09/01-GC11, 338-343		X					X	X	X	X	X							X		
Fr09/01-GC12, 419-425	X	X							X	X								X		
Fr09/01-GC14, 485-490		X				?	X		X	X		X								
Fr09/01-GC15, 232-236		X					X		X	X	X	X	X			X				
Fr09/01-GC16, 285-290		X				X	X		X	X			X			X				
Fr09/01-GC18, 205-210		X					X		X	X	X					X		X		
Fr09/01-GC21, 275-280		X					X	X	X	X	X		X			X		X		
Fr09/01-GC22, 430-435		X					X		X	X	X					X		X		
Fr09/01-GC23, 418-424		X					X		X	X	X		X			X		X		X
Fr09/01-GC24, 235-240		X					X		X	X	X		X			X		X		
Fr09/01-GC25, 318-325		X							X	X	X					X		X		X
Fr09/01-GC26, 334-340		X					X		X	X	X	X			X			X		
Fr09/01-GC27, 219-225		X					X		X	X	X					X		X		

Two of the dredge samples from dredge FR09/01-DR1 contain late Early Eocene faunas which should be studied in greater detail than done for this study. In particular, sample DR1B1 contains a rich siliceous assemblage (mainly radiolaria, with some diatoms present), as well as rare, but well preserved foraminiferal assemblage. A similar radiolarian-rich sediment has been noted by Hornibrook et al. (1989) from the *Morozovella crater* Zone in northern New Zealand. In this part of the North Island, sediments of this age are within an allochthanous sequence, the source of which is believed to be in the northeast; the radiolarian-rich sediments from the Fairway Basin are from the northwest. This record may be of interest for regional tectonics. Further study of this sample may be useful to provide another data point for correlation between the calcareous and siliceous planktic zonal schemes. Dredge haul DR5A6 contains an Early Pliocene assemblage in micrite within a volcanic breccia.

To summarise, it is recommended that:

- a more detailed study of the older cores (in particular the longer ones GC12 (from the north) and GC25 (from further south) and G22 (from the south) should be made, as well as selected surface samples;
- further study of the calcareous and siliceous planktic groups be undertaken on sample DR01B1 which may provide another data point for correlation between the calcareous and siliceous planktic zonal schemes.

9. DISCUSSION AND CONCLUSIONS

The geological history of this region is part of the poorly understood and globally significant Southwest Pacific story of Cretaceous and Cainozoic subduction and back-arc rifting. From west to east are the eastern Lord Howe Rise, Fairway Basin, northern West Norfolk Ridge, New Caledonia Basin and Norfolk Ridge. The results of the cruise are summarised in Tables 2-5 and Figure 4. The cruise was an overall success, and the cruise data have improved our understanding of the geology of an important part of the Southwest Pacific. The structural nomenclature of the region has been significantly modified, as outlined in Section 3.

One of the main objectives of the French-New Caledonian ZoNéCo 11 multichannel seismic survey (September-October, 2004) is to further confirm: i) the likely thinned-continental nature of the Fairway and northern New Caledonia Basins, with the help of seismic refraction data; and ii) the BSR's occurrence and extension within the northern and central segments of the Fairway Basin.

9.1. Sedimentary basin sequences

Using the seismic interpretations of van de Beuque *et al*. (1998), Auzende *et al*. (2000c) and van de Beuque *et al*. (2003) as a basis, but adding DSDP and our own information, we suggest the following sequences are probably present in the region studied:

- Lower Cretaceous siliciclastic sediments resting on basement
- Upper Cretaceous siliciclastic sediments
- Paleocene and Eocene chalks and radiolarites with chert
- Oligocene to Middle Miocene chalk
- Middle Miocene to Recent ooze and volcaniclastic turbidites

The seismic program provided 2795 km of 24 channel, limited-penetration profiles, which are of excellent quality. The program enabled us to clarify the structural framework and nomenclature of the area (Section 3), showing that the Fairway Basin and New Caledonia Basin are separated by an intermittent ridge, and that both terminate at roughly 31º30'S. Table 10 shows interpreted average thicknesses in the various basins as shown on our seismic profiles. The nine new seismic profiles across the Fairway Basin, and the four profiles that entered the previously unknown southern part of the New Caledonia Basin, help to elucidate the history of a complex region of ribbon continents and deep ocean basins. Sediment diapirs (e.g. Figure 27) and a sporadic BSR occur in both basins, suggesting that both have some petroleum potential. The diapirs are probably of Upper Cretaceous mudstone, whereas the cross-cutting BSR, controlled by pressure and temperature, is generally in Oligocene or Miocene chalk.

Table 10. Average sediment thickness (metres) as indicated by our seismic profiles

Sequence	**Central Fairway**	**Northern South Fairway**	**Southern South Fairway**	**North New Caledonia Basin**	**South New Caledonia Basin**
Neogene	500-600	400-600	400-600	400-500	100-700
Palaeogene	200-900	300-1000	~500	300-600	500-700
Cretaceous	500-1200	300-800	750-1000	0-700	? absent
Total	~2000	~2000	~2000	700-1800	600-1500

Before this cruise, the Fairway Basin was known to form a distinct sedimentary basin along the eastern side of the Lord Howe Rise for 550 km, from 22°S to 26°40'S. We now know that it extends another 500 km southward to 31°30'S. It is a roughly north-south basin about 1050 km long and 150 km wide. We can now split it into three parts:

- The northwest trending *North Fairway Basin* from 22°S to 23°30'S (not surveyed on this voyage)
- The north-south trending *Central Fairway Basin* from 23°30'S to 26°40'S
- The north-south trending, largely deeper water *South Fairway Basin* from 26°40'S to 31°30'S.

In the Central Fairway Basin in the north (largely in New Caledonian jurisdiction), two new east-west cross-sections were added to the existing few. More diapirs were discovered, more evidence of a bottom-simulating reflector (BSR) suggesting the presence of gas hydrates, and more evidence of young faulting. In short, the survey increased our knowledge of a part of the basin known to have petroleum potential. The sequence we profiled is up to 2000 m thick. The uppermost transparent section, assumed to be Miocene and younger calcareous ooze and chalk, is 500-600 m thick. A middle, well-bedded sequence, probably Palaeogene pelagic ooze and turbidites, is 200-900 m thick. A lower, poorly bedded sequence, probably an Upper Cretaceous siliciclastic sequence, is 500-1200 m thick.

In the South Fairway Basin, the seismic profiling has provided six east-west cross-sections in an area of Australian jurisdiction where there were none. These profiles show that the north-south, deeper water depression south of 26º20'S is indeed a southern extension of the Fairway Basin, with the main difference probably being thinner continental crust. The South Fairway basin is limited by the Lord Howe Rise to the west and the northern extension of the West Norfolk Ridge to the east, and is roughly 600 km long and 150 km wide. Thus it has an area of 90,000 km^2, larger than Tasmania, and about 40% of it lies within the Norfolk Island EEZ. It contains sediments more than 2 seconds thick in places, shallow and deep diapirs (especially common north of 29°S), and a BSR in some regions. Water depths are 1200 m to 3600 m. Clearly, the South Fairway Basin has some petroleum potential, although the apparent maximum thickness of sediment <3 km) in the small part of the basin that we surveyed does reduce its potential.

In the northern South Fairway Basin, north of ~29ºS, the sequences are much the same as those in the Central Fairway Basin. About 400-600 m of transparent Miocene and younger pelagic carbonate overlies 300-1000 m of bedded Palaeogene marine sediment, and 300-800 m of poorly bedded Upper Cretaceous sediment. In the southern South Fairway Basin, 200-300 m of interbedded

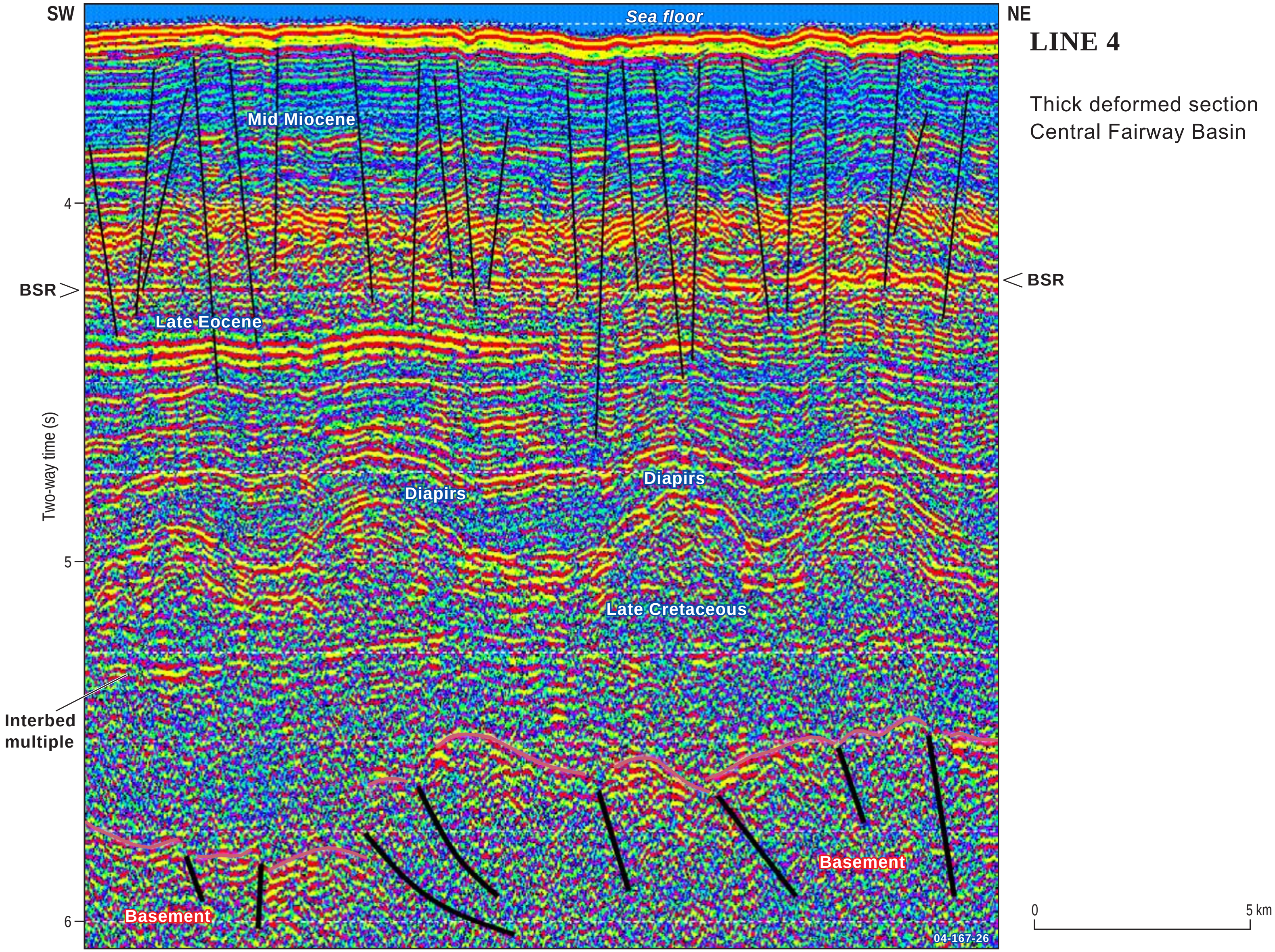

Figure 27. Detail of profile 232-4 showing diapirs and bottom simulating reflector (BSR)

sediments, interpreted as Miocene and younger turbidites and ooze, overlie 200-300 m of transparent sediments, interpreted to be Early Miocene ooze, ~500 m of variably bedded Palaeogene marine sediment, and 750-1000 m of poorly bedded strata, interpreted to be Upper Cretaceous siliciclastic sediment.

In the southern part of the New Caledonia Basin (near Norfolk Island) the true sediment thickness is unclear, because basement commonly was not reached by our low-powered seismic system, but it reaches 1500 m in places. The sedimentary section is flat-lying in general, with some areas of folding and diapirism. The generally seismically diffuse lower sequence, of probable Paleocene-Eocene age, contains rare strong reflectors. The upper sequence is transparent on both sides of the basin, but contains well-bedded sequences, probably turbidites, in the basin centre.

9.2. Petroleum indications

A major aim of the survey was to extend our knowledge of characteristics, documented in Exon *et al*. (1998), van de Beuque et al. (1998b, 2003), Auzende *et al*. (2000a, b, c) and Dickens *et al*. (2001), that suggested that the region had petroleum potential. These characteristics include:

- A sedimentary section at least 3 km thick in places, which is probably adequate to generate hydrocarbons.
- An assumed Cretaceous sequence contains diapirs that might well contain organic-rich mudstone formed in the early rift between Lord Howe Rise to the west and the Norfolk Ridge and New Caledonia to the east. Such diapirs might also form structural traps for petroleum as they do world-wide.
- A bottom-simulating reflector (BSR) occurs at 500-600 m below sea bed in the Cainozoic sequences, in water depths of 1500-3600 m, and could well represent gas hydrates.
- DSDP coring had shown these Cainozoic sequences to be calcareous oozes and chalks that are poor in organic carbon, and hence unlikely to generate biogenic gas. Accordingly, if there are gas hydrates, they are likely to have been generated by thermogenic processes at depth.
- Minute quantities of gases that were sampled from Quaternary piston cores taken by R.V. *L'Atalante* suggested that perhaps thermogenic gases were being generated at depth (Dickens *et al*. (2001). However, the results were equivocal.

Gas sampling and pore waters

It was hoped that core samples taken aboard would also help us to address the composition of any gas hydrates (represented by a BSR) at depth, and petroleum potential in general, by determining the origin and composition of any enclosed gas, and the nature of pore water variations. However, our coring results did not provide any definitive information about the origin and composition of any gas leaking from gas hydrates, because no significant gas was recovered (Appendices 1 and 9). The cores did not get below the oxidising zone of whitish chalks, and hence were not valid tests of any gas leaking from the postulated gas hydrates. It appears that the oxidising zone is too deep everywhere (Appendices 1 and 2) to allow piston or gravity coring to recover gas. Furthermore, the pore waters do not show the sharp chemical gradients of sulphate, chloride, and methane, which would indicate that significant accumulations of gas hydrates were present. Further testing will need direct gas hydrate samples, obtained either by deep drilling, or by giant box coring of areas where the BSR crops out.

Diapirs

The new seismic evidence shows that sediment diapirs occur well south of where they were previously known. Diapirs occur in the North and Central Fairway Basin (Auzende *et al*., 2000 a, c); the Central Fairway Basin (Lines 1, 3 and 4); the South Fairway Basin (Lines 5, 6, 7, 9 and 11); the southern New Caledonia Basin (Lines 7 and 9); the East Lord Howe Spur (Lines 10 and 11); and the Taranaki Basin (Line 11). This suggests that mobilisation of fluidised sediment, almost certainly of Cretaceous age, is common. This sediment is more likely to be mud than salt, because the high Cretaceous palaeolatitudes favoured deposition of mud rather than salt. If the sediment is carbonaceous mudstone, the diapirs could represent petroleum source rocks, as well as forming structures that might form petroleum traps.

Bottom simulating reflector: what generates it?

Extensive, cross-cutting, bottom simulating reflectors (BSRs) were known to exist in seismic profiles from the North Fairway Basin, the Central Fairway Basin, the northernmost South Fairway Basin and the northern New Caledonia Basin, before the present survey (Exon *et al*., 1998; Auzende *et al*., 2000b, c). These BSRs occur at depths of 500-600 m below the sea floor. BSRs are generated by a change in interval velocity, and can be caused by the presence of gas hydrates or by sediment diagenesis. Gas hydrate BSRs are normally caused by a downward decrease of interval velocity (negative polarity), from a hydrate-cemented zone above to a water or gas saturated zone below. In contrast, diagenetic BSRs are normally caused by a downward increase of interval velocity (positive polarity), from less-cemented sediments above to more-cemented sediments below. In this region, all authors, starting with Exon *et al*. (1998), have assumed that the BSR is generated by hydrate, partly because the necessary pressure and temperature conditions appear to fit its depth within the section. However, the seismic polarity suggests a contact between low velocity sediments above and high velocity sediments below, not the normal situation with hydrate-generated BSRs. On the present survey, a definite BSR was identified in data only from the Central Fairway Basin (Line 1) and the East Lord Howe Spur (Line 10).

The cross-cutting BSR in the region could possibly be a diagenetic feature, with more-cemented material below it. Silica diagenesis commonly generates a BSR in the deep ocean, but major silica diagenesis in the silica-deficient Oligocene and younger pelagic carbonates in this region seems unlikely. For example, Gardner *et al*. (1986) showed that, in DSDP Site 591, corrected carbonate percent is 90-95 % throughout, to its base at 500 m in Lower Miocene chalk. In several nearby DSDP drill sites, Packham and van der Lingen (1973) found two rapid increases in sonic velocity, related to step-wise lithification of the oozes to chalks with burial (but not to silicification), which they suggest may possibly correlate to seismic reflectors. At Site 206 for example (location in Figure 4) the lower increase occurred about 500 m deep in Upper Oligocene chalk, whereas silica-rich chalks and chert are first abundant in the Eocene below 614 m. The site's total depth was 734 m, more than 100 m deeper than any BSR observed in the region, and there is no seismic reflector directly associated with the change from Oligocene silica-poor chalks to Eocene silica-rich chalks. We conclude that the regional BSR is not related to silica diagenesis.

In this region, carbonate diagenesis depends mostly on the assemblages of the nannofossils that dominate the carbonates (James Kennett, University of California at Santa Barbara, pers. comm., 2002). These assemblages are controlled by surface water temperatures. In the nearby DSDP sites, warm-water loving discoasters, which are subject to diagenetic dissolution and re-precipitation, alternate with resistant cooler water assemblages. Therefore, reflections from diagenetic carbonate horizons should parallel bedding, unlike the BSRs that cut across stratigraphic horizons in the study area.

If neither silica nor carbonate diagenesis generates the BSR, it is probably generated by gas hydrates. The seismic evidence from this region suggests that the BSR is unlikely to be generated by thick, high-velocity gas hydrates overlying low-velocity free gas (the normal situation), because the seismic polarity indicates a contact between low velocity sediments above and high velocity sediments below.

Pecher (2004) carried out a full waveform inversion study on a Fairway Basin deep seismic line (AGSO LHRNR-BA) to determine how the BSR might have been generated. The technique generated best-fit velocity models by inverting a common-depth point gather for its full waveform. He suggested that 'two scenarios could generate positive-polarity BSRs in gas hydrate settings, a thin gas hydrate layer with a sharp top and without any significant amount of free gas beneath it, and a free-gas layer with a gradational top but a sharp base.' The results suggest that a free gas zone with a sharp base is unlikely to cause this BSR. The full waveform inversion 'cannot unambiguously distinguish between a single velocity step, mimicking a diagenetic BSR, and a thin high-velocity layer, simulating a gas-hydrate layer.' However, results do favour the presence of a thin high-velocity layer. Pecher cautioned that the superposition of stratigraphically controlled velocities and BSR-related velocities may lead to a complex velocity function.

Thus, the evidence does not support the presence of a diagenetic BSR, but the evidence for a gas hydrate BSR is not conclusive. In the end, only sampling across the BSR, at depth or from outcrops on the continental slope, will conclusively prove whether it is associated with gas hydrates.

9.3. Quaternary sediments

Late Quaternary foram-bearing nannofossil ooze and nannofossil ooze were recovered in 22 successful cores, in water depths of 1297-3517 m. These gravity cores averaged 360 cm long (and totalled 80 m), much less than the 630 cm average of the piston cores taken by *L'Atalante* in 1998 in the north and central Fairway Basin. Nevertheless, the present set of cores will allow studies of the composition, character and climate history of the region over nearly eight degrees of latitude. Many of the cores are figured in Appendix 2. Lack of significant colour changes in the northern cores, where pale colours and only slight variations prevail, suggest purely oxidising conditions. In the south, somewhat stronger colours and more variation are common, suggesting fluctuations in redox conditions, which were probably related to the inflow of varied bottom water through time.

Twenty-one samples from low in cores have been examined for planktic foraminifera and calcareous nannofossils. All core samples contain abundant and well preserved Pleistocene planktic foraminifera and nannofossils. The foraminiferal core assemblages are typically subtropical to warm temperate, dominated largely either by the *Globorotalia (Truncorotalia)* or the *Gr. inflata* groups.

The nannofossils show a clear relationship between location and age of the base of the cores. This suggests that there is a systematic variation in sedimentation rates, as most cores are of similar lengths (300-400 cm). The four oldest cores, all from the north, have the lowest average sedimentation rates (~4 mm/1000 years). They are on slopes, so may be subject to winnowing. The other northern cores have lower sedimentation rates (~10 mm/1000 years) than the southern cores (~25 mm/1000 years), perhaps because productivity has been higher south of 26º45'S than further north.

9.4. Older rocks

Dredge 1 from the Central Fairway Basin contains chalk and radiolarite, with Early Eocene foraminifera and late Early Eocene nannofossils. The volcanic breccia of Dredge 5 from the southern Lord Howe Rise contains poorly preserved Early Pliocene foraminifera and Late Miocene to Late Pliocene nannofossils in a micrite infilling, and Late Middle Miocene foraminifera in the associated ferromanganese crust. Accordingly, the volcanic rocks are Late Middle Miocene or older in age.

10. REFERENCES

Auzende, J-M., Beneton, G., Dickens, G., Exon, N., François, C., Holdway, D., Juffroy, F., Lafoy, A., Leroy, A., Van de Beuque, S. & Voutay, O., 2000a. Mise en évidence de diapirs mésozoiques sur la bordure orientale de la ride de Lord Howe (Sud-Ouest Pacifique: campagne ZoNeCo 5. *Comptes Rendus Academie Science, Paris, Sciences de la Terre et des Planètes*, 330: 209-215.

Auzende, J-M., Dickens, G.R., Van de Beuque, S., Exon, N.F., François, C., Lafoy, Y., & Voutay, O., 2000b. Thinned crust in southwest Pacific may harbor gas hydrate. *EOS, Transactions of American Geophysical Union*, 81(17): 182-185.

Auzende, J.M., Van de Beuque, S., Dickens, G., Francois, C., Lafoy, Y., Voutay, O. & Exon, N. 2000c. Deep sea diapirs and bottom simulating reflector in Fairway Basin (SW Pacific). *Marine Geophysical Researches*. 21(6), 579-587.

Berggren W.A., Kent, D.V., Swisher, C.C. III, & Aubry, M.-P., 1995a. A revised Cenozoic geochronology and chronostratigraphy. *In:* Berggren, W.A. et al. (eds.). *Geochronology, time scales and global correlation,* SEPM Special Publication, 54, 129-212.

Berggren, W.A., Hilgen, F.J., Langereis, C.G., Kent, D.V., Obradovich, J.D., Raffi, I., Raymo, M.E., and Shackleton, N.J., 1995b. Late Neogene chronology: New perspectives in high-resolution stratigraphy. *Geological Society of America Bulletin* 107, 1272-1287.

Bernardel, G., Lafoy, Y., van de Beuque, S., Missegue, F. & Nercessian, A., 1999. Preliminary results from AGSO Law of the Sea Cruise 206: an Australian/French collaborative deep-seismic marine survey in the Lord Howe Rise/New Caledonia region. *Australian Geological Survey Organisation Record* 1999/14.

Bolli, H.M. & Saunders, J.B., 1985. Oligocene to Holocene low latitude planktic foraminifera. *In* Bolli, H. M., Saunders, J. B. & Perch Nielsen, K., (eds.) *Plankton Stratigraphy 1*, pp. 155-262. Cambridge University Press, Cambridge, U.K.

Bown, P.R. & Young, J.R., 1998. Techniques. *In*: Bown, P.R., (ed.) *Calcareous Nannofossil Biostratigraphy*, pp. 16-28. Chapman & Hall, London.

Bradshaw, J.D., Andrews, P.B., & Adams, C.J., 1973. Carboniferous to Cretaceous. In: Burns, R.E., Andrews, J.E., et al., 1973. *Initial Reports of the Deep Sea Drilling Project*, 21, U.S. Government Printing Office, Washington, D.C.

Burns, R.E., Andrews, J.E. et al., 1973. *Initial Reports of the Deep Sea Drilling Project*, 21. U.S. Government Printing Office, Washington, D.C., 931 p.

Chaproniere, G.C.H., 1991. Pleistocene to Holocene planktic foraminiferal biostratigraphy of the Coral Sea, offshore Queensland, Australia. *BMR Journal of Australian Geology and Geophysics,* 12, 195-221.

Chaproniere, G.C.H., 1996. Quaternary foraminiferal biostratigraphy. In: G.C. Young and J.R. Laurie (Eds), *An Australian Phanerozoic Timescale*, 187-190. Oxford University Press, Melbourne.

Chaproniere, G.C.H., Styzen, M.J., Sager, W.W., Nishi, H., Quinterno, P.J. and Abrahamsen, N., 1994. Late Neogene biostratigraphic and magnetostratigraphic synthesis, Leg 135. *Proceedings of the Ocean Drilling Project, Scientific Results* 135, 857-877.

Dickens, G.R., Castillo, M.M. and Walker, J.C.G., 1997a. A blast of gas in the latest Paleocene: Simulating first-order effects of massive dissociation of oceanic methane hydrate. *Geology* 25, 259-262.

Dickens, G.R., Paull, C.K., Wallace, P. and ODP Leg 164 Scientific Party, 1997b. Direct measurement of *in situ* methane quantities in a large gas hydrate reservoir. *Nature* 385, 426-428.

Dickens, G.R. and Quinby-Hunt, M.S., 1997. Methane hydrate stability in pore water: A simple theoretical approach for geophysical applications. *Journal of Geophysical Research* 102, 773-783.

Dickens, G., Exon, N., Holdway, D., Lafoy, Y., Auzende, J-M., Dunbar, G. and Summons, R., 2001. Quaternary sediment cores from the Southern Fairway Basin on the northern Lord Howe Rise (Tasman Sea). *Australian Geological Survey Organisation Record,* 2001/31, 29 p. and CD-ROM

Dillon, W.P. and Paull, C.K., 1983. Marine gas hydrates, II. Geophysical evidence. *In*: Cox, J.L. (Editor), *Natural Gas Hydrates*: *Properties*, *Occurrences and Recovery*, Butterworth, London, pp. 73-90.

Dubois, J., Ravenne, C., Aubertin, A., Louis, J., Guillaume, R., Launay, J., & Montadert, L., 1974. Continental margins near New Caledonia. *In*: C.A. Burk & C.L. Drake (Eds), *The Geology of Continental Margins,* Springer-Verlag, New York, 521-535.

Eade, J.V., 1988. The Norfolk Ridge system and its margins. *In*: A.E.M. Nairn, F.G. Stehli & S. Uyeda (Eds), *The Ocean Basins and Margins, Vol. 7B, The Pacific Ocean,* Plenum Press, N.Y. and London, 303-322.

Exon, N.F., Dickens, G.R., Auzende, J-M., Lafoy, Y., Symonds, P.A. and Van de Beuque S., 1998. Gas hydrates and free gas on the Lord Howe Rise, Tasman Sea. *Petroleum Exploration Society of Australia Journal* 26, 148-58.

Exon, N.F., Quilty, P.J., Lafoy, Y. and Auzende, J-M., 2004. Miocene volcanic seamounts on northern Lord Howe Rise: lithology, age, ferromanganese crusts, and origin. *Australian Journal of Earth Sciences* 51(2), 291-300.

Gaina, C., Müller, R.D., Royer, J-Y., Stock, J., Hardebeck, J. & Symonds, P., 1998. The tectonic history of the Tasman Sea: a puzzle with 13 pieces. *Journal of Geophysical Research*, 103 (B6), 12413-12433.

Gardner, J.V., Dean, W.E., Bisagno, L. and Hemphill, E., 1986. Late Neogene and Quaternary coarse-fraction and carbonate stratigraphies for Site 586 on Ontong-Java Plateau and Site 591 on Lord Howe Rise. *In*: Kennett, J.P., von der Borch, C.C., et al., 1986. *Initial Reports of the Deep Sea Drilling Project*, 90. U.S. Government Printing Office, Washington D.C., 1201-1224.

Hayes, D.E., & Ringis, J., 1973. Seafloor spreading in the Tasman Sea. *Nature*, 243, 454-58.

Herzer, R.H., Chaproniere, G.C.H., Edwards, A.R., Hollis, C.J., Pelletier, B., Raine, J.I., Scott, G.H., Stagpoole, V., Strong, C.P., Symonds, P., Wilson, G.J., & Zhu, H., 1997. Seismic stratigraphy and structural history of the Reinga Basin and its margins, southern Norfolk Ridge system. *New Zealand Journal of Geology & Geophysics*, 40, 425-451.

Herzer, R.H., Sykes, R., Kilops, S.D., Funnell, R.H., Burggraf, D.R., Townend, J., Raine, J.I. & Wilson, G.J., 1999. Cretaceous carbonaceous rocks from the Norfolk Ridge system, southwest Pacific: implications for regional petroleum potential. *New Zealand Journal of Geology & Geophysics*, 42, 57-73.

Hine, N., & Weaver, P.P.E., 1998. Quaternary. *In*: Bown, P.R., (ed.) *Calcareous Nannofossil Biostratigraphy*, pp. 266-283. Chapman & Hall, London.

Hinz, K. et al., 1985. Geophysical, geological and geochemical studies on the Lord Howe Rise. *Bundesanstalt für Geowissenschaften und Rohstoffe Report*, 193 p.

Hiramatsu, C. and DeDekker, P., 1997. The late Quaternary calcareous nannoplankton assemblages from three cores from the Tasman Sea. *Palaeogeography*, *Palaeoclimatology*, *Paleoecology* 131(3-4), 391-412.

Hornibrook, N. de B., Brazier, R.C., and Strong, C.P., 1989. Manual of New Zealand Permian to Pleistocene Foraminiferal Biostratigraphy. *New Zealand Geological Survey Paleontological Bulletin* 56, 1-175.

Jones, J.G. and McDougall, I., 1973. Geological history of Norfolk and Philip Islands, southwest Pacific Ocean. *Journal Geological Society of Australia* 20, 239-254.
Kennett, J.P., Houtz, R.E. et al., 1974. *Initial Reports of the Deep Sea Drilling Project*, 29. U.S. Government Printing Office, Washington D.C., 1517 p.
Kennett, J P, Houtz, R E, Andrews, P B, et al., 1974. Cenozoic paleoceanography in the Southwest Pacific Ocean, Antarctic glaciation, and the development of the Circum-Antarctic Current. In: Kennett, J.P., Houtz, R.E. et al., 1974. *Initial Initial Reports of the Deep Sea Drilling Project*, 29. U.S. Government Printing Office, Washington D.C., 1155-1169.
Kennett, J.P., von der Borch, C.C., et al., 1986. *Initial Reports of the Deep Sea Drilling Project*, 90. U.S. Government Printing Office, Washington D.C., 1517 p
Kroenke, L.W., 1984. Cenozoic tectonic development of the Southwest Pacific. *CCOP/SOPAC Technical Bulletin* 6, 122 p.
Kvenvolden, K.A., 1993. Gas hydrates - geological perspective and global change. *American Geophysical Union Reviews of Geophysics*, 31(2), 173-187.
Kvenvolden, K.A., 1995. A review of the geochemistry of methane in natural gas hydrate. *Organic Geochemistry*, 23, 997-1008.
Kvenvolden, K.A. and Cooper, A.K., 1987. Natural gas hydrates of the offshore circum-Pacific margin – a future energy resource? In: Horn, M.K. (Ed.), *Transactions of the 4th Circum-Pacific Energy and Mineral Resources Conference*; Circum-Pacific Council for Energy and Mineral Resources, 285-297.
Lafoy, Y., Pelletier, B., Auzende, J.M., Missegue, F. and Mollard, L., 1994. Tectonique compressive Cenozoique sur les rides de Fairway et Lord Howe entre Nouvelle-Caledonie et Australie, *Comptes Rendu Acadamie Science Paris*, 319, serie IIa, 1063-1069.
Lafoy, Y., Bernardel, G. and Van de Beuque, S., 1998a. Campagne de sismique multitraces entre la marge Est Australienne et le Sud de l'arc des Nouvelles-Hébrides, *Rapport de la campagne Rig-Seismic 206, Programme FAUST, Rapport ZoNéCo*, 40 p.
Lafoy, Y., Van de Beuque, S., Bernardel, G., Missegue, F., Nercissian, A., Auzende, J-M., Symonds, P. & Exon, N., 1998b. Scientists study deep geological structure between New Hebrides arc and eastern Australian margin. *Eos, Transactions American Geophysical Union*, 79(50), 613-614.
Lafoy, Y., Exon, N., and Hill, P., Fellows, M., Perry, K., Mitts, P., 2001. Reconnaissance géophysique et géologique du bassin de Fairway (Sud-Ouest Pacifique): résultats préliminaires des données acquises dans la zone économique de la Nouvelle-Calédonie, 1ère partie de la campagne FAUST 3 (R/V Franklin, 13 nov .- 6 déc. 2001), Décembre 2001, 13 p.
Lafoy, Y., Brodien, I, Vially, R., Exon, N.F., in prep. Structural style of the submarine basin and ridge system west of New Caledonia (Southwest Pacific). *Marine Geophysical Researches* (submitted).
Launay, J., Dupont, J., Lapouille, A., Ravenne, C., & de Broin, C.E., 1977. Seismic traverses across the northern Lord Howe Rise and comparison with the southern part (South-west Pacific). *In*: *Symposium on International Geodynamics in Southwest Pacific*, Noumea, 27 August-2 September 1976, *Editions Technip*, Paris, 155-163.
McDougall, I., & van der Lingen, G.J., 1974. Age of rhyolites on the Lord Howe Rise and the evolution of the southwest Pacific Ocean. *Earth and Planetary Science Letters*, 21, 117-126.
Martini, E., 1971. Standard Tertiary and Quaternary calcareous nannoplankton zonation. In Farinacci, A. (ed.). Proceedings of the Second Planktonic Conference Roma 1970, Rome, Edizioni Tecnoscienza, p. 739-785.
Mortimer, N., Herzer, R.H., Gans, P.B., Parkinson, D.L. and Seward, D., 1998. Basement geology from Three Kings Ridge to West Norfolk Ridge, southwest Pacific Ocean: evidence from petrology, geochemistry and isotopic dating of dredge samples. *Marine Geology* 148, 135-162.
Nees, S., 1997. Late Quaternary palaeoceanography of the Tasman Sea: The benthic foraminiferal view. *Palaeogeography*, *Palaeoclimatology*, *Paleoecology* 131(3-4), 365-390.

Nelson, C.S., 1986. Lithostratigraphy of Deep Sea Drilling Project Leg 90 drill sites in the Southwest Pacific: an overview. *In*: Kennett, J.P., Houtz, R.E. et al., 1974. *Initial Reports of the Deep Sea Drilling Project*, 29. U.S. Government Printing Office, Washington D.C., 1471-1491

Okada, H., & Bukry, D., 1980. Supplementary modification and introduction of code numbers to the low-latitude coccolith biostratigraphic zonation. *Marine Micropaleontology*, 5, 321-325.

Packham, G.H. and van der Lingen, G.J., 1973. Progressive carbonate diagenesis at Deep Sea Drilling Sites 206, 207, 208, and 210 in the Southwest Pacific and its relationship to sediment physical properties and seismic reflectors. *In*: Burns, R.E., Andrews, J.E. et al., 1973. *Initial Reports of the Deep Sea Drilling Project*, 21, U.S. Government Printing Office, Washington D.C., 495-521.

Pecher, I.A., 2004. Waveform inversion applied to a bottom simulating reflection on the eastern Lord Howe Rise. *NZ Institute of Geological and Nuclear Sciences Science Report* 2004/27.

Perch-Nielsen, K., 1985. Cenozoic calcareous nannofossils. *In*: Bolli, H. M., Saunders, J. B. & Perch Nielsen, K., (eds.) *Plankton Stratigraphy 1*, pp. 427-554. Cambridge University Press, Cambridge, U.K.

Ravenne, C., de Broin, C.E., Dupont, J., Lapouille, A. & Launay, J., 1977. New Caledonia Basin – Fairway Ridge: structural and sedimentary study. *International Symposium on Geodynamics in Southwest Pacific*, Editions Technip, Paris, 145-154.

Roeser, H. & Shipboard Party, 1985. Geophysical, geological and geochemical studies on Lord Howe Rise. *Bundesanstalt fur Geowissenschaften und Rohstoffe Report*, *Cruise SO36 (1).*

Schreckenberger, B., Roeser, H.A., & Symonds, P.A., 1992. Marine magnetic anomalies over the Lord Howe Rise and the Tasman Sea: Implications for the magnetization of the lower continental crust. *Tectonophysics*, 212, 77-97.

Shaw, R.D., 1978. Sea floor spreading in the Tasman Sea: a Lord Howe Rise - Eastern Australian reconstruction. *Bulletin of the Australian Society of Exploration Geophysicists*, 9 (3), 75-81.

Stagg, H.M.J., Alcock, M.B., Borissova, I. & Moore, A.M.J., 2002. Geological framework of the southern Lord Howe Rise and adjacent areas. Geoscience Australia Record 2002/25, 142 p and CD-ROM

Uruski, C., & Wood, R., 1991. A new look at the New Caledonia Basin, an extension of the Taranaki Basin, offshore North Island, New Zealand. *Marine and Petroleum Geology*, 8, 379-391.

Van de Beuque, S., Auzende, J-M., Lafoy, Y. & Missegue, F., 1998a. Tectonique et volcanisme tertiare sur la ride de Lord Howe (Sud-Ouest Pacifique) *Comptes Rendu Academie Science Paris, Sciences de la terre et des planetes*, 326, serie II, 663-669.

Van de Beuque, S., Auzende, J-M., Lafoy, Y., Bernardel, G., Nercissian, A., Regnier, M., Symonds, P. & Exon, N., 1998b. Transect sismique continu entre l'arc des nouvelles-hébrides et la marge orientale de l'Australie: program FAUST (French Australian Seismic Transect). *Comptes Rendu Academie Science Paris, Sciences de la terre et des planetes*, 327, serie II, 761-768.

Van de Beuque, S., Stagg, H.M.J., Sayers, J., Willcox, J.B. & Symonds, P.A., 2003. Geological framework of the northern Lord Howe Rise and adjacent areas. *Geoscience Australia Record* 2003/01, 108 p.

Vially, R., Lafoy, Y., Auzende, J.M., France, R., 2003. Petroleum potential of New Caledonia and its Offshore Basins, AAPG International Conference, Barcelona, Spain, Sept. 21-24, 2003, 1-6.

Walley, A.M., 1992. Cretaceous – Cainozoic palaeogeography of the New Zealand – New Caledonia region. *Bureau of Mineral Resources Record* 1992/11.

Weaver, P.P.E., 1993. High resolution stratigraphy of Quaternary sequences. *In* Hailwood, E.A., & Kidd, R.B., (eds.) High resolution stratigraphy. *Geological Society Special Publication* 70, 137-154.

Weissel, J.K., & Hayes, D.E., 1977. Evolution of the Tasman Sea reappraised. *Earth and Planetary Science Letters*, 36, 77-84.

Willcox, J.B., Sayers, J., Stagg, H.M.J. & Van de Beuque, S., 2001. Geological framework of the Lord Howe Rise and adjacent ocean basins. *In*: Hill, K.C. & Bernecker, T. (eds.) *Eastern*

Australasian Basins Symposium, A Refocused Energy Perspective for the Future. Petroleum Exploration Society of Australia, Special Publication, 211-225.

Willcox, J.B., Symonds, P.A., Bennett, D. & Hinz, K., 1981. Lord Howe Rise area, offshore Australia: preliminary results of a co-operative Federal Republic of Germany / Australia geophysical survey. *Bureau of Mineral Resources, Geology & Geophysics, Report* 228.

Willcox, J.B., Symonds, P.A., Hinz, K. & Bennett, D., 1980. Lord Howe Rise, Tasman Sea – preliminary geophysical results and petroleum prospects. *BMR Journal of Australian Geology & Geophysics*, 5, 225-236.

Young, J. R., 1998. Neogene. *In* Bown, P.R., (ed.) *Calcareous Nannofossil Biostratigraphy*, pp. 225-265. Chapman & Hall, London.

Appendix 1: Pore water sulfate, chloride, and methane concentrations in sediment gravity cores from the Fairway and New Caledonia Basins: Results from *Franklin* Cruise FR9/01

Patrick J. Mitts [1,2], Charles K. Paull [1], William Ussler III [1], Gerald R. Dickens [3,4], and Kirsten L. Perry[4]

1) Monterey Bay Aquarium Research Institute, 7700 Sandholt Road, Moss Landing, CA USA 95039
2) Moss Landing Marine Laboratory, 8272 Moss Landing Road, Moss Landing, CA USA 95039
3) Rice University Department of Earth Science, MS 126, PO Box 1892 Houston, TX, USA 77251-1892
4) James Cook University, School of Science and Engineering, Townsville, Queensland, Australia 4811

Abstract

Pore waters were collected from sediment gravity cores (up to 519 cm in length) in the Fairway and New Caledonia Basins of the South Pacific Ocean during 2001 to constrain whether significant shallow gas hydrate deposits occur there. Analyses of these pore waters do not show sharp chemical gradients of sulfate, chloride, and methane, characteristics that would be anticipated if significant accumulations of gas hydrates were present in the near subsurface.

The Gas Hydrate Problem

Gas hydrates are crystalline solids composed of a lattice of water molecules that trap gas molecules (Sloan, 1997). Gas hydrates are stable only under conditions of low temperatures/high pressures and sufficient gas concentrations. These states occur at water depths below ~500 m in many areas of the worlds oceans where there is a supply of methane. Because the mass of methane stored in gas hydrates is believed to be enormous, gas hydrates may represent a potential energy resource (Max, 2000) and a modulator of the ocean/atmosphere carbon cycle (Dickens et al., 1997 a.).

Accurate measurements of methane levels in gas-rich sea floor sediments are difficult to make because, without special tools, significant amounts of gas can escape during core recovery (Dickens et al., 1997b.; Paull and Ussler, 2001). Pore water sulfate profiles provide an independent proxy for the likelihood that gas hydrates occur in the sub-surface (Borowski et al., 1997, 1999). Sulfate levels in sediment are strongly affected by microbial activity. Some pore water sulfate can be consumed by sulfate-reducing bacteria, which utilize solid organic matter ($SO_4^{2-} + 2\ CH_2O \rightarrow H_2S + 2\ HCO_3^-$). Where this process dominates, pore water sulfate gradients typically display slightly convex upward profiles that converge with seawater sulfate values at the sediment-seawater interface (Figure 1). Anaerobic methane oxidation (AMO) is another biogeochemical reaction that can deplete sulfate in anaerobic sediments (Reeburgh, 1976; Borowski et al., 1997, 1999). This reaction ($SO_4^{2-} + CH_4 \rightarrow HS^- + HCO3^- + H_2O$), mediated by a microbial consortium (Boetius et al., 2000), is driven by an upward flux of methane to a sulfate methane interface (SMI) (Figure1). Where this process dominates, pore water sulfate gradients are often linear from seawater sulfate values at the sediment-seawater interface to essentially no sulfate below the SMI. Higher methane fluxes from below will usually produce steep, linear sulfate concentration profiles (Borowski et al., 1999) (Figure 1).

Chloride concentrations can be used to assess significant evaporation or dilution of pore water samples that may occur during sampling and storage. Chloride may also be used as a proxy for gas hydrates. Gas hydrate formation removes water and gas from sediment pore waters but excludes dissolved ions (Hesse and Harrison, 1980). As gas hydrates form, the surrounding pore waters thus become enriched in chloride. However, over time, this excess chloride will diffuse away forming a smooth concentration profile. During core recovery, gas hydrates can decompose, causing anomalous freshening of pore water (Hesse and Harrison, 1980).

Gas Hydrates in the Tasman Sea?

A series of recent geophysical cruises in the northern Tasman Sea have documented a large (> 70,000 km^2) north-south structural basin on the eastern flank of the northern Lord How Rise (Exon et al., 1998; Auzende et al., 2000). This basin (Figure 2), the southern Fairway Basin, contains several km of sediment and a prominent bottom-simulating reflector (BSR). Using available estimates for sonic velocities and thermal gradients in sediment on the LHR, the BSR lies at pressures and temperatures where gas hydrate is in equilibrium with free gas. Hence, it has been suggested that gas hydrate might occur in the Southern Fairway Basin (Exon et al., 1998) although this raises a dilemma because there does not appear to be an adequate supply of organic matter to generate the requisite methane (Auzende et al., 2000). Previous work on a set of piston cores collected from the southern Fairway Basin in 1998 did not detect significant decreases in pore water sulfate as expected for a region with gas hydrate and high upward fluxes of methane (Dickens et al., 2001). However, these samples were not collected or analyzed under ideal conditions.

The joint Australian/French cruise FR9/01 aboard the Australian R/V *Franklin* in November and December 2001 (Exon et al., 2001) was planned to further investigate the petroleum potential of the Southern Fairway Basin, including the inferred presence of gas hydrate. The survey collected ~ 2,800 km of seismic profiles on 11 transit lines and 22 gravity cores in an area that included both French and Australian Territorial waters (Figure 2). Among the research activities were the collection and analysis of pore waters and associated gases.

Methods

The gravity cores for pore water and gas analyses averaged 360 cm in length (Tables 1, 2). Gravity cores were collected using a one-ton, 7-meter metal core barrel that enclosed a 6-meter long, ~ 7 cm diameter PVC core liner and metallic core catcher. When the cores were recovered they were cut into 1-m sections beginning at the base of the core to facilitate handling. The 1-m sections were split in half on board ship, archive halves described, and 5-cm sections were sub-sampled from the working half of the cores for pore water analysis.

A total of 75 sub-samples were collected for pore-water analysis at semi-regular intervals within the cores, typically one near the top, middle, and bottom. Pore water samples collected near the base of the gravity cores along with other samples specifically collected from visually darker sediment layers were also of interest for methane gas analysis. An additional 21 samples of core top waters (CTW) were collected to provide seawater controls. CTW were immediately refrigerated and sediments were allowed to settle before the waters were drawn through a 0.2 μm filter into a 60 cc syringe.

To collect the pore waters, sediment samples were immediately transferred to a 7.6 cm diameter Reeburg-style hollow plastic liner with a paper filter below (Reeburg, 1967). Each sample was placed on a squeezing rack and topped with a dental dam. Compressed air was then used to squeeze the pore waters into a 60 cc syringe attached to a 1.6 mm tubing outlet below the sample.

The 75 pore water samples yielded an average of 13 cc of water (Table 3). Ambient air was added to each syringe after squeezing of pore waters and vigorously shaken for two minutes to extract the dissolved gasses.

The extracted gasses from 21 samples were stored after pore waters were expelled from the syringes. To do this, the syringes were individually placed into a bucket of surface seawater with a 15 cc serum vial filled with the seawater. Vials were then inverted under water and the residual gas in the syringes were injected into the vials and topped with a rubber stopper. The vials were then crimp sealed for storage and transport. All vials were refrigerated during storage and shipment prior to analysis at Monterey Bay Aquarium Research Institute (MBARI), except for a 24-hour period of non-refrigeration during the airplane flight back to California.

Water and gas samples from science cruise FR9/01 were labelled LHR-01 (Lord Howe Rise 2001) prior to analysis at MBARI. The data tables and graphs in this report reflect the LHR-01 nomenclature. The mid-point of the sample intervals reported in Tables 3-6 are used on the graphs in Figures 3 and 4.

Pore water samples were analyzed for chloride and sulfate concentrations by ion chromatography and the gas samples analyzed for methane content by gas chromatography at MBARI in March 2002. The ion chromatograph was calibrated using the International Association for the Physical Sciences of the Oceans (IAPSO) seawater standard. After every five samples, an IAPSO standard was measured to calculate machine drift. Methane was analyzed using a Shimadzu mini-2 gas chromatograph (GC) equipped with a flame ionization detector. Calibration of the GC was achieved using a methane-in-nitrogen gas standard, which was run in triplicate before and after sets of analyses.

Results and Discussion

The chloride concentration values from LHR-01 ranged from 428 mM to 757 mM, with a mean value of 581 mM and standard deviation (+1 σ) of 47.0 mM (Table 4). Sulfate concentration values range from 21.7 mM to 32.4 mM with a mean value of 29.0 mM and standard deviation of 1.5 mM (Table 5).

Five of the chloride and sulfate values are anomalous in that they are significantly enriched or depleted in both species relative to other samples. These samples are: GC-2 (7-10cm) [757 mM chloride and 30.7 mM sulfate], GC-02 (354-360 cm) [648 mM chloride and 32.4 mM sulfate], GC-04 - CTW (434 mM chloride and 22.2 mM sulfate), GC-06 (318-328 cm) [429 mM chloride and 21.7 mM sulfate], and GC-16 (62-68 cm) [631 mM chloride and 32.4 mM sulfate]. All five of these samples probably have been affected by post-collection evaporation or dilution because both chloride and sulfate concentrations are offset similarly.

If the outliers are excluded, chloride concentration values have a mean value of 572 mM + 22 mM (Table 4) and sulfate concentrations have a mean value of 28.8 mM + 1.0 mM (Table 5). These values are close to those determined for IAPSO (Figure 3 and 4). They confirm the absence of steep pore water sulfate profiles in the Southern Fairway Basin (Dickens et al., 2000).

Methane concentrations have a mean value of 1.90 ppm + 0.21 ppm (Table 6). These methane concentrations are slightly higher than for the core top samples but common in sulfate bearing sediments worldwide (Paull and Ussler, 2001). They provide no evidence for the existence of underlying gas hydrate deposits.

The area surveyed during the cruise lies beneath low-productivity surface waters and in a region that receives minimal terrestrial input. As observed by previous work (Dickens et al., 2000), sediments collected during the FR/09 cruise are primarily foraminiferal ooze. They probably accumulate very slowly with very little organic carbon and thus cannot support a shallow system with significant sulfate depletion and methane production. While some methane is present in most marine sediments (< 10 ppm), methane hydrate formation requires significantly greater methane concentrations.

Conclusions

The sulfate, chloride, and methane concentration data from the cores collected on FR9/01 do not support the presence of gas hydrates in shallow sediment. Moreover, if gas hydrates are present in deeper sediment, the sulfate profiles indicate that the upward flux of methane from these deposits must be extremely low (Figure 1).

References

Auzende, J.M., Dickens, G., Van de Beuque, S., Exon, N., Francois, C., Lafoy, A., and Voutay, O., 2000. Thinned crust in southwest Pacific may harbor gas hydrate. *EOS*, *Transactions of American Geophysical Union* 81(17), 182-185.

Boetius, A., Ravenschlag, K., Schubert, C.J., Rickert, D., Widdel, F., Gieseke, A., Amann, R., Jorgensen, B.B., Witte, U., and Pfannkuche, O., 2000. A marine microbial consortium apparently mediating anaerobic oxidation of methane. *Nature* 407, 623-626.

Borowski, W.S., Paull, C.K., and Ussler, W. III, 1996. Marine pore-water sulfate profiles indicate in situ methane flux from underlying gas hydrate. *Geology* 24(7), 655-658.

Borowski, W.S., Paull, C.K., and Ussler, W. III, 1997. Carbon cycling within the upper methanogenic zone of continental rise sediments overlying the Blake Ridge gas hydrate deposits: *Marine Chemistry*, 299-311.

Borowski, W.S., Paull, C.K., and Ussler, W. III, 1999. Global and local variations of interstitial sulfate gradients in deep-water, continental margin sediments: Sensitivity to underlying methane and gas hydrates: *Marine Geology* 159, 131-154.

Dickens, G.R, Castillo, M.M., and Waller, J.C.G., 1997a. A blast of gas in the latest Paleocene: simulating effects of massive dissociation of oceanic methane hydrate: *Geology* 25, 259-262.

Dickens, G.R., Paull, C.K., Wallace, P., and the ODP Leg 164 Scientific Party, 1997 b. Direct measurement of in situ methane quantities in a large gas hydrate reservoir: *Nature* 385, 426-428.

Dickens, G. R., Exon, N., Holdway, D., Lafoy, Y., Auzende, J.M., Dunbar, G., and Summons, R., 2001. Quaternary sediment cores from the Southern Fairway Basin on the northern Lord Howe Rise (Tasman Sea), *AGSO Record* 2001/31, 56 pp.

Exon, N.F., Dickens, G.R., Auzende, J.M., Lafoy, Y., Symonds, P.A. & van de Beuque, S., 1998. Gas hydrates and free gas on the Lord Howe Rise, Tasman Sea. *PESA (Petroleum Exploration Society of Australia) Journal*, 26, 148-158.

Exon, N., Hill, P., Lafoy, Y., Fellows, M., Perry, K., and Mitts, P., 2001. *Franklin Voyage Summary*, No. FR09/2001, 20 pp.,
http://www.marine.csiro.au/franklin/plans/2001/fr0901s.html.

Hesse, R. and Harrison, W.E., 1981. Gas hydrates (clathrates) causing pore water freshening and oxygen isotope fractionation in deep-water sedimentary sections of terrigenous continental margins. *Earth and Planetary Science Letters* 55, 453-462.

Max, M.D., 2000. Natural Gas Hydrates. *Klewar Academic Publishers*, Howell, MA,
410 p.

Packham, G.H. and van der Lingen, G.J., 1973. Progressive carbonate diagenesis at Deep Sea Drilling Sites 206, 207, 208, and 210 in the Southwest Pacific and its relationship to sediment physical properties and seismic reflectors. *In* Burns, R.E., Andrews, J.E. et al., *Initial Reports of the Deep Sea Drilling Project*, Washington D.C., 21, 495-521.

Paull C.K., and Ussler, W. III, 2001. History and Significance of Gas Sampling During the DSDP and ODP, in: *Natural Gas Hydrates Occurrence, Distribution, and Detection*, Paull, C.K., and

Dillon, W.P., *eds*., Geophysical Monograph no. 24, American Geophysical Union, Washington D.C., 53-65.
Reeburgh, W.S., 1967. An improved interstitial water sampler: *Limnology & Oceanography* 12, 163-165.
Reeburgh, W.S., 1976. Methane Consumption in Cariaco Trench Waters and Sediments. *Earth and Planetary Science Letters* 28, 337-344.
Sloan, E.D., 1997. Clathrate Hydrates of Natural Gasses. *Marcel Dekker*, Monticello, NY, 705 pp.

Figure 1: Map of FR9/01 survey

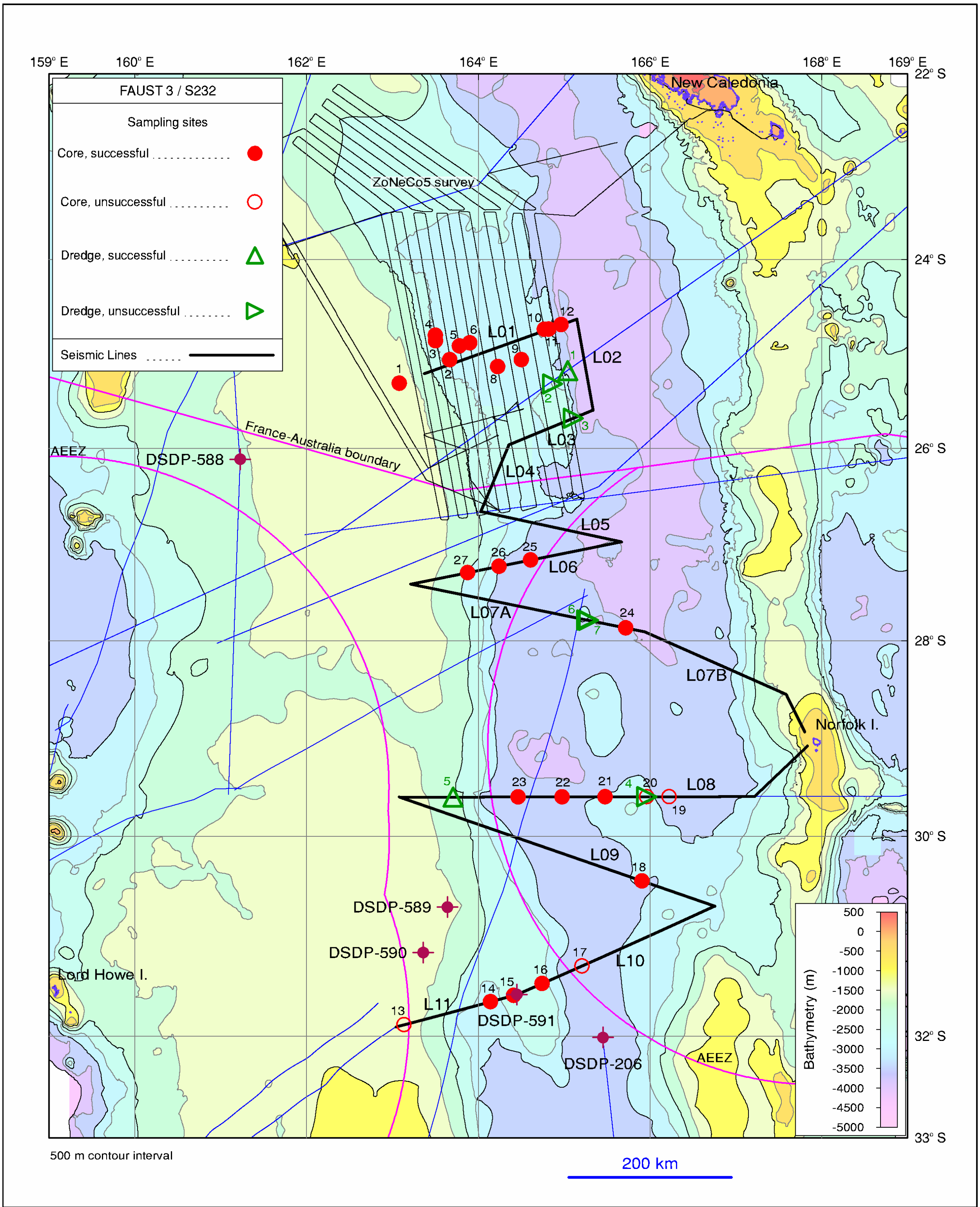

(Fig. 1): Map of Fr9/01 seismic lines, coring sites, and dredge locations. Map by Peter Hill, Geoscience Australia, from Exon et al., (2001)

Figure 2: Hydrate Stability Diagram

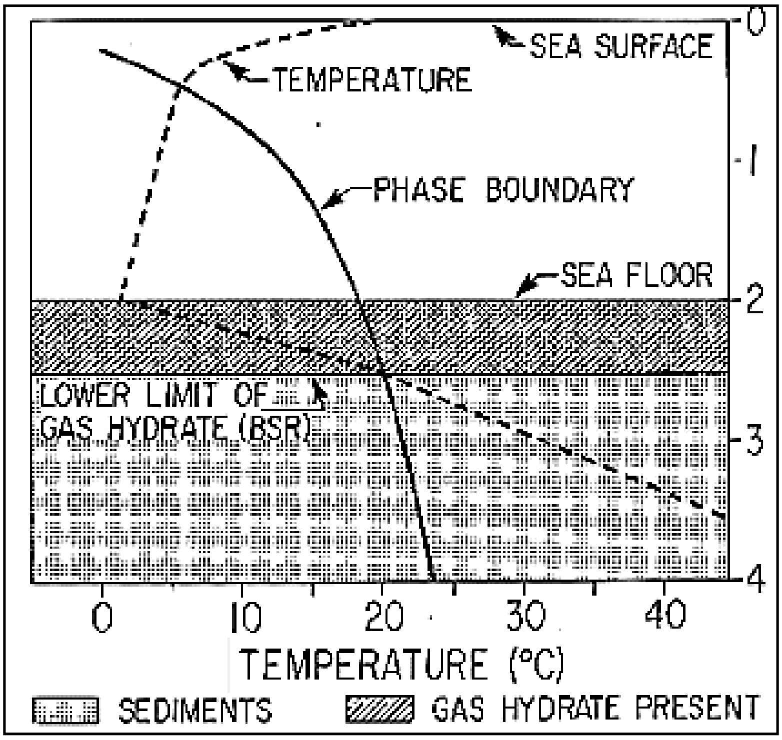

(Fig. 2): Hydrate stability diagram showing hydrate stability zone below the seafloor.
From USGS website: http://woodshole.er.usgs.gov/project-pages/hydrates/what.html

Figure 3: Sulfate Diffusion Profiles

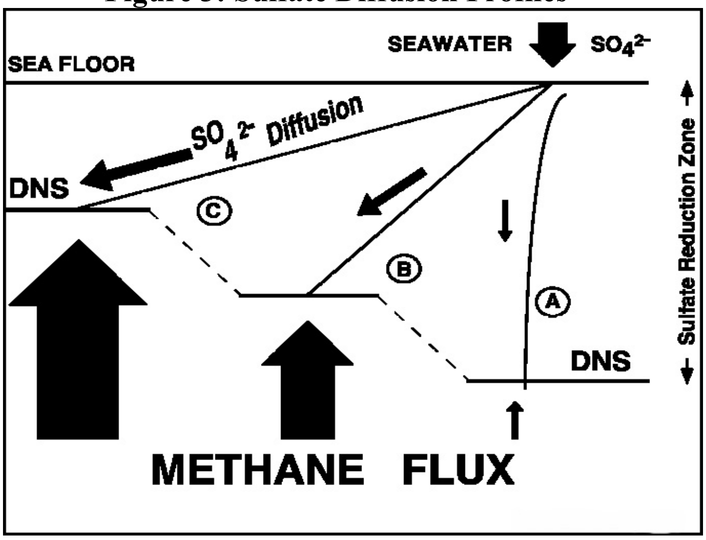

(Fig. 3): When methane flux increases and/or approaches the seafloor bottom, the sulfate concentration profile gradients change from a convex vertical gradient with no methane flux to less steepened gradient profiles with higher methane flux from sediments below.
From Borowski et al., 1996.

Figure 4a: Ion Exclusion During Gas Hydrate Formation

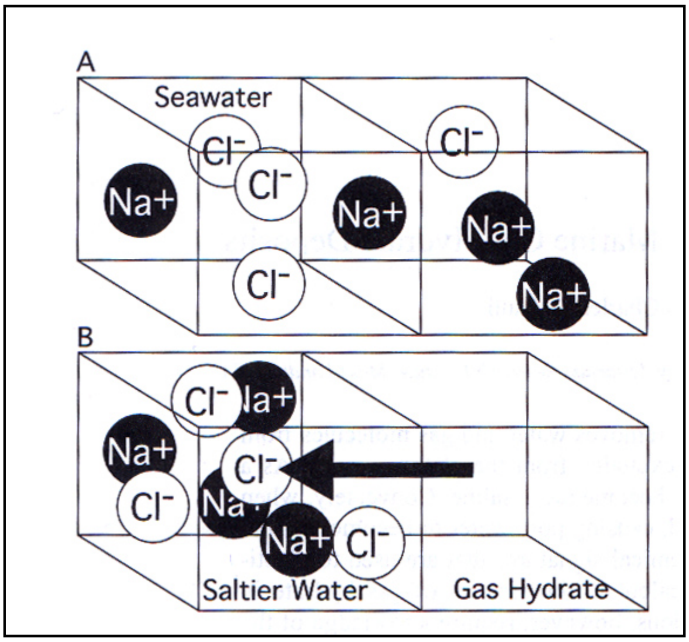

(Fig. 4a): Diagram showing how sediment pore waters are depleted in chloride during gas hydrate formation. From Ussler and Paull, 2001.

Figure 4b: Fresh Water Formation

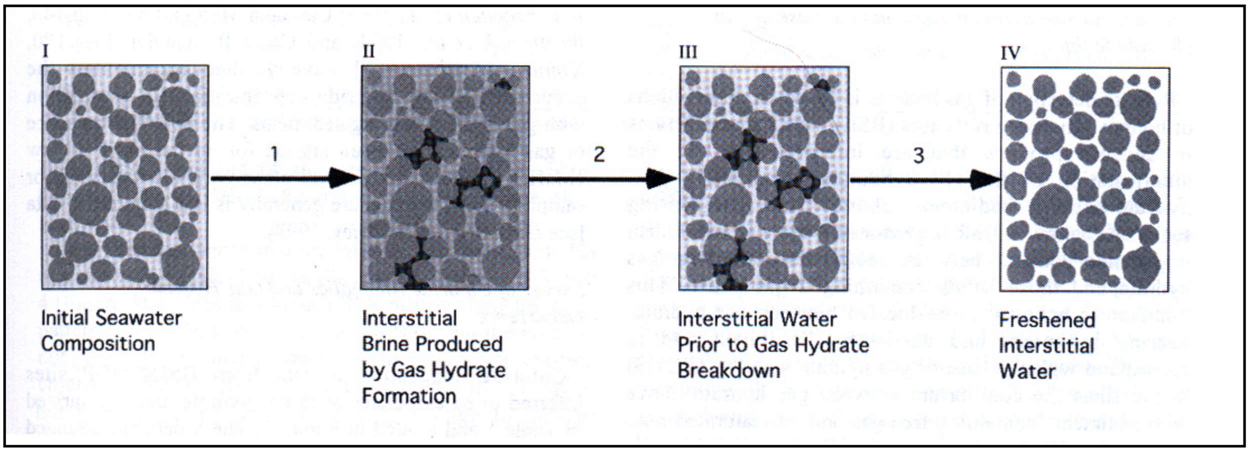

(Fig. 4b): Diagram showing fresh water formation with breakdown of gas hydrates. From Ussler and Paull, 2001.

Figure 5: Correlation of chloride depletion and gas hydrate concentrations

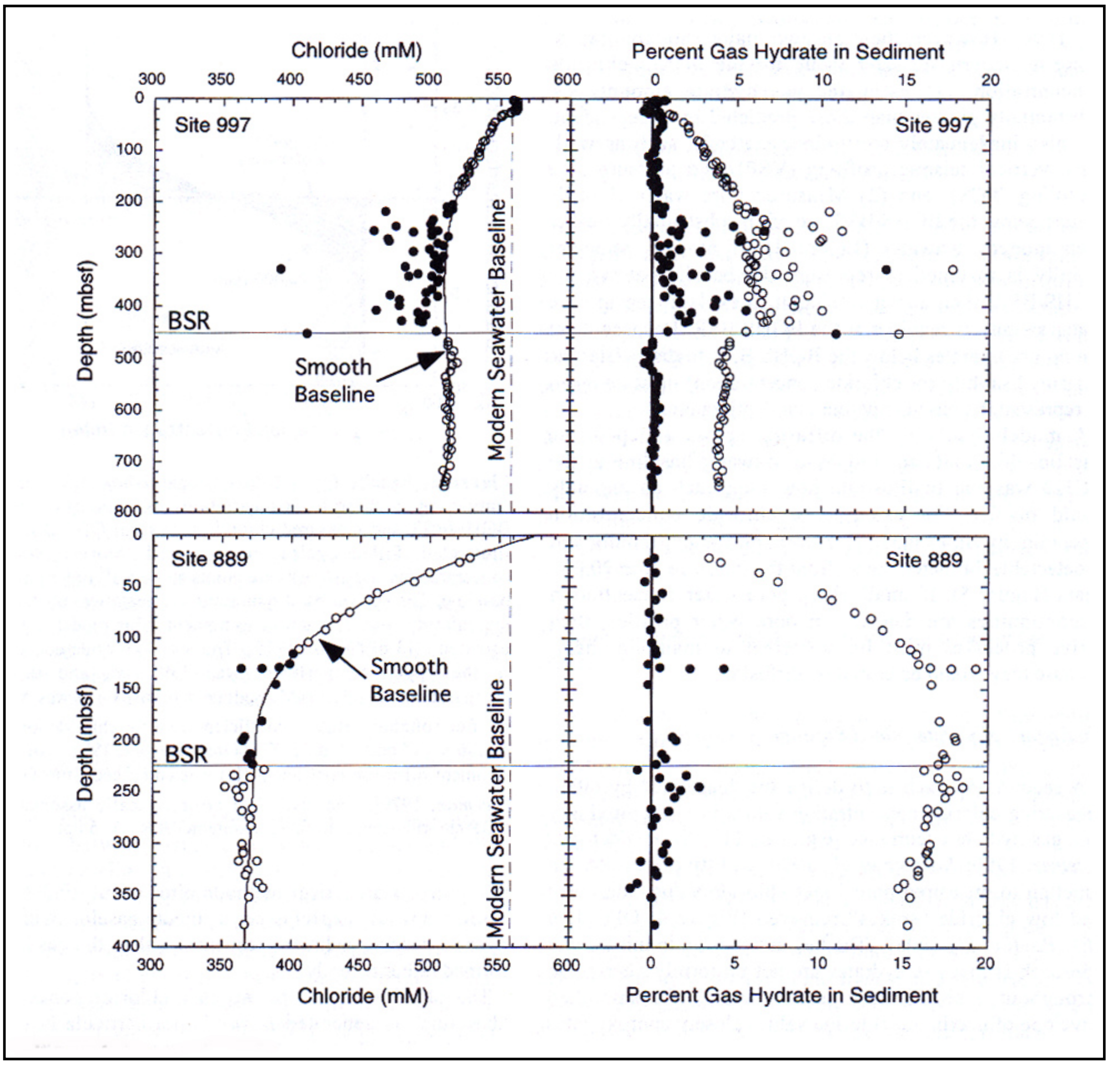

(Fig. 5): Diagrams showing chloride depletion profiles and percentage of gas hydrates in the sediment column at depth. Profiles shown are from known gas hydrate deposits in the Blake Ridge off North Carolina, USA (Site 997) and Hydrate Ridge (Site 889).
From Ussler and Paull, 2001.

Table 1. FR9/01 cores from New Caledonian jurisdiction

Core	Latitude	Longitude	Depth (m)	Length (cm)	Description	Seismic interpretation
GC01	-25º18.67	163º04.75	1297	450	Pale foram-bearing nanno ooze	N/A
GC02	-25°03.71	163°40.02	2635	369	Pale brown foram-bearing nanno ooze	1a
GC03	-24°51.70	163°30.09	2522	339	Pale brown foram-bearing nanno ooze	DpBSR + 1b
GC04	-24°48.18	163°29.99	2586	329	Pale foram-bearing nanno ooze	DS + 1b
GC05	-24°54.98	163°46.75	2706	305	Pale brown foram-bearing nanno ooze	DpBSR + 1a
GC06	-24°53.00	163°53.98	2764	338	Pale foram-bearing nanno ooze	DD + 1a
GC07	-24°18.60	164°03.60	2835	N/A	Not attempted	DD + 1a + PM
GC08	-25°08.10	164°13.50	2700	369	Pale foram-bearing nanno ooze (repeat section from 328 cm)	DD + 1b + PM
GC09	-25°03.71	164°30.05	2840	350	Pale brown foram-bearing nanno ooze	DpBSR + 1a
GC10	-24°44.33	164°46.14	2580	445	Pale brown foram-bearing nanno ooze	
GC11	-24°44.28	164°49.13	2820	350	Pale brown foram-bearing nanno ooze	
GC12	-24°41.39	164°57.83	3517	455	Brown foram-bearing nanno ooze	

Table 2. FR9/01 cores from Australian jurisdiction

Core	Latitude	Longitude	Depth (m)	Length (cm)	Description	Seismic interpretation
GC13	-31° 53.0	163 08.0	1188	10 cm	Pale olive muddy foram sand	PO
GC14	-31° 39.35	164 08.47	2720	519 cm	0-16 cm: pale brown foram-rich nanno ooze. 16-496: olive to white nanno ooze. 496-519: repeat 0-16.	PO
GC15	-31° 35.59	164 24.64	2140	246 cm	0-90 cm: pale brown & light grey nanno ooze. 90-246 cm: pale yellow & white nanno ooze	DSDP 591 DD
GC16	-31° 28.49	164 44.53	2100	320 cm	0-29 cm: pale brown & light grey foram-rich nanno ooze. 29-320: light grey & pale olive nanno ooze	MD, F, PM
GC17	-31° 17.94	165 12.46	3320	None	Traces of foram sand	PO
GC18	-30° 26.87	165 54.33	2590	240 cm	Interbedded v pale brown & light grey foram-bearing nanno ooze	BR, WNR
GC19	-29° 35.74	166 13.33	2905	None	Fingers torn off core catcher	DD, NCB
GC20	-29° 35.75	165 57.65	2483	None	Bounced off hard rock, core cutter damaged. Ooze traces.	BR
GC21	-29° 35.78	165 28.60	2810	400 cm	0-290 cm: pale brown & yellow foram-bearing nanno ooze. 290-400 cm: repeat of top section	DD, WNR
GC22	-29° 35.86	164 58.51	3405	445 cm	Multicoloured nanno ooze, with distinct beds 20-30 cm thick: white, pale yellow, pale & dark greenish grey.	DD
GC23	-29° 35.88	164 27.77	3392	433 cm	Multicoloured nanno ooze, with distinct beds 20-40 cm thick: yellow, yellowish brown, pale & dark greenish grey.	DD
GC24	-27° 52.02	165 43.00	3450	266 cm	Pale brown & pale yellow nanno ooze	SB, DNS, BSR, NCB
GC25	-27° 09.78	164 36.54	3239	407 cm	0-359 cm: pale brown & pale yellow nanno ooze. 359-407: repeat	DNS, SB
GC26	-27° 13.74	164 14.43	2935	377 cm	Pale yellow, pale brown & greenish grey nanno ooze	DNS
GC27	-27° 17.67	163 52.50	1875	248 cm	Pale brown, pale yellow, light grey & white nanno ooze	SB, DNS

Seismic Survey Annotations:

DNS: near-surface diapir — F: Fault — BSR: Bottom simulating reflector
DpBSR: Diapir piercing the BSR — PM: pock mark — BR: basement ridge
DD: Deep diapir — SB: surface bulge — WNR: West Norfolk Ridge
MD: Minor diapir — PO: paleo-oceanography — WNCB: West New Caledonia Basin

Echofacies (3.5 kHz):

1a: Layered, flat (long wave amplitude) 1b: Layered, wavy (short wave amplitude)

Tables 1, 2 from Exon et al., 2001

Table 3. Cores from ZoNéCo 5 Survey

Core	Latitude	Longitude	Depth (m)	Length (cm)	Seismic profile interpretation
KG 01	-25º 35.74	164º 28.58	2735	682	PM, BSR, F
KG 02	-25° 30.27	164° 27.55	2753	602	PM, BSR, F
KG 03	-25° 37.64	164° 19.20	2653	688	PM, BSR, F
KG 04	-25° 43.26	164° 20.35	2647	610	PM, BSR,
KG 05	-25° 39.80	164° 11.07	2604	735	BSR
KG 06	-25° 46.33	164° 12.23	2530	702	PM, BSR, F, DD
KG 07	-25° 51.70	164° 13.30	2569	430	PM, BSR, F, DD
KG 08	-26° 19.80	164° 23.70	1250	683	Background Core
KG 09	-26° 38.60	164° 14.00	2473	425	F
KG 10	-26° 32.64	164° 05.35	2390	648	DpBSR, F, DD
KG 11	-26° 19.64	163° 54.89	2060	583	PM, BSR, D
KG 12	-26° 16.50	163° 54.24	2031	758	BSR, F
KG 13	-26° 00.77	163° 51.31	1968	703	PM, BSR, F

(Table 3): Data interpolated from Dickens et al., 1999

Table 4. Pore water and gas yields from sub-samples

Core #	Interval	Amount Water (cc)	Amount Gas (cc)		Core #	Interval	Amount Water (cc)	Amount Gas (cc)
1	CTW-1	25	25		**15**	CTW-15	25	25
1	(5-11)	17	13		**15**	(85-90)	4	25
1	(112-114)	8	22		**15**	(127-132)	12	12
1	(221-224)	5	25		**15**	(152-156)	5	25
2	CTW-2	6	24		**15**	(232-256)	10	20
2	(7-10)	7	23		**16**	CTW-16	25	25
2	(354-360)	6	24		**16**	(32-38)	6	25
3	CTW-3	25	25		**16**	(62-68)	5	25
4	CTW-4	25	25		**16**	(185-190)	13	13
4	(8-12)	9	23		**16**	(285-290)	10	10
4	(70-75)	9	18		**18**	CTW-18	25	25
4	(99-102)	12	12		**18**	(13-18)	6	24
4	(171-176)	13	13		**18**	(100-105)	5	25
4	(200-206)	15	20		**18**	(205-210)	11	10
4	(305-309)	10	20		**21**	CTW-21	25	25
5	CTW-5	25	25		**21**	(15-20)	9	20
5	(0-5)	21	21		**21**	(145-150)	12	11
5	(142-148)	12	13		**21**	(275-280)	12	12
5	(297-300)	13	13		**21**	(385-390)	3	24
6	CTW-6	25	25		**22**	CTW-22	25	25
6	(10-15)	9	19		**22**	(30-37)	19	19
6	(118-123)	11	11		**22**	(72-80)	27	25
6	(318-323)	9	20		**22**	(188-193)	12	12
8	CTW-8	25	25		**22**	(262-268)	29	25
8	(58-63)	16	16		**22**	(305-310)	23	23
8	(320-325)	11	11		**22**	(430-435)	10	10
8	(355-360)	15	16		**23**	CTW-23	25	25
9	CTW-9	25	25		**23**	(10-15)	16	16
9	(40-45)	16	16		**23**	(90-95)	12	12
9	(160-165)	12	13		**23**	(192-198)	8	22
9	(330-335)	7	23		**23**	(358-364)	(-)	(-)
10	CTW-10	25	25		**23**	(418-424)	5	25
10	(39-44)	15	15		**24**	CTW-24	25	25
10	(298-303)	8	20		**24**	(35-40)	11	11
10	(433-438)	13	13		**24**	(111-116)	12	12
11	CTW-11	25	25		**24**	(235-240)	8	22
11	(39-44)	14	14		**25**	CTW-25	25	25
11	(210-215)	10	10		**25**	(34-40)	13	13
11	(338-343)	7	25		**25**	(225-234)	16	16
12	CTW-12	25	25		**25**	(318-325)	14	14
12	(39-44)	18	18		**26**	CTW-26	25	25
12	(230-235)	14	14		**26**	(43-50)	15	15
12	(419-425)	7	25		**26**	(190-196)	16	16
14	(33-38)	12	12		**26**	(334-340)	13	13
14	(133-138)	13	13		**27**	CTW-27	25	25
14	(285-290)	12	12		**27**	(14-20)	16	16
14	(385-390)	13	13		**27**	(122-129)	17	17
14	(485-490)	10	10		**27**	(219-226)	7	23

(Table 4): Gas and pore water yields from sediment sub-samples and core top waters (CTW) collected during FR9/01 survey

Figure 6: Pore water sampling protocol and sample processing

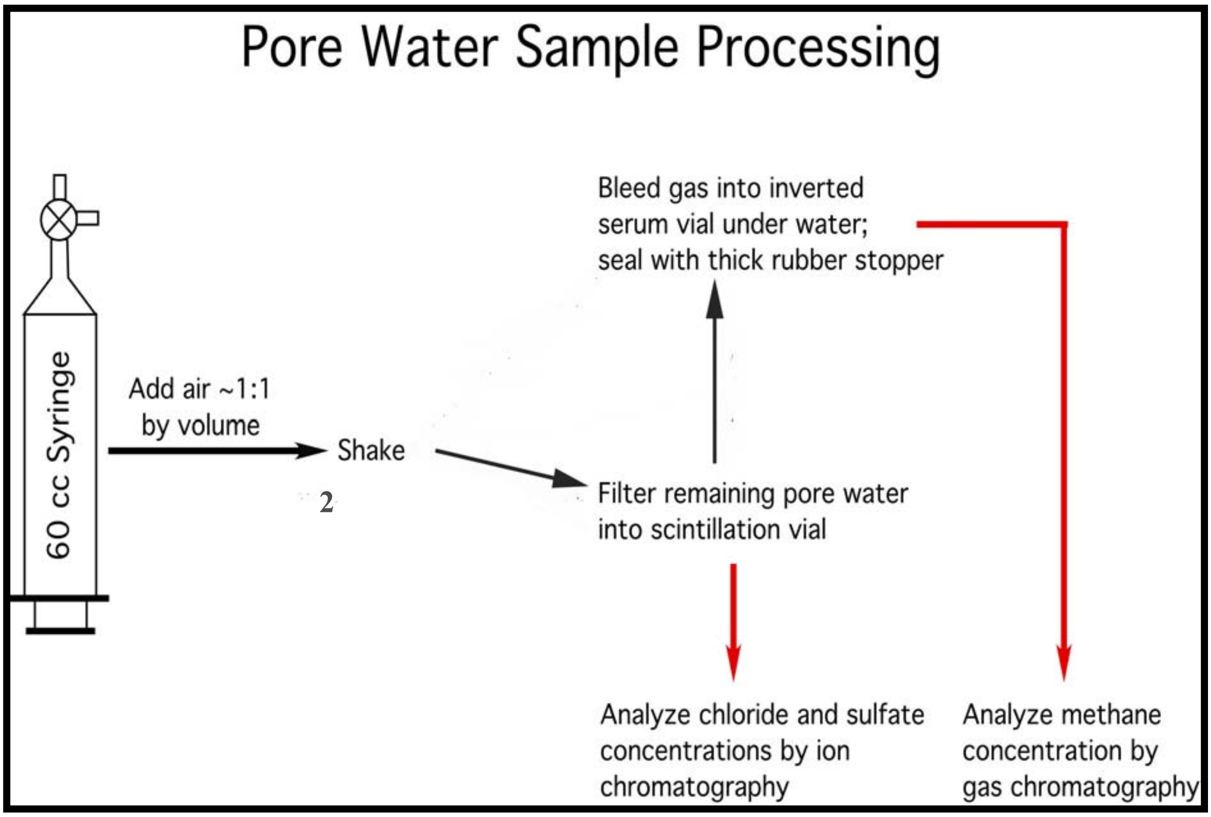

(Fig. 6): Schematic of pore water and gas sampling as diagram by Ussler, this report.

Table 5: FR/09 (LHR-01) Chloride Values

Core #	Interval	Chloride (mM)		Core #	Interval	Chloride (mM)
LHR01_GC-01	CTW-1	559.13		**LHR01_GC-15**	(85-90)	588.60
LHR01_GC-01	(5-11)	564.49		**LHR01_GC-15**	(127-132)	599.10
LHR01_GC-01	(112-114)	576.29		**LHR01_GC-15**	(232-236)	624.07
LHR01_GC-02	CTW-2	563.15		**LHR01_GC-16**	CTW-16	564.31
LHR01_GC-02	(7-10)	*757.11*		**LHR01_GC-16**	(32-38)	560.41
LHR01_GC-02	(354-360)	648.32		**LHR01_GC-16**	(62-68)	631.03
LHR01_GC-03	CTW-3	512.77		**LHR01_GC-16**	(185-190)	563.44
LHR01_GC-04	CTW-4	*428.63*		**LHR01_GC-16**	(285-290)	572.51
LHR01_GC-04	(8-12)	601.95		**LHR01_GC-18**	CTW-18	574.59
LHR01_GC-04	(70-75)	604.52		**LHR01_GC-18**	(13-18)	582.37
LHR01_GC-04	(99-102)	616.82		**LHR01_GC-18**	(100-105)	564.36
LHR01_GC-04	(171-176)	594.77		**LHR01_GC-18**	(205-210)	563.77
LHR01_GC-04	(200-206)	586.35		**LHR01_GC-21**	(15-20)	564.57
LHR01_GC-04	(305-309)	586.35		**LHR01_GC-21**	(145-150)	576.75
LHR01_GC-05	CTW-5	562.46		**LHR01_GC-21**	(275-280)	589.09
LHR01_GC-05	(0-5)	546.74		**LHR01_GC-21**	(385-390)	561.87
LHR01_GC-05	(142-148)	586.10		**LHR01_GC-22**	CTW-22	563.36
LHR01_GC-05	(297-300)	615.09		**LHR01_GC-22**	(30-37)	541.88
LHR01_GC-06	CTW-6	560.90		**LHR01_GC-22**	(72-80)	553.33
LHR01_GC-06	(10-15)	596.05		**LHR01_GC-22**	(188-193)	536.77
LHR01_GC-06	(118-123)	585.17		**LHR01_GC-22**	(262-268)	572.52
LHR01_GC-06	(318-323)	*434.62*		**LHR01_GC-22**	(305-310)	544.56
LHR01_GC-08	CTW-8	561.36		**LHR01_GC-22**	(430-435)	538.45
LHR01_GC-08	(58-63)	580.12		**LHR01_GC-23**	CTW-23	562.24
LHR01_GC-08	(320-325)	595.85		**LHR01_GC-23**	(10-15)	561.08
LHR01_GC-08	(355-360)	576.02		**LHR01_GC-23**	(90-95)	568.92
LHR01_GC-09	CTW-9	560.29		**LHR01_GC-23**	(192-198)	600.55
LHR01_GC-09	(40-45)	567.10		**LHR01_GC-23**	(418-424)	614.24
LHR01_GC-09	(160-165)	553.57		**LHR01_GC-24**	CTW-24	556.80
LHR01_GC-09	(330-335)	582.51		**LHR01_GC-24**	(35-40)	575.78
LHR01_GC-10	CTW-10	582.01		**LHR01_GC-24**	(111-116)	558.51
LHR01_GC-10	(39-44)	580.68		**LHR01_GC-24**	(235-240)	566.15
LHR01_GC-10	(433-438)	600.78		**LHR01_GC-25**	CTW-25	561.88
LHR01_GC-11	CTW-11	523.43		**LHR01_GC-25**	(34-40)	560.69
LHR01_GC-11	(39-44)	594.58		**LHR01_GC-25**	(225-234)	582.27
LHR01_GC-11	(210-215)	565.53		**LHR01_GC-25**	(318-325)	553.83
LHR01_GC-11	(338-343)	623.33		**LHR01_GC-26**	CTW-26	565.19
LHR01_GC-12	CTW-12	563.92		**LHR01_GC-26**	(43-50)	558.74
LHR01_GC-12	(39-44)	577.00		**LHR01_GC-26**	(190-196)	568.49
LHR01_GC-12	(230-235)	580.33		**LHR01_GC-26**	(334-340)	572.76
LHR01_GC-12	(419-425)	609.50		**LHR01_GC-27**	CTW-27	558.19
LHR01_GC-14	(33-38)	572.69		**LHR01_GC-27**	(14-20)	555.90
LHR01_GC-14	(133-138)	589.53		**LHR01_GC-27**	(122-129)	554.93
LHR01_GC-14	(285-290)	591.57		**LHR01_GC-27**	(219-226)	582.61
LHR01_GC-14	(385-390)	612.54		**Median**		581.35
LHR01_GC-14	(485-490)	587.93		**Stdev**		47.590

(Table 5): FR/09 (LHR-01) chloride values; Note outliers in red at GC-07 (7-10 cm), GC-04 (CTW), and GC-06 (318-323).

Figure 7: FR/09 (LHR-01) Chloride Values Plotted with MSW value 559.9 mM

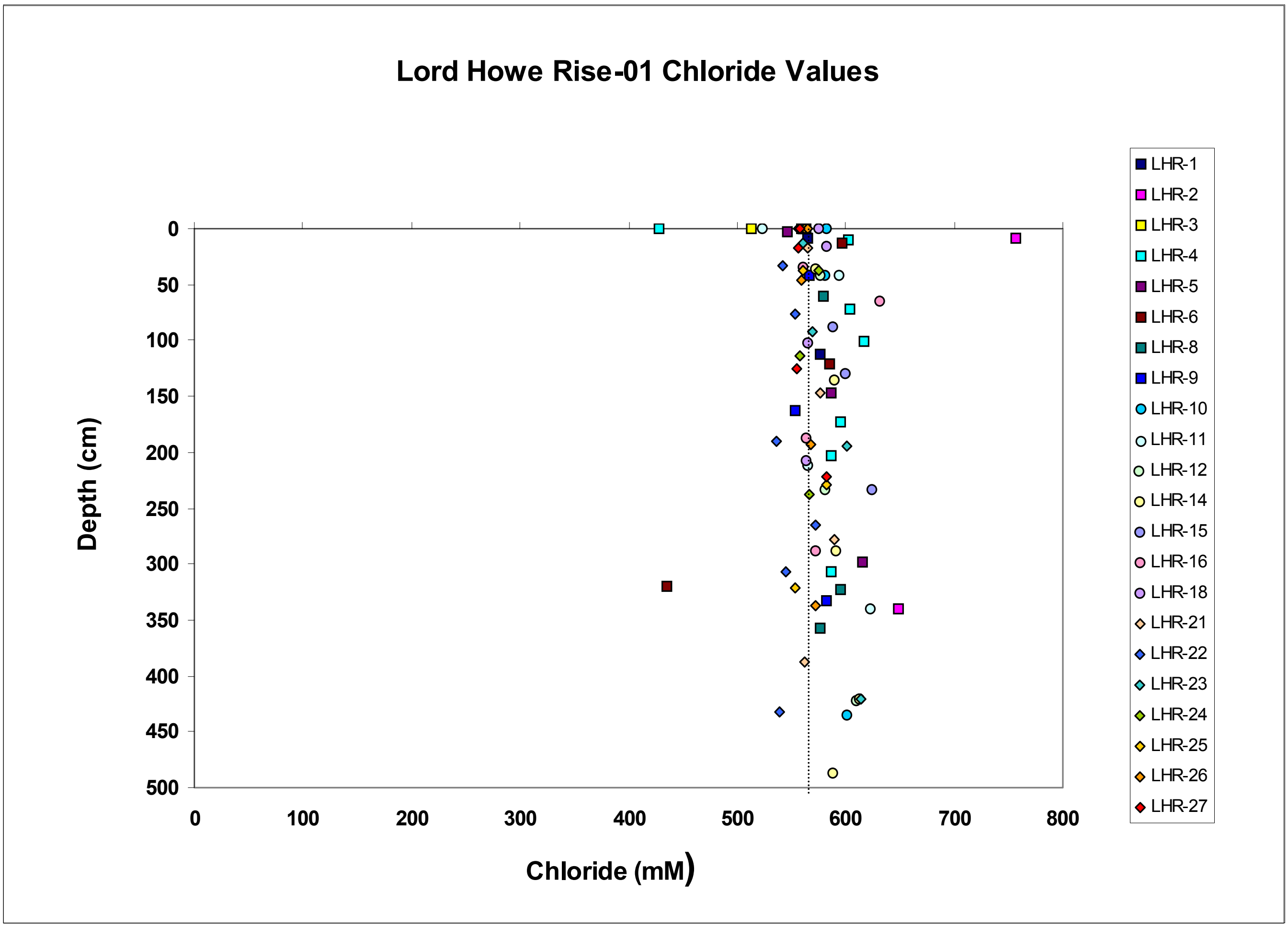

(Fig. 7): FR/09 (LHR-01) Chloride Values Plotted with MSW value 559.9 mM.

Table 6: FR/09 (LHR-01) Sulfate Values

Core #	Interval	Sulfate (mM)		Core #	Interval	Sulfate (mM)
LHR01_GC-01	CTW-1	28.83		**LHR01_GC-15**	(127-132)	29.43
LHR01_GC-01	(5-11)	28.93		**LHR01_GC-15**	(232-236)	29.67
LHR01_GC-01	(112-114)	29.09		**LHR01_GC-16**	CTW-16	29.11
LHR01_GC-02	CTW-2	29.10		**LHR01_GC-16**	(32-38)	28.51
LHR01_GC-02	(7-10)	*30.66*		**LHR01_GC-16**	(62-68)	32.38
LHR01_GC-02	(354-360)	32.42		**LHR01_GC-16**	(185-190)	28.40
LHR01_GC-03	CTW-3	26.27		**LHR01_GC-16**	(285-290)	28.61
LHR01_GC-04	CTW-4	*22.17*		**LHR01_GC-18**	CTW-18	29.58
LHR01_GC-04	(8-12)	30.41		**LHR01_GC-18**	(13-18)	29.67
LHR01_GC-04	(70-75)	30.41		**LHR01_GC-18**	(100-105)	28.75
LHR01_GC-04	(99-102)	31.13		**LHR01_GC-18**	(205-210)	28.36
LHR01_GC-04	(171-176)	29.93		**LHR01_GC-21**	(15-20)	28.68
LHR01_GC-04	(200-206)	29.38		**LHR01_GC-21**	(145-150)	29.09
LHR01_GC-04	(305-309)	29.52		**LHR01_GC-21**	(275-280)	29.41
LHR01_GC-05	CTW-5	29.02		**LHR01_GC-21**	(385-390)	28.29
LHR01_GC-05	(0-5)	27.84		**LHR01_GC-22**	CTW-22	29.11
LHR01_GC-05	(142-148)	29.24		**LHR01_GC-22**	(30-37)	27.26
LHR01_GC-05	(297-300)	30.69		**LHR01_GC-22**	(72-80)	28.08
LHR01_GC-06	CTW-6	28.98		**LHR01_GC-22**	(188-193)	26.37
LHR01_GC-06	(10-15)	30.25		**LHR01_GC-22**	(262-268)	28.29
LHR01_GC-06	(118-123)	29.23		**LHR01_GC-22**	(305-310)	26.60
LHR01_GC-06	(318-323)	*21.72*		**LHR01_GC-22**	(430-435)	25.29
LHR01_GC-08	CTW-8	28.99		**LHR01_GC-23**	CTW-23	29.00
LHR01_GC-08	(58-63)	29.15		**LHR01_GC-23**	(10-15)	28.31
LHR01_GC-08	(320-325)	29.64		**LHR01_GC-23**	(90-95)	28.39
LHR01_GC-08	(355-360)	28.81		**LHR01_GC-23**	(192-198)	29.44
LHR01_GC-09	CTW-9	28.89		**LHR01_GC-23**	(418-424)	29.93
LHR01_GC-09	(40-45)	28.56		**LHR01_GC-24**	CTW-24	28.72
LHR01_GC-09	(160-165)	27.87		**LHR01_GC-24**	(35-40)	28.88
LHR01_GC-09	(330-335)	29.25		**LHR01_GC-24**	(111-116)	28.15
LHR01_GC-10	CTW-10	30.00		**LHR01_GC-24**	(235-240)	28.12
LHR01_GC-10	(39-44)	29.27		**LHR01_GC-25**	CTW-25	29.09
LHR01_GC-10	(433-438)	29.92		**LHR01_GC-25**	(34-40)	28.16
LHR01_GC-11	CTW-11	26.94		**LHR01_GC-25**	(225-234)	28.73
LHR01_GC-11	(39-44)	30.04		**LHR01_GC-25**	(318-325)	27.34
LHR01_GC-11	(210-215)	28.26		**LHR01_GC-26**	CTW-26	29.25
LHR01_GC-11	(338-343)	31.29		**LHR01_GC-26**	(43-50)	28.09
LHR01_GC-12	CTW-12	29.06		**LHR01_GC-26**	(190-196)	28.39
LHR01_GC-12	(39-44)	29.13		**LHR01_GC-26**	(334-340)	28.46
LHR01_GC-12	(230-235)	29.31		**LHR01_GC-27**	CTW-27	28.91
LHR01_GC-12	(419-425)	30.55		**LHR01_GC-27**	(14-20)	28.31
LHR01_GC-14	(33-38)	28.76		**LHR01_GC-27**	(122-129)	27.69
LHR01_GC-14	(133-138)	29.49		**LHR01_GC-27**	(219-226)	28.37
LHR01_GC-14	(285-290)	28.77				
LHR01_GC-14	(385-390)	29.42				
LHR01_GC-14	(485-490)	27.92		**Median**		28.99
LHR01_GC-15	(85-90)	28.99		**StDev**		1.54

(Table 6): FR/09 (LHR-01) sulfate values; Note outliers in red at GC-07 (7-10 cm), GC-04 (CTW), and GC-06 (318-323) .

Table 7: ZoNéCo 5 Sulfate Values

Core#	Interval (cm)	SO4 (mM)		Core#	Interval (cm)	SO4 (mM)
ZoNeCo-5_KG-01	(43-50)	27.3		**ZoNeCo-5_KG-06**	(446-465)	23.8
ZoNeCo-5_KG-01	(211-221)	25.8		**ZoNeCo-5_KG-06**	(682-694)	22.6
ZoNeCo-5_KG-01	(342-355)	25.8		**ZoNeCo-5_KG-07**	(62-76)	23.6
ZoNeCo-5_KG-01	(595-605)	27.2		**ZoNeCo-5_KG-07**	(153-176)	27.0
ZoNeCo-5_KG-02	(52-62)	25.5		**ZoNeCo-5_KG-07**	(320-323)	26.3
ZoNeCo-5_KG-02	(166-177)	25.5		**ZoNeCo-5_KG-07**	(411-419)	23.1
ZoNeCo-5_KG-02	(366-376)	26.5		**ZoNeCo-5_KG-08**	(262-273)	24.5
ZoNeCo-5_KG-02	(480-490)	24.3		**ZoNeCo-5_KG-08**	(315-326)	25.2
ZoNeCo-5_KG-02	(575-585)	23.0		**ZoNeCo-5_KG-08**	(411-419)	23.1
ZoNeCo-5_KG-03	(38-47)	27.3		**ZoNeCo-5_KG-09**	(23-31)	26.7
ZoNeCo-5_KG-03	(155-165)	26.3		**ZoNeCo-5_KG-09**	(114-130)	24.1
ZoNeCo-5_KG-03	(234-246)	25.8		**ZoNeCo-5_KG-09**	(312-327)	24.3
ZoNeCo-5_KG-03	(328-338)	25.7		**ZoNeCo-5_KG-09**	(405-415)	25.2
ZoNeCo-5_KG-03	(405-417)	26.5		**ZoNeCo-5_KG-10**	(14-27)	24.6
ZoNeCo-5_KG-03	(493-504)	27.3		**ZoNeCo-5_KG-10**	(176-188)	24.0
ZoNeCo-5_KG-03	(584-594)	27.2		**ZoNeCo-5_KG-10**	(474-484)	27.5
ZoNeCo-5_KG-04	(74-89)	27.3		**ZoNeCo-5_KG-10**	(574-587)	23.1
ZoNeCo-5_KG-04	(168-181)	25.3		**ZoNeCo-5_KG-11**	(61-81)	23.5
ZoNeCo-5_KG-04	(257-271)	24.5		**ZoNeCo-5_KG-11**	(276-290)	25.5
ZoNeCo-5_KG-04	(553-571)	26.0		**ZoNeCo-5_KG-11**	(372-386)	26.2
ZoNeCo-5_KG-05	(15-29)	29.0		**ZoNeCo-5_KG-11**	(553-566)	24.5
ZoNeCo-5_KG-05	(168-180)	24.5		**ZoNeCo-5_KG-12**	(60-77)	25.2
ZoNeCo-5_KG-05	(277-290)	24.5		**ZoNeCo-5_KG-12**	(277-282)	25.2
ZoNeCo-5_KG-05	(317-328)	28.2		**ZoNeCo-5_KG-12**	(471-482)	26.7
ZoNeCo-5_KG-05	(410-423)	23.3		**ZoNeCo-5_KG-12**	(723-735)	23.3
ZoNeCo-5_KG-05	(610-620)	26.8		**ZoNeCo-5_KG-13**	(64-86)	26.2
ZoNeCo-5_KG-06	(30-48)	26.0		**ZoNeCo-5_KG-13**	(272-289)	23.5
ZoNeCo-5_KG-06	(157-159)	27.7		**ZoNeCo-5_KG-13**	(343-359)	26.8
ZoNeCo-5_KG-06	(273-283)	22.8		**ZoNeCo-5_KG-13**	(675-685)	23.3
ZoNeCo-5_KG-06	(310-325)	25.3		**Median**		25.5
				Stdev		1.55

(Table 7): Data from Dickens et al., 1999

Figure 8: Sulfate profiles from LHR-01 samples

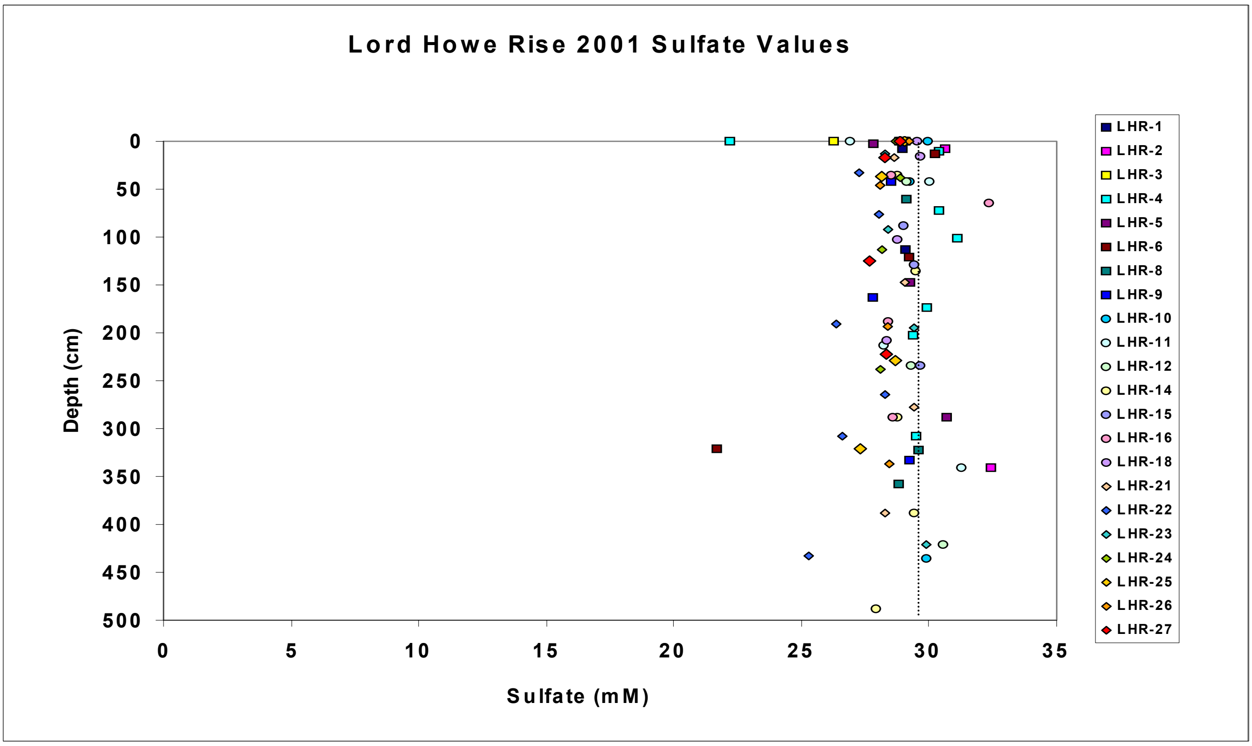

(Fig. 8): Sulfate profiles from LHR-01 samples.

Figure 9: Sulfate profiles plotted from ZoNéCo 5 data

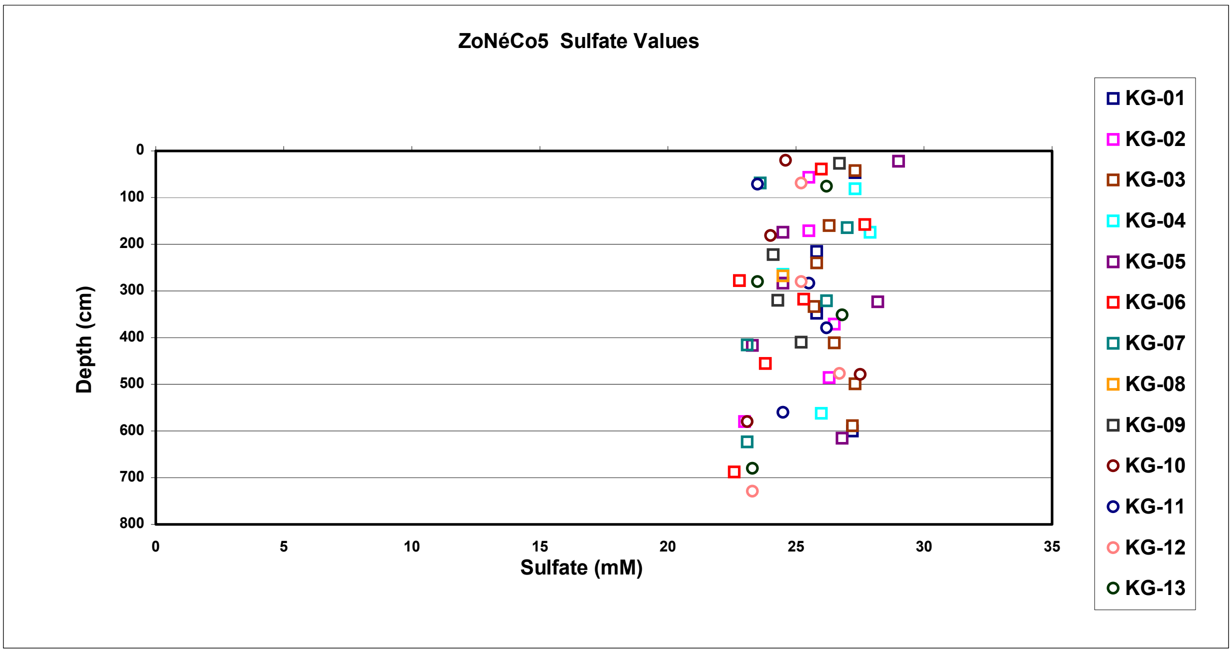

(Fig. 9): Sulfate profiles plotted from ZoNéCo 5 data of Dickens et al, 1999

Table 8: FR9/01 (LHR-01) and ZoNéCo 5 Methane Concentrations

Core #	Interval	Methane (ppm)		Core #	Interval	Methane (ppm)
LHR01_GC-04	(305-309)	1.77		**ZoNeCo-5_KG-01**	(142-152)	0.20
LHR01_GC-05	(297-300)	1.96		**ZoNeCo-5_KG-01**	(642-650)	0.35
LHR01_GC-06	(318-323)	2.05		**ZoNeCo-5_KG-02**	(142-150)	1.52
LHR01_GC-08	(320-325)	1.98		**ZoNeCo-5_KG-02**	(480-490)	2.19
LHR01_GC-09	(330-335)	1.64		**ZoNeCo-5_KG-03**	(139-149)	0.77
LHR01_GC-10	(433-438)	1.97		**ZoNeCo-5_KG-03**	(141-149)	0.39
LHR01_GC-11	(338-343)	1.83		**ZoNeCo-5_KG-03**	(511-519)	2.08
LHR01_GC-12	(419-425)	1.67		**ZoNeCo-5_KG-04**	(60-70)	0.49
LHR01_GC-14	(385-390)	2.47		**ZoNeCo-5_KG-05**	(600-610)	0.44
LHR01_GC-15	(232-236)	1.53		**ZoNeCo-5_KG-05**	(729-739)	0.47
LHR01_GC-16	(62-68)	1.9		**ZoNeCo-5_KG-06**	(180-190)	0.03
LHR01_GC-16	(285-290)	2.09		**ZoNeCo-5_KG-06**	(660-670)	0.30
LHR01_GC-18	(205-210)	1.97		**ZoNeCo-5_KG-07**	(80-90)	1.57
LHR01_GC-21	(275-280)	1.73		**ZoNeCo-5_KG-07**	(401-410)	0.22
LHR01_GC-22	(262-268)	2.37		**ZoNeCo-5_KG-08**	(59-60)	0.30
LHR01_GC-22	(305-310)	2.11		**ZoNeCo-5_KG-08**	(580-590)	0.81
LHR01_GC-22	(430-435)	1.94		**ZoNeCo-5_KG-09**	(80-90)	0.63
LHR01_GC-23	(418-424)	1.85		**ZoNeCo-5_KG-09**	(393-397)	1.11
LHR01_GC-24	(111-116)	1.56		**ZoNeCo-5_KG-09**	(415-422)	0.27
LHR01_GC-25	(318-325)	1.73		**ZoNeCo-5_KG-10**	(80-90)	0.21
LHR01_GC-26	(334-340)	1.79		**ZoNeCo-5_KG-10**	(559-560)	1.67
				ZoNeCo-5_KG-11	(83-93)	0.29
Median		1.90		**ZoNeCo-5_KG-11**	(569-579)	0.59
Std Dev		0.24		**ZoNeCo-5_KG-11**	(742-752)	0.15
				ZoNeCo-5_KG-12	(82-92)	0.49
				ZoNeCo-5_KG-13	(112-122)	0.00
				ZoNeCo-5_KG-13	(675-685)	1.09
				Median		0.47
				Std Dev		0.57

(Table 8): FR9/01 (LHR-01) methane values measured in ppm and ZoNéCo 5 methane concentrations in ppm from Dickens et al, 1999.

Figure 10: LHR-01 Methane profile plots

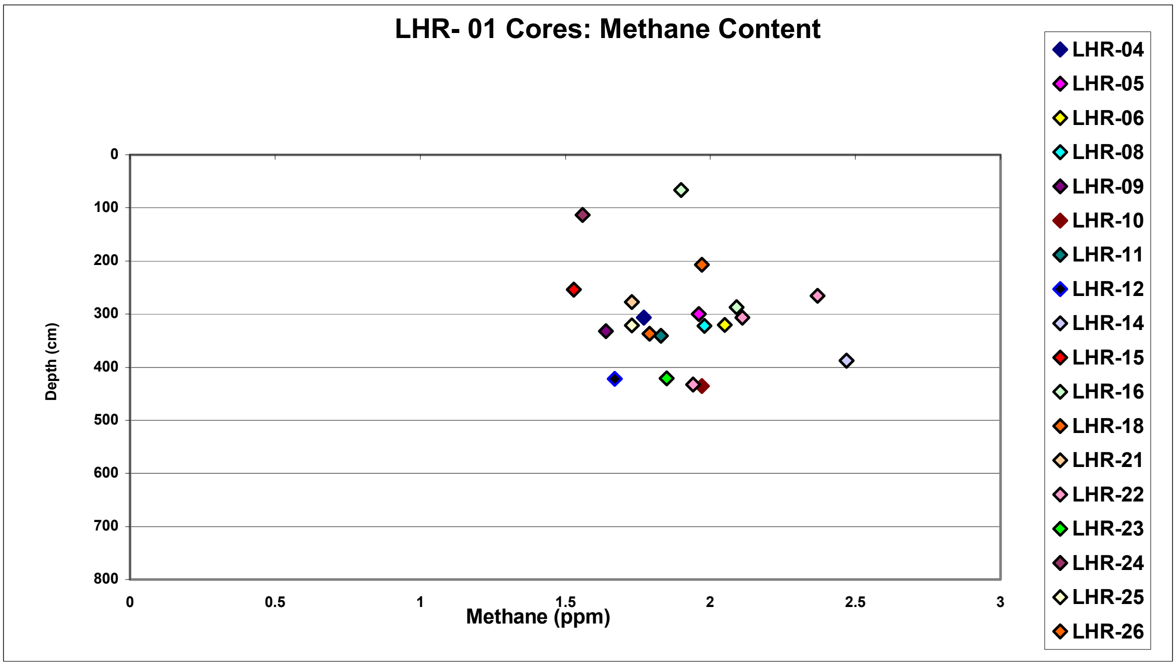

Fig. 10: LHR-01 Methane profile plots in ppm.

Figure 11: Methane profiles plotted from ZoNéCo 5 data

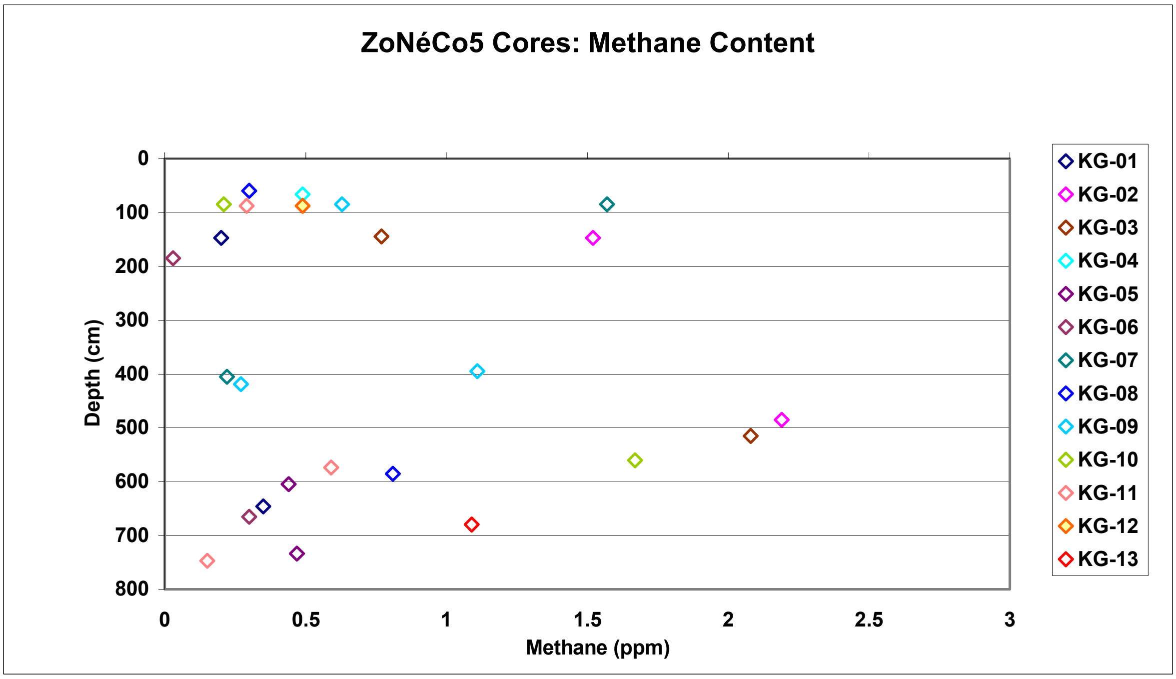

(Fig. 11): ZoNéCo 5 methane profile plots in ppm from Dickens et al, 1999 data.

Figure 12: Location Map of Blake Ridge Survey

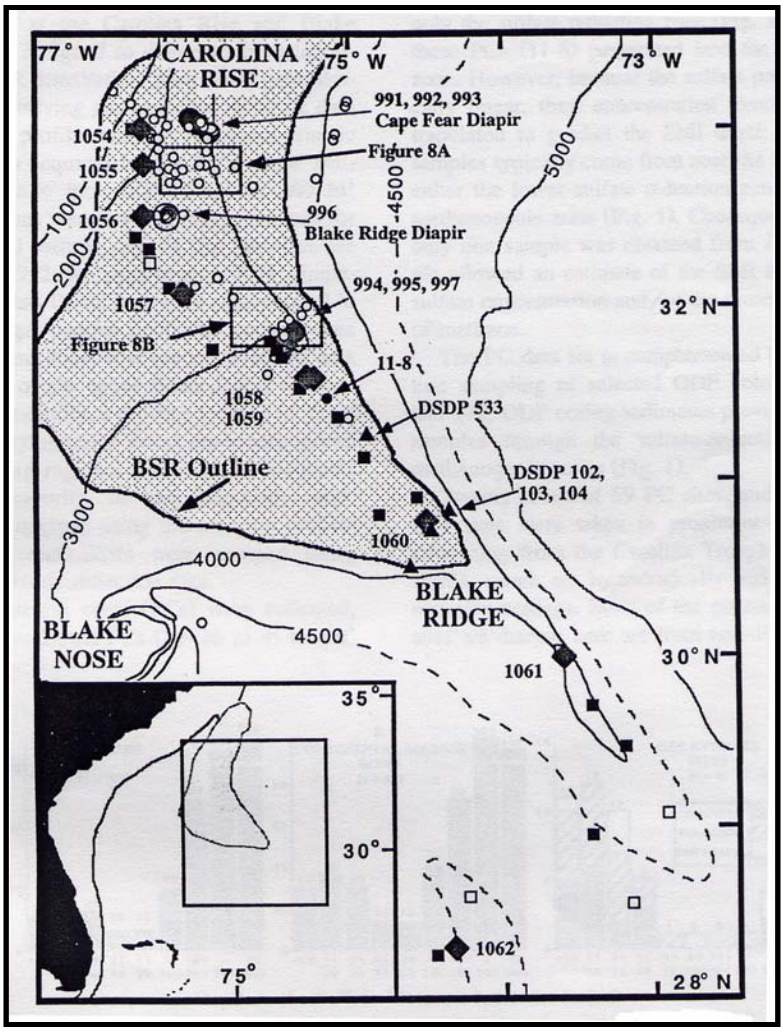

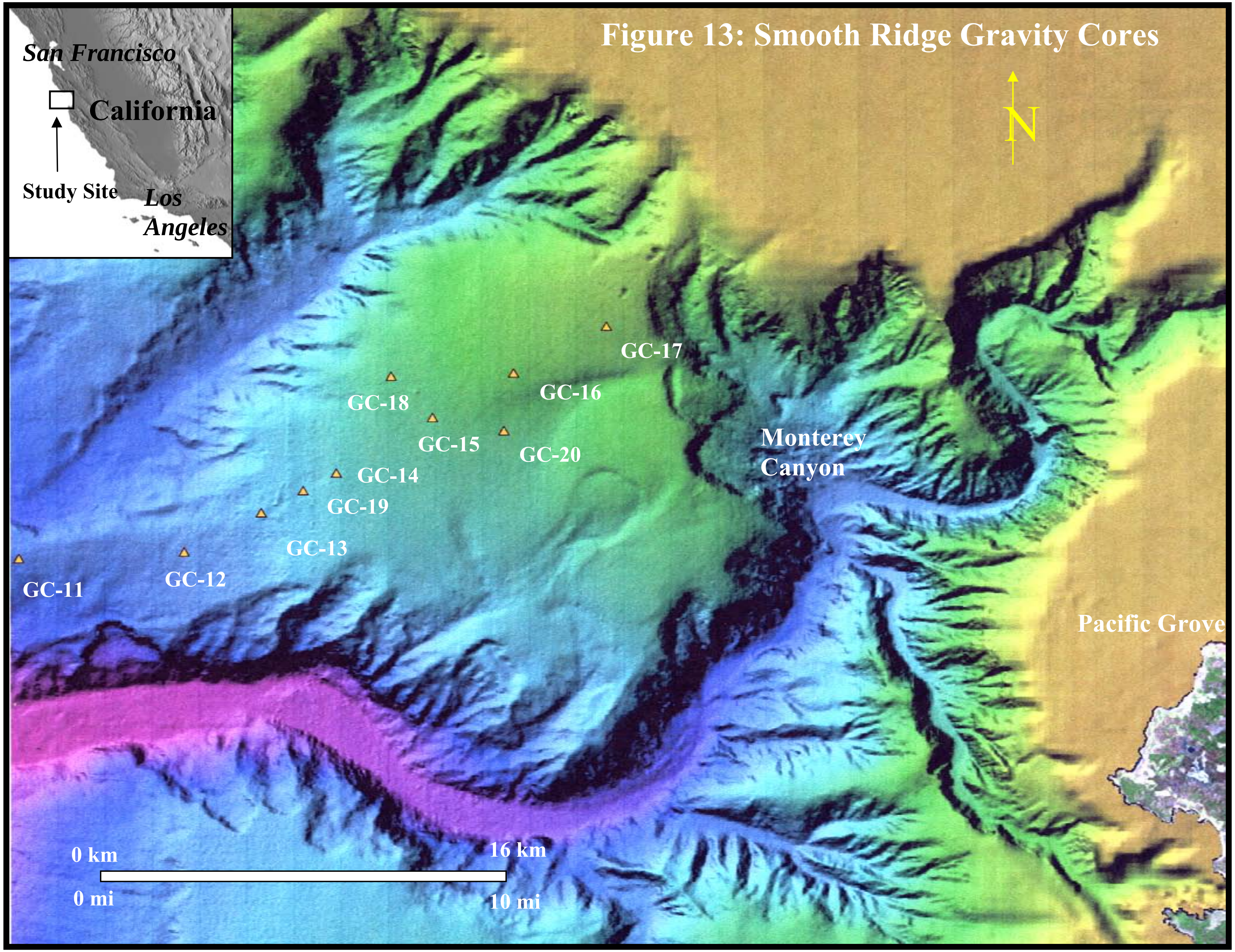

Figure 13: Smooth Ridge Gravity Cores

Figure 15: Blake Ridge and Smooth Ridge sulfate profiles

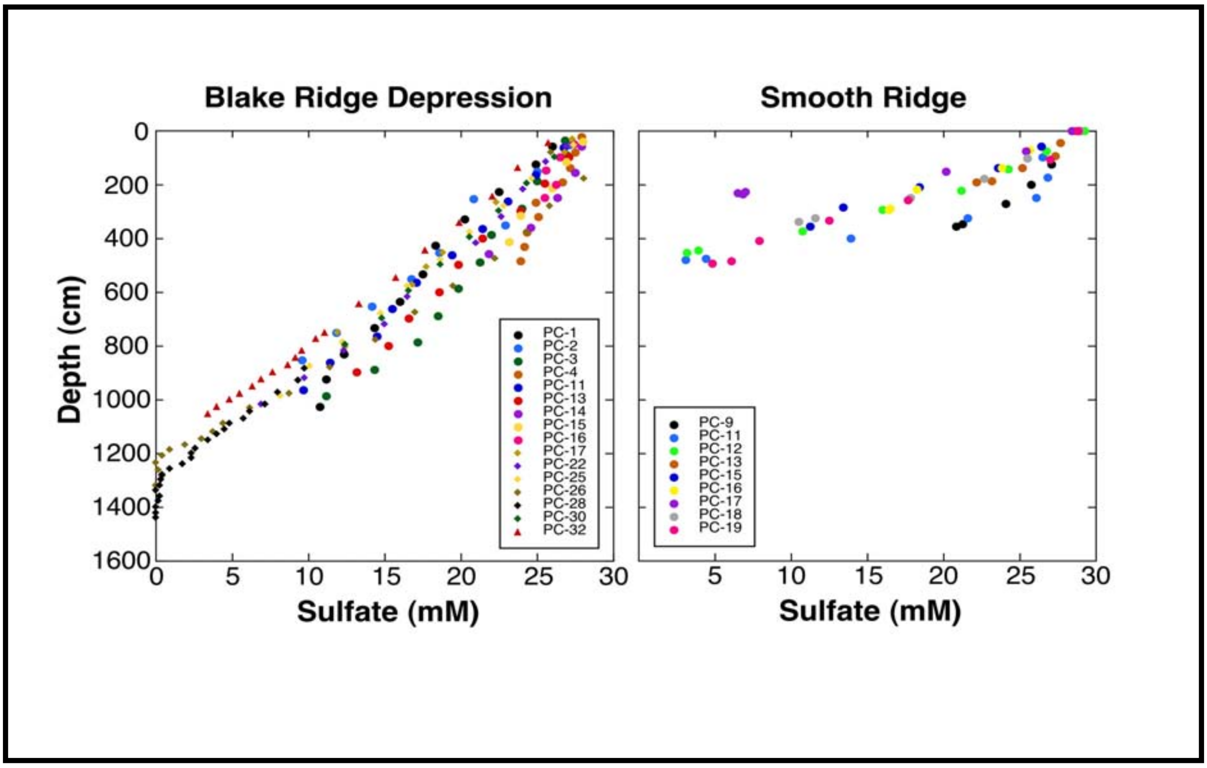

(Fig. 15): Blake Ridge and Smooth Ridge sulfate profiles note the gradients of the sulfate concentration curves with those from LHR-01 (Fig. 9)
(Ussler and Paull, unpublished data)

Appendix 2. Fairway Basin core descriptions

Dr Neville Exon and Andrew Heap, Geoscience Australia
Mrs Kirsten Perry, James Cook University

The gravity cores from *Franklin* Cruise FR 9/2001 (Geoscience Australia Cruise 232) were halved and described aboard the vessel under the leadership of Neville Exon and Kirsten Perry. The cores have a nominal diameter of 8 centimetres. They are documented in Tables 4 and 5, and their locations are shown in Figure 4 in the main report. None have been X-rayed, so we cannot be sure whether core sequences that show no structure whatsoever are completely undisturbed or (more likely) have been completely bioturbated. These Quaternary cores, from beneath an oceanic low productivity area (24-32ºS) far from land, consist of calcareous ooze and have a great paucity of organic matter (c.f. Appendix 9) and general lack of pyrite. They are generally nannofossil oozes with variable quantities of foraminifera. The detailed examination of the foraminifera by George Chaproniere (Section 8) shows that planktonic foraminifera make up > 95 % of total foraminifera. The general absence of pteropods suggests that sedimentation occurred below the local Aragonite Compensation Depth, which hence must lie shallower than 1300 m below sea level. Location details are given in Tables 4 and 5 in the main body of the text. Kirsten Perry is engaged in a detailed study of the cores for her PhD.

Here we provide simplified logs of representative cores, in five strings – four along east-west seismic profiles, and one basinal string from north to south. The cores are generally oxidized and light coloured. In general terms, the core colours represent degrees of oxidation. From most to least oxidized the colours (average Munsell soil colour in brackets) are grouped as pale brown to pale yellow (10YR7/4 to 2.5Y 7/3), white, grey (5Y 6/1), greenish grey (GLEY 1 6/2) and pale olive (5Y 6/3). Shannon Muir drew up the core logs for publication and tried to match the Munsell colours.

Kirsten Perry used a Geotek multisensor logger to measure bulk density, P-wave velocity and magnetic susceptibility on 16 half cores for her doctoral studies, and the raw data will be available in Geoscience Australia's MARS sediment database. Initial processing by Andrew Heap shows that the logs of these homogeneous pelagic carbonate do not vary much with depth. The bulk density is generally 1.1-1.3 gm/cc and the P-wave velocity is correspondingly low. The magnetic susceptibility is very low, but generally slightly higher in the upper part of the core.

Northern cores along seismic profile 232/1 (Figure 1)

Thirteen cores were taken from west to east in New Caledonian waters. The shallowest was on the Lord Howe Rise and the deepest in the New Caledonia Basin. Five representative cores are illustrated in Figure 1. All are light coloured foram-bearing nannofossil ooze, dominantly very pale brown or pale yellow in colour, with common pale grey beds. Scattered burrow mottling occurs in some beds and poorly defined bedding in others. About a third of the core sequences show no structure whatsoever. There is little apparent change in the cores from GC01 in water 1297 m deep, to GC12 in water 3517 m deep. However, the base of GC01, GC02 and GC12 is Early to Middle Pleistocene, whereas the base of GC06 and GC10 is Late Pleistocene, suggesting variation in depositional rates. Assuming the pelagic rain is constant along the profile, this variation is probably caused by transport and erosion in shallow water, and dissolution in deep water.

Central cores along seismic profile 232/5 (Figure 2)

Three cores were taken further south, from east to west in Australian waters. All were taken in the Central Fairway Basin, on the flank of the Lord Howe Rise. All are light coloured foram-bearing nannofossil ooze, and they are very similar to the cores illustrated in Figure 1. They are largely very pale brown to yellow in colour, with minor grey beds and one light greenish grey bed. Mottled, poorly bedded and massive beds are all common. There is little apparent change from GC27 in water 1866 m deep, to GC25 in water 3239 m deep. The base of GC27 and GC12 is Late Pleistocene, whereas the base of GC26 is Late Pleistocene. The slower deposition at GC26 may be caused by greater erosion.

Southern cores along seismic profile 232/8 (Figure 3)

Three cores were taken further south, from east to west in Australia waters. All were taken in the Southern Fairway Basin in deep water. All are foram-bearing nannofossil ooze as in the cores further north. The shallowest core, GC 21 in 2818 m depth, is dominantly pale brown to yellow like the northern cores. However, the abundance of greenish grey beds in the two deeper cores suggests that they have not been heavily oxidised, probably because the bottom waters have been oxygen-poor during some periods. The shallower core shows more burrow mottling, and the deeper cores more bedding. The base of all three cores is Late Pleistocene.

Southernmost cores along seismic profile **232/11** *(Figure 4)*

These three cores from the East Lord Howe Spur and the Taranaki Basin, are less oxidised overall than those from other areas. All are foram-bearing nannofossil ooze. One of the shallower cores, GC15 from 2147 m deep, is dominantly pale brown or yellow, but the other relatively shallow core, GC16, contains only one thin brown bed and is dominantly olive in colour. The deepwater core from the Taranaki Basin, GC14, contains white, pale brown and olive beds. Bedding is not common. Burrow mottling is rare in GC14, probably because of relatively reducing conditions. The base of all three cores is Late Pleistocene.

North-south basinal core profile (Figure 5)

In order to investigate further the north-south variation in cores, one basinal core from each of the above profiles is displayed here. All are in water depths of 2700-3500 metres. The two northern cores, GC12 and GC25, are dominantly pale brown or yellow and oxidised, with some grey beds in GC12. GC22 is dominantly pale grey and greenish grey suggesting less oxidation southward. GC14 is the most mixed of all the cores, with white beds dominant, but also some pale brown or yellow and some pale olive beds. The impression is clear that conditions were more oxidising and homogeneous in the north, and more reducing and variable in the south.

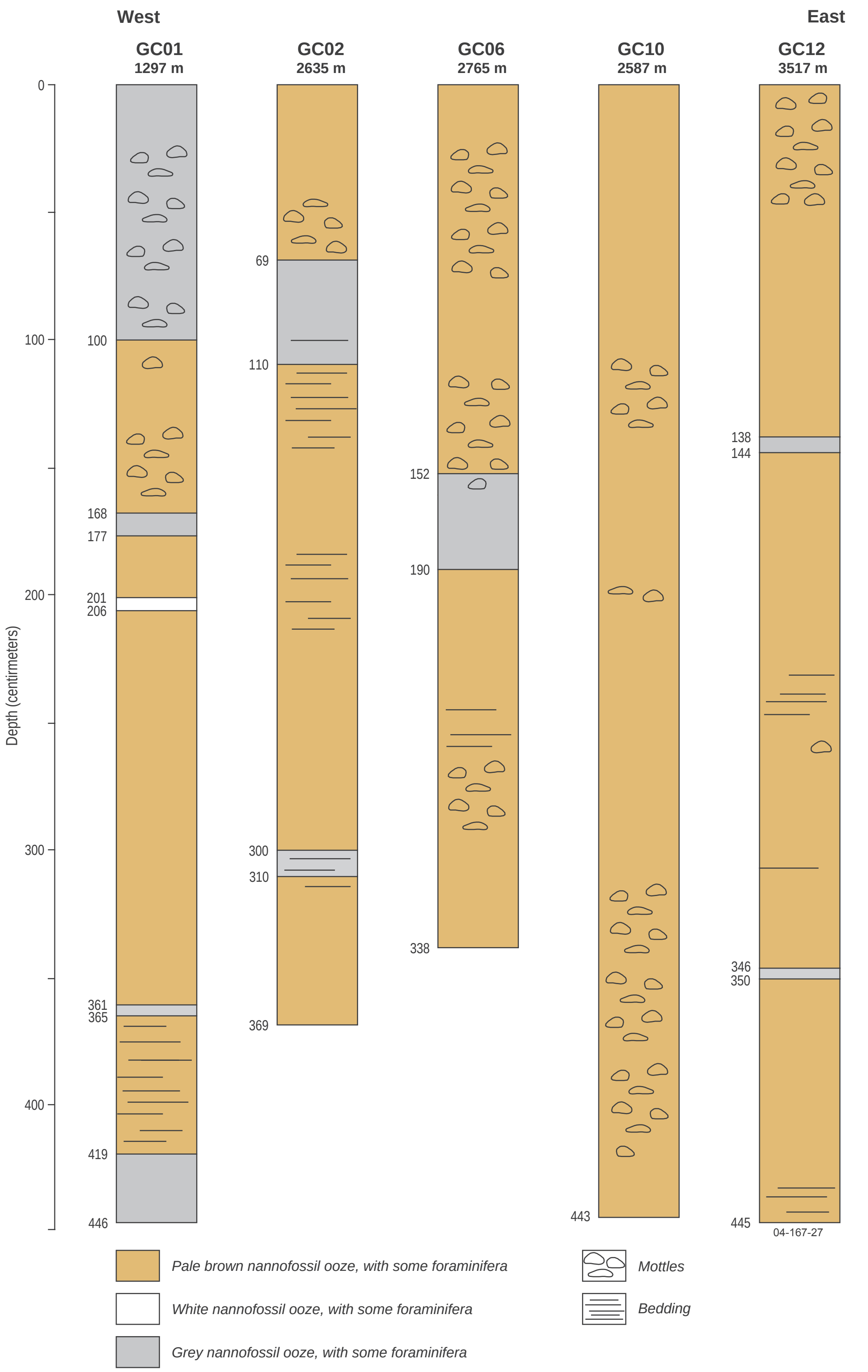

Figure 1. Representative cores taken downslope from GC01 on the Lord Howe Rise, eastward through Central Fairway Basin to northern New Caledonia Basin, latitude 25°S.

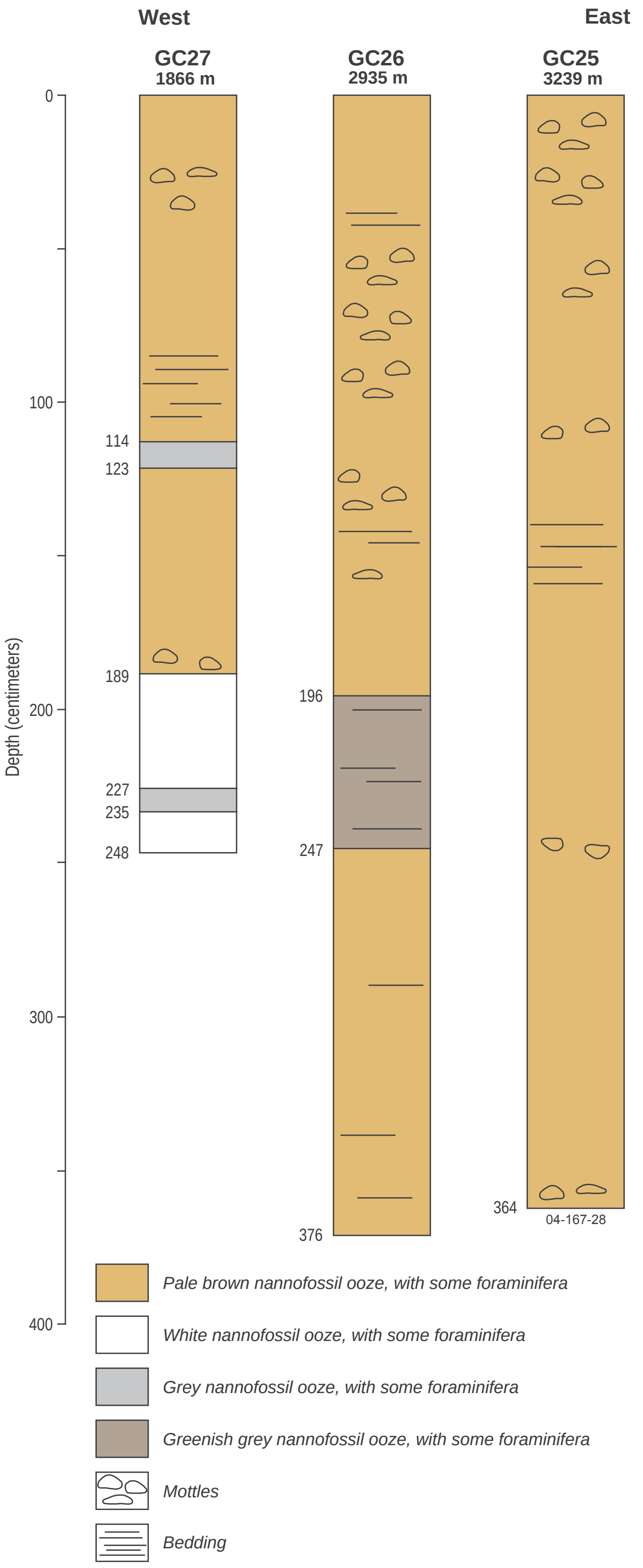

Figure 2. Cores taken upslope and westward in South Fairway Basin, latitude 27°S.

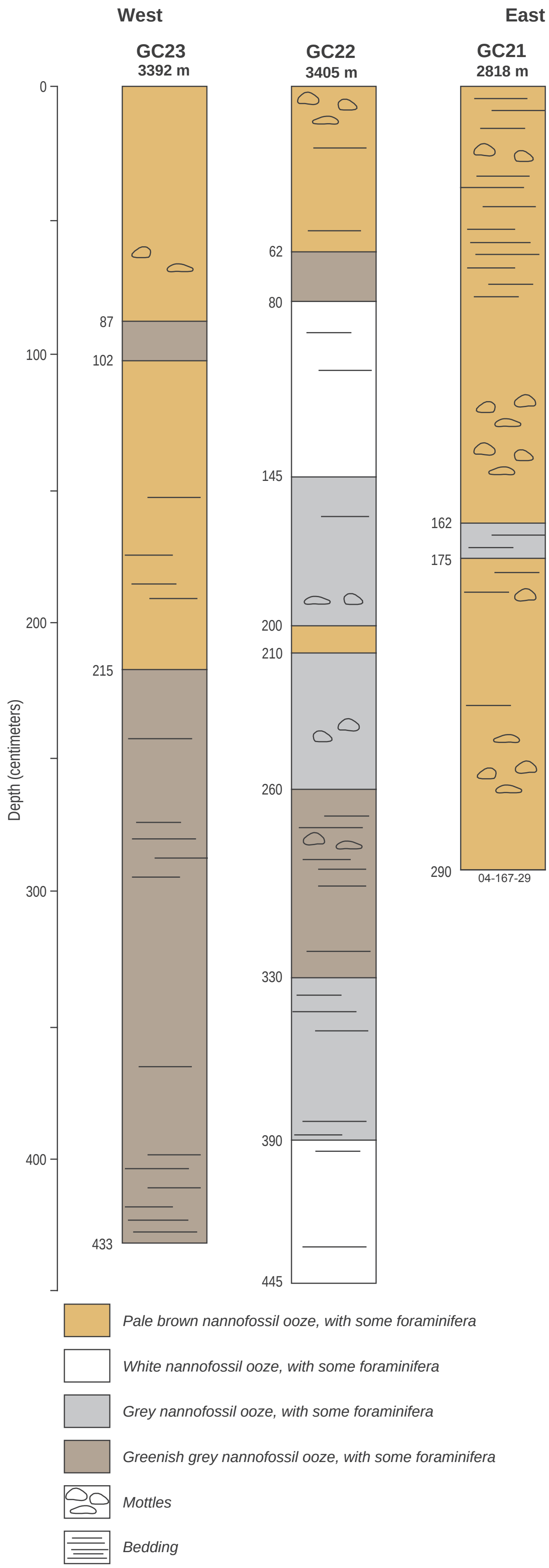

Figure 3. Cores taken from GC21 on West Norfolk Ridge, across South Fairway Basin to the west, latitude 29°30'S.

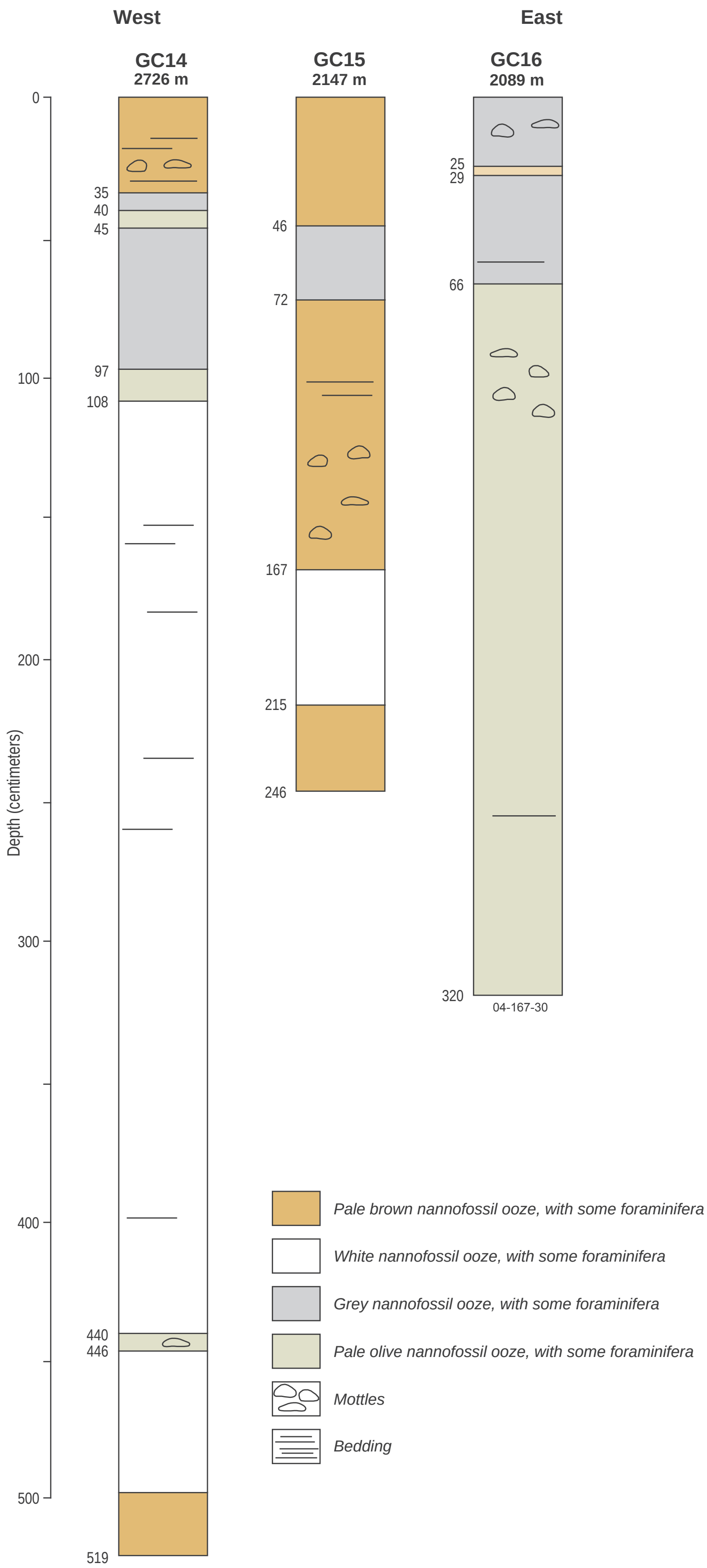

Figure 4. Cores taken eastward from Taranaki Basin to East Lord Howe Spur, latitude 31°30'S.

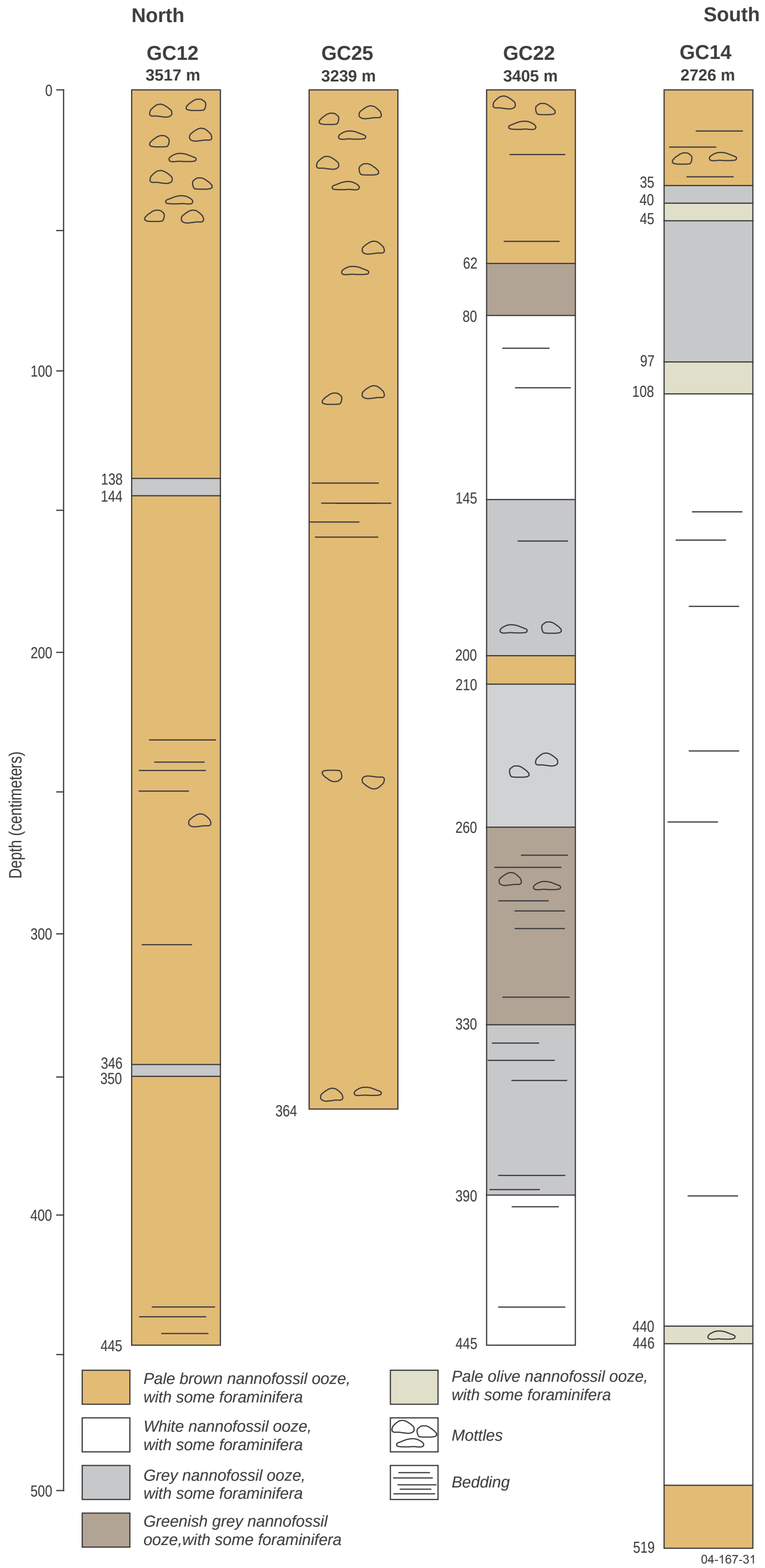

Figure 5. North-south string of deep water cores, taken over about 700 kilometres from latitude 25°S to latitude 31°30'S.

Appendix 3: Cruise Narrative

We departed from Brisbane at 1045 local time on 13 November (0045 on Julian Day 317) and headed down the Brisbane River and into Moreton Bay on a bright sunny day with a moderate breeze in our face. Once in the open sea we made 10-11 knots over the ground at a heading of 80º, into a current from the northeast. Around 1800 we deployed the new Geoscience Australia magnetometer in the hope of getting a magnetic profile across the Tasman Basin. With no response from the equipment, it was hauled in for overhaul at 2300.

On 14 November, we were still underway to the first station and refining our plans. During the day, from 1230 until 1430, a CTD cast and several XBT casts were carried out at the one station, to compare data sets. At 1800, tests showed a break in the magnetometer cable and it was cut beyond the break and re-terminated, leaving the cable 50 m shorter at 200 m long. The cable was redeployed at 2300 and worked well as we climbed the western flank of Lord Howe Rise. The magnetometer was now 150 m behind the ship at the end of the neutrally buoyant cable.

New Caledonian sampling and seismic survey

At 2300 on 15 November (1100 on Julian Day 319) we deployed the 6 m gravity corer in 1300 m water depth on the eastern flank of Lord Howe Rise in New Caledonian territory. We recovered 450 cm of light grey to very pale brown nannofossil ooze, with decreasing forams and increasing stiffness down the core. Early on 16 November we deployed the seismic system in good weather on the long Seismic **Line 1** to the east across the Fairway Basin. The system consisted on a hired compressor, two GI airguns suspended from a rail beneath a buoy, and a 300 m long, 24 channel *Stealtharray* solid seismic cable. This system towed well at 8 knots. A 40 minute ship's engine failure around 0300 on 16 November necessitated pulling the seismic cable in by hand. Seismic surveying recommenced after a long turn (Line 1, part 2), but was cut short by a compressor failure at 1030, caused by rust, dirt and water in its fuel tank. Another short period of seismic acquisition was ended by more dirt in the filter at 1415.

At 1800 on 16 November we decided to stop waiting on seismic acquisition and started coring in the Fairway Basin. GC2 recovered 369 m of pale nannofossil ooze at 2130, and then we took cores GC3-6, and GC8-9, consisting of similar sediments in cores of similar length. The cores were split, described and sampled for headspace gas, hydrocarbon isotopes and pore water. This coring program ended at 1850 on 17 November, and we headed back westward to complete Seismic Line 1.

Craig Wintle and the ship's engineers had jury rigged the diesel motor that drives the compressor to take clean fuel from a 200 litre drum, and a test of several hours suggested that this was likely to be a success. It involved hand pumping of fuel for 10 minutes every 2 hours, but worked. At 2245 on 17 November we reached the area for the continuation of Seismic **Line 1** (part 3) and started to deploy the seismic gear. At 0030 on 18 November the first shot was fired. The 205 km long Line 1 was completed at 1245 on 18 November and Seismic **Line 2** to the south in the New Caledonia Basin was started at 1330. Shortly afterward the bearings failed of a pulley tensioning the six belts connecting the motor and the compressor, and seismic acquisition stopped. Profiling recommenced at 1630 after the bearings were replaced, and the 110 km long Line 2 was completed at 0100 on 19 November.

Seismic **Line 3** to the west up the eastern flank of the Lord Howe Rise started at 0130 on 19 November and was terminated at 0230. The drive belts between the diesel motor and the compressor had burnt out, as had the bearings of the tensioning pulley for the belts. The ship's engines failed from 0500 to 0830. Email discussions started with ships' agents in Noumea and the supplier of the equipment in Australia about sourcing and delivery of diesel/compressor spares. To reduce the pressure on the single mechanical technician, and to do useful work while repairs continued, we returned to Seismic **Line 1** to attempt to sample older sediments on the buried basement block just west of the New Caledonia Basin. Cores GC10-12 were taken between 1800 on November 19 and 1300 on November 20.

The vessel then headed south about 60 km to dredge the northern end of a large basement block west of the New Caledonia Basin. Two dredges were attempted between 0400 and 1330 on 20 November. DR1 was successful in recovering Neogene chalks. DR2 lost the dredge to some hard outcrop. DR3 was attempted between 1600 and 1900 in the central part of the block, 50 km south, and recovered only ooze. At 2100 seismic profiling recommenced on Line 3 running to the west, and this 107 km long profile was completed with only minor further problems at 0650 on 21 November. Seismic **Line 4** to the SSW, 95 km long, commenced at 0700 and was completed at 8 knots at 1240. This took us out of New Caledonian territory 1.7 days later than originally planned.

Australian seismic survey

After a turn during which the compressor was checked and adjusted, Seismic **Line 5** to the ESE commenced at 0230 on 21 November. The 187 km long line was finally completed at 0430 on 22 November, and then the compressor belts shredded again. They are operating at a temperature of 140°C, which is much higher than one would expect. We again discussed the option of going to Norfolk Island to pick up spares if the remaining two sets of belts failed, and asked Steve Dutton in Canberra to pursue spares and air transport more vigorously. At 1000 we started Seismic **Line 6** to the WSW, but the compressor failed again at 1200 because of fuel problems. At 1430 the line recommenced and it continued with minor problems until 0300 on 23 November when firstly the airguns needed attention, and secondly the compressor threw off a belt. Profiling recommenced at 0800 but at 1115 dirty fuel caused another delay. Line 6, 242 km long, was finally completed at 1515 on 23 November. The compressor was checked on the turn and a leaking seal on the second stage was replaced. The airguns were also recovered to fix an air leak. During the day arrangements were made to fly spares to Norfolk Island for collection at the end of the next seismic line, including heavier duty belts.

At 1820 on 23 November, Seismic **Line 7** to the ESE started. It continued without problems until 0745 on 24 November, when dirty fuel caused a brief failure. It was decided to continue the line to Norfolk Island, and the remainder of the program was modified accordingly. Only minor further stoppages occurred on 24 November with the vessel recording at 8 knots and data quality being good. The same applied on 25 November until we terminated the line off Norfolk Island at 1200 and pulled in the seismic gear. Spare parts such as belts, bearings and oil filters for the diesel compressor were transferred to the vessel by boat, and we started Seismic **Line 8** to the southwest at 1600, and later west at 2330. It was designed to join the western end of east-west *Rig Seismic* Seismic **Line 177**/LHRNR-C, southwest of Norfolk Island. The 550 km long line ended on the morning of 27 November.

Seismic **Line 9** to the ESE commenced at 0840 on 27 November. After early problems, with the computer acquisition system locking up and with tape drives, there were no major problems on this 370 km long line. The magnetometer failed at 1200 and was restarted at 1800. The line ended at 1315 on 28 November. Seismic **Line 10** to the WSW commenced at 1430 on 28 November. It was designed to tie DSDP Site 591. The magnetometer failed when brought in for the loop before this line, but was brought back into action fairly quickly. Seismic **Line 10**, 241 km long, ended at 0610 on 29 November. Seismic **Line 11** to the WSW commenced at DSDP Site 591 at 0625

Seismic **Line 11**, 139 km long was completed on the easternmost Lord Howe Rise at 1530 on 29 November, tying to *Rig Seismic* **Line 46/6**. This ended the seismic program and all the equipment was aboard and stowed away by 1700 on 29 November. Unfortunately, the tail assembly of the magnetometer was damaged during recovery.

Australian sampling program

Southern area: Core GC13 was attempted twice in 1188 m of water on the eastern Lord Howe Rise at the end of Seismic **Line 11** between 1710 and 1915 on 29 November. Only 10 cm of foram sand was recovered, indicating current activity at that depth. We then headed ENE back along Lines 11 and 10, into the southernmost Fairway Basin for a concerted sampling program. GC14 recovered 5.19 m of nanno ooze from 2726 m of water at 0130 on 30 November. GC15 recovered 2.46 m of ooze from 2147 m of water at 0430. GC16 recovered 3.2 m of foram ooze from 2089 m of water at 0750. GC17 failed the first time, recovering only traces of foram sand and ooze from 3320 m of water at 1156. A second attempt at 1347 also failed.

Then northeast to Seismic **Line 9**, where GC18 recovered 240 cm of nanno ooze from a lightly sedimented basement high in water 2590 m deep, at 2140 on 30 November.

Central area: After a transit of 100 km to the north, Core GC19 was taken at 0440 on 1 December in the flat southern New Caledonia Basin on Line 8. It failed, but the sheared fingers of the core catcher showed that it had penetrated. We then moved west along Seismic **Line 8**, to a lightly sedimented basement high on the eastern flank of the northern extension of the West Norfolk Ridge. On the evidence of damage to the core cutter, Core GC20 skidded off the outcrop in water 2483 m deep at 0740. Dredge DR4, taken west to east up the basement slope from water depths of 2580 to 2420 m, recovered only foram nanno ooze, and left the station at 1045. Core GC21, in transparent ooze on the western part of the ridge, was taken at 1620 in a water depth of 2818 m, and recovered 400 cm of nanno ooze. Core GC22 was located in the flat bottom of the eastern part of the Fairway Basin. It was taken at 2140 on 1 December in water 3405 m deep, in a fairly reflective surface layer, and recovered 445 cm of multicoloured nannofossil ooze. Core GC23 was located in the flat bottom of the western part of the Fairway Basin. It was taken at 0110 on 2 December in water 3390 m deep, in a fairly reflective surface layer, and recovered 433 cm of multicoloured nannofossil ooze. Dredge DR5, taken east to west on rugged basement, recovered volcaniclastic rocks and manganese crust at 0700 from water 1700 m deep on the eastern edge of the Lord Howe Rise.

Northern area: After a 270 km transit northeast, Core GC24 was taken at 2220 on 2 December in moderately transparent sediment in the flat depression of the New Caledonia Basin, on Seismic **Line 7**. It recovered 226 cm of pale brown and pale yellow nanno ooze from 3450 m water depth. Dredges DR6 and DR7 were planned to sample the eastern slope of basement high on the northern West Norfolk Ridge. Dredge DR6 sampled the slope in water depths of 3080-2840 m and recovered only nanno ooze at 0500 on 3 December. Dredge DR7 sampled the slope in water depths of 3280-3100 m and recovered only nanno ooze at 0830. After a transit of 145 km to the northwest to Seismic **Line 6**, Core GC25 was taken in transparent sediments at 1430 and recovered 407 cm of nanno ooze. Core GC26 was taken at 1810 in transparent sediments in the Fairway Basin at the foot of the Lord Howe Rise slope, in water 2935 m deep. It recovered 377 cm of nanno ooze. Core GC27 was taken in water 1866 m deep, in weakly bedded sediments on the slope of the westernmost Fairway Basin. It recovered 248 cm of nanno ooze at 2130. The core was on deck at 2150 on 3 December, and we set course for Brisbane with the magnetometer deployed. The magnetometer could not be made to operate, and was hauled in at 2250.

On 4 and 5 December, much time was taken up in report writing, scientific discussions and a final science meeting, and packing up samples and equipment. Two short engine stoppages slowed us down, but otherwise the return to Brisbane went uneventfully. Late on 3 December coring ended, and we berthed at 0915 on the morning of 6 December, and all samples and some equipment were despatched to Canberra. Equipment for the non-seismic Geoscience Australia cruise FR1/02, to sail in January, was left aboard.

Appendix 4: Key Equipment

Charge-Air DC330/2000 diesel compressor of 2000 psi capacity for airguns
2 x GI airguns, each of capacity 45/105 cubic inches
Seismic winch
Stealtharray solid seismic cable 450 m long, with 300 m active section and 24 channels
Plotter for seismic profiles and sampling locations
Seismic processing work station
MMC *Seaspy Overhauser* magnetometer and towing winch
Gravity corer, 1 tonne, for 6m cores
Dredges, chain bag and pipe
Refrigerated container for cores
Benches in CTD laboratory
Rock saw
Core splitter
Equipment for gas sampling
Equipment for pore water sampling equipment from Moss Landing Marine Labs
Ship's winches, and deck machinery
Coring cradle
DGPS navigation
Scientific echosounder (12 kHz)

Appendix 5: Shipboard Personnel Lists

Scientific personnel list

Neville Exon	Geoscience Australia	Chief Scientist, Geology
Peter Hill	Geoscience Australia	Geophysicist
Yves Lafoy	Direction de l'Industrie, des Mines et de l'Energie, New Caledonia	Geoscientist
Melissa Fellows	Geoscience Australia	Sedimentologist
Kirsten Perry	James Cook University	Sedimentologist
Patrick Mitts	Moss Landing Marine Labs, USA	Geochemist
Jon Stratton	Geoscience Australia	Geological technician
Lyndon O'Grady	Geoscience Australia	Geological technician
Craig Wintle	Geoscience Australia	Mechanical technician
David Holdway	Geoscience Australia	Electronics technician
Lindsay Pender	CSIRO Marine Research	Computer specialist
Stephen Thomas	CSIRO Marine Research	Electronics technician

Crew list

Ian Taylor	Master
Arthur Staron	Chief Officer
John Boyes	2nd Officer
Gordon Gore	Chief Engineer
Gregory Pearce	1st Engineer
Hugh McCormick	Electrical Engineer
Malcolm McDougall	Senior Integrated Rating (Bosun)
Tony Hearne	Integrated Rating
Graham McDougall	Integrated Rating
Louis Jacomas	Integrated Rating
Howard (Danny) Davies	Greaser
Marc Sweeney	Chief Cook
Bernard Sorenson	2nd Cook
Shaun McQuaid	Chief Steward

Appendix 6: Ferromanganese crusts

Dr Neville Exon, Geoscience Australia

Dredge haul 232/DR5 was taken on a volcanic edifice on the eastern Lord Howe Rise at 29º35.9'S, 163º42.3'E, in a water depth of ~1700 m. The dredge haul consisted of basaltic volcaniclastic rocks including hyaloclastite, hyaloclastite breccia, and minor basalt, encrusted with ferromanganese. Two ferromanganese crusts were analysed for metal content. Sample DR5B1 was a smooth slightly layered crust 3 cm thick, containing some white inclusions. Sample DR5B2 was a smooth dense crust about 3 cm thick that incorporated some volcanic clasts.

Analyses were carried out by ANALABS of Welshpool, Western Australia (Report WM060656) in 2001, on samples ground with a Zirconia ring mill. Some elements or oxides were analysed using XRF, but the bulk of the elements by ICP-AES or ICP-MS. The more important results are listed below (Table 1).

Table 1: Analyses of major components of Lord Howe Rise ferromanganese crusts

Sample/ GA no.	Mn %	Fe %	Mn:Fe	Cu %	Ni %	Co %	SiO2 %	Al2O3 %	MgO %	CaO %	LOI %
DD5B1/ 6406362B	27.02	11.86	2.26	0.15	0.77	0.38	7.17	3.13	3.74	3.38	18.95
DR5B2/ 6406363B	21.81	18.72	1.16	0.03	0.30	0.55	5.36	1.37	2.08	3.46	20.58

The Lord Howe Rise crusts are similar in Mn, Fe, Cu, Ni and Co contents to average Pacific Ocean crusts (Table 2). As compared to the most economically interesting Pacific crusts, from the Central Pacific for example, the Lord Howe Island crusts are low in Cu and Co, but high in Cu. In many respects they are quite like those from Christmas Island (Exon *et al.*, 2002) and the Tasmanian region (Exon, 1997), but are higher in Ni and Co. These crusts are of no commercial interest.

Table 2. Ferromanganese crust comparisons

Samples	No	Mn (%)	Fe (%)	Cu (%)	Ni (%)	Co (%)	Cu+Ni+Co (%)
Pacific Ocean	319	22	15	0.08	0.44	0.63	1.15
Central Pacific	311	23	15.7	0.47	0.12	0.79	1.38
Marshall Islands		20.3	12.5	0.04	0.39	0.85	1.28
Tasmanian	31	16.2	17.2	0.08	0.32	0.34	0.74
Christmas Island (Indian Ocean)	14	16.2	13.9	0.11	0.35	0.44	0.90
Lord Howe Rise	2	24.4	15.3	0.09	0.54	0.47	1.10

Pacific and Central Pacific crusts after Hein et al. (1992). Marshall Island crusts after (Hein et al., 1990). Tasmanian crusts after Exon (1997). Christmas Island crusts after Exon et al. (2002).

References

Exon, N.F., 1997. Ferromanganese crust and nodule deposits from the continental margin south and west of Tasmania. *Australian Journal of Earth Sciences* 44, 701-710.

Exon, N.F., Raven, M.D. & de Carlo, E.H., 2002. Ferromanganese nodules and crusts from the Christmas Island region, Indian Ocean. *Marine Georesources & Geotechnology* 20(4), 275-297.

Hein, J.R. *et al.*, 1990. Geological, geochemical, geophysical and oceanographic data and interpretations of seamounts and Co-rich ferromanganese crusts from the Marshall Islands, KORDI-USGS R.V. *Farnella* cruise F10-89-CP. *US Geological Survey Open File Report*, 90-407.

Hein, J.R., Schultz, M.S. and Gein, L.M., 1992. Central Pacific cobalt-rich ferromanganese crusts: historical perspective and regional variability. *Circum-Pacific Council for Energy and Mineral Resources, Earth Science Series* 16, 261-283.

Appendix 7: Thin-section rock descriptions for Fairway Basin volcanics (232/DR05A)

Dr Neville Exon, Geoscience Australia

Sample	Description and age
DR5A1	Brownish-grey, fine-grained vesicular basalt with skeletal feldspars, and olivine with chlorite alteration. Vesicles 1-2 mm, filled with calcite
DR5A2	Hyaloclastite consisting largely of brown, vesicular fine-grained, iron-altered glassy basalt with skeletal feldspars, and aggregates of fairly fresh ?pyroxene. Contains rounded pebbles of grey vesicular glassy basalt with minor skeletal feldspar set in dark iron-altered glass, with aggregates of fairly fresh ?pyroxene, and some olivine with strong chlorite alteration. Veins filled with calcite and chlorite
DR5A3	Hyaloclastite consisting largely of brown, vesicular iron-altered glass, and some micrite. Darker and lighter patches a few mm across suggest welding of various glassy components. Vesicles filled with calcite and zeolite. Attached foram-bearing micrite* also contains granule of glass. Foram age in infilling micrite is middle early Pliocene (Chapter 7); in the encrusting Mn it is late middle Miocene (Appendix 7). Thick Mn crust
DR5A4	Hyaloclastite consisting largely of light coloured palagonitised glass, with iron-altered ferromagnesian phenocrysts. Also contains clasts of iron-stained similar glass, and veins of foram-bearing micrite*.
DR5A5	Hyaloclastite consisting largely of welded fragments, 1-2cm in size. Mix of light coloured palagonitised glass, and iron-stained similar glass. Iron-altered ferromagnesian phenocrysts and zeolitic infillings are commonly present. Thick Mn crust

Location: 29º 35.9'S, 163º42.3'W, water depth ~1700 m.

Appendix 8: Foraminiferal assemblage in Mn crust on volcaniclastic edifice

Dr Patrick Quilty, University of Tasmania

Sample 232/DR05A3. GA reference 6406742 (Q0965)

Location: 29º 35.9'S, 163º42.3'W, water depth ~1700 m.

Lithology: Mn oxide covered (intermixed) white lithified chalk/ooze, encrusting hyaloclastite.

Method: Examined first as thin section and then as sample broken down by gentle crushing which released a good fauna. Fauna is not good for statistics but can get an impression of faunal structure.

Fauna:

Planktonic species:
Globigerina nepenthes
Orbulina universa
Globoquadrina altispira altipsira
Globorotalia miozea
Globorotalia scitula
Globorotalia cf. *menardii*
Catapsydrax parvulus
Globigerinoides trilobus (several forms)

Benthic forms:
Diverse, dominated by *Ehrenbergina*
Common *Virgulina, Bolivina, Neouvigerina*
Less common *Cibicides, Osangularia,* etc

Age: Later Middle Miocene, N14/15.

Environment of deposition: Probably mid-shelf or equivalent, this judgement based on abundance and diversity of benthic fauna. An interesting and unusual aspect of the fauna is the relative abundance of infaunal species suggesting a high nutrient environment, perhaps near upwelling. This judgement is tentative because of the lack of statistical validity of the fauna.

Appendix 9: Petroleum geochemistry

Dr Chris Boreham, Geoscience Australia

Headspace gas samples from shallow core sediments were analysed in Geoscience Australia's laboratories. Results are the average of duplicate samples, except when marked with an asterisk (*). 70ESRD is a standard.

SAMPLE No.	No.	TOP (m)	BASE (m)	METHANE (ppm)	ETHANE (ppm)	PROPANE (ppm)
70ESTD				2360	2170	2050
20020026	232GC01	0.33	0.43	0.7	0	0.05
20020027	232GC01	0.54	0.64	0	0.15	0.05
20020028	232GC01	4.15	4.25	2.5	0.15	0.05
20020029	232GC01	4.25	4.35	1.5	0	0
20020030	232GC02	0.2	0.3	0	0	0
20020031	232GC02	0.3	0.4	0.7	0	0.05
20020032	232GC02	3	3.1	1.7	0.0	0.0
20020033*	232GC03	0.5	0.6	0.5	0	0
20020034	232GC03	0.6	0.7	1.5	0.2	0.1
20020035	232GC03	1.5	1.6	0	0.05	0.1
20020036	232GC03	1.6	1.7	2.7	0.2	0.1
20020037	232GC03	3.03	3.13	no analysis	no analysis	no analysis
20020038	232GC03	3.13	3.23	2	0.2	0
20020039	232GC04	0.5	0.6	0.65	0.2	0
20020040*	232GC04	0.6	0.7	3.1	0.2	0.1
20020041	232GC04	2.82	2.92	0.3	0.0	0.0
20020042	232GC04	2.92	3.02	0.05	0.15	0
20020043	232GC05	0.5	0.6	0.8	0.0	0.1
20020044	232GC05	0.6	0.7	0.4	0.2	0.1
20020045	232GC05	2.7	2.8	5.4	0.5	0.3
20020046	232GC05	2.8	2.9	0.3	0.05	0
20020047	232GC06	0.15	0.25	3.1	0.0	0.0
20020048	232GC06	0.25	0.35	0.6	0	0
20020049	232GC06	2.98	3.08	0.15	0.05	0
20020050	232GC06	3.08	3.18	0.5	0.1	0.0
20020051	232GC08	0.38	0.48	1.5	0	0.05
20020052	232GC08	0.48	0.58	0.1	0.0	0.0
20020053	232GC08	3.1	3.2	0.5	0	0
20020054	232GC08	3.35	3.45	0	0.15	0
20020055	232GC08	3.45	3.55	0.1	0	0
20020056	232GC09	0.2	0.3	2.4	0.05	0
20020057*	232GC09	0.3	0.4	0	0	0.6
20020058	232GC09	3.1	3.2	2.05	0	0.15
20020059	232GC09	3.2	3.3	1.05	0.05	0

20020060	232GC10	4.18	4.28	0.3	0	0
20020061	232GC10	4.28	4.28	no analysis	no analysis	no analysis
20020062*	232GC11	3.18	3.28	0.3	0	0.1
20020063	232GC11	3.28	3.3	0	0	0
20020064	232GC12	2.35	2.45	0.1	0	0

These results indicate that there are negligible amounts of hydrocarbons in the surface cores in this region, probably because of the oxidation of the sediments.

Appendix 10. Carbon contents and isotopic analysis of Fairway Basin sediments

Dr Roger Summons, Geoscience Australia (in 1999)

Samples from Lamont-Doherty Earth Science Laboratory piston cores RC12-108 and RC12-113 from the Fairway Basin (Lord Howe Rise) were analysed in Geoscience Australia's Isotope and Organic Geochemistry Laboratory in 1999 (File rslordhowe1toc). The attached Table 1 shows that the cores contain low organic carbon contents and also that TOC decreases systematically from the 6-7 cm sediments where it is ~0.25% to 0.1% by 300cm. The samples are also predominantly carbonate (93-98 %), with up to 98% lost on acid digestion.

The bulk carbon isotopic content of the carbonates (Table 2) is near zero for the near surface samples and appears to be unaffected by any anomaly expected to be introduced by large-scale methane oxidation. Both 300cm samples are significantly heavier at +1.5%o than those that are shallower. This indicates that there may be some isotopic trend down-core that could be examined by more detailed sampling.

These samples do not appear to offer any hope of detecting effects arising from the presence or oxidation of nearby subsurface methane clathrate.

Table 1. Organic carbon and carbonate contents

Latitude	Longitude	Water depth (m)	Core	Depth in core (cm)	*TOC wt %	**Weight % carbonate	GA No.
24º53'S	163º31'E	2454	RC12-113	6-7	0.24	97	19990205
				100-101	0.19	96	19990206
				200-201	0.14	95	19990207
				300-301	0.10	98	19990208
26º02.5'S	165º49'E	3354	RC12-108	6-7	0.27	95	
				100-101	0.14	93	
				200-201	0.13	95	
				300-301	0.10	97	

*TOC error +/- 5% or 0.05, whichever is the greatest
** Calculated by % loss to acid digestion: equates in general to % carbonate

Table 2. Carbon Isotopic Analysis

GA No.	Sample Depth	Type	$\delta^{13}C_{PDB}$(%o)	Av. $\delta^{13}C_{PDB}$(%o)
19990205	6-7cm	carbonate repeat	0.09 -0.01	**0.04**
19990206	100-101cm	carbonate repeat	-0.24 -0.24	**-0.24**
19990207	201-202cm	carbonate repeat	0.07 0.06	**0.07**
12220208	300-301cm	carbonate repeat	1.45 1.42	**1.44**
19990209	6-7 cm	carbonate repeat	-0.02 -0.07	**-0.05**
19990210	100-101cm	carbonate repeat	-0.12 -0.15	**-0.14**
19990211	200-201cm	carbonate repeat	0.21 0.17	**0.19**
19990212	300-301cm	carbonate	1.52	**1.52**